Architecture and Structure of a Fold-and-Thrust Belt During Initial Inversion of a Salt-Bearing Passive Margin (Jurassic of the Eastern Alps, Austria)

Oscar Fernández[1], Hugo Ortner[2], William E.H. Munday[1], Michael Moser[1], Diethard Sanders[2], Bernhard Grasemann[1], and Thomas Leitner[3]

[1]University of Vienna
[2]University of Innsbruck
[3]Salinen AG

April 09, 2024

Abstract

Inversion of the Austroalpine Triassic salt-bearing passive margin, represented by the Northern Calcareous Alps (Eastern Alps), started in the Late Jurassic. Subsequent deformation during the Cretaceous and Cenozoic mostly preserved the Late Jurassic deformation fabric in the central Northern Calcareous Alps, making it an outstanding location to understand the early history of inversion of salt-bearing margins. Thrusting and folding in the central NCA during the Late Jurassic were strongly conditioned by the distribution of Triassic salt structures, the thickness of supra-salt stratigraphy, the lateral propagation of deformation, and the possible influence of sub-salt basement faults. Syn-orogenic sediments make it possible to reliably reconstruct the timing of structural inversion. The description of Late Jurassic structures presented here indicates that initial inversion of the Northern Calcareous Alps led to the development of coherent deformation systems that accumulated limited amounts of shortening, totaling few tens of kilometers. This differs from previous interpretations of Late Jurassic deformation of the area, that involve major amounts of allochthony (many tens of kilometers). As a specific example of coherent structural development, we present here an 80 km long linked system of thrusts and folds (the Totengebirge–Trattberg contractional system), whose outstanding continuity has gone previously unrecognized. The anatomy of this system and its temporal evolution are described in detail and discussed in the framework of the Jurassic to recent evolution of the Eastern Alps.

Hosted file

`Fernandez_etal_Jurassic_shortening_NCA.docx` available at https://authorea.com/users/765582/articles/788544-architecture-and-structure-of-a-fold-and-thrust-belt-during-initial-inversion-of-a-salt-bearing-passive-margin-jurassic-of-the-eastern-alps-austria

Hosted file

`Fernandez_etal_Jurassic_shortening_NCA_SuppInf.docx` available at https://authorea.com/users/765582/articles/788544-architecture-and-structure-of-a-fold-and-thrust-belt-during-initial-inversion-of-a-salt-bearing-passive-margin-jurassic-of-the-eastern-alps-austria

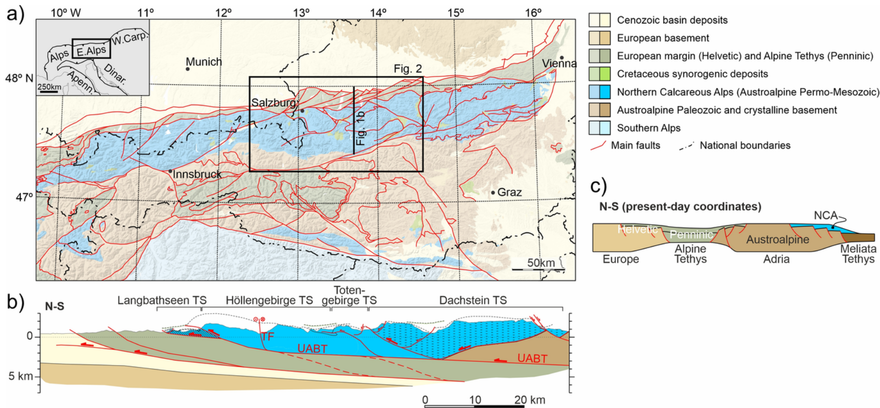
a)
Munich
Salzburg
Innsbruck
Vienna
Graz
Fig. 2
Fig. 1b
Cenozoic basin deposits
European basement
European margin (Helvetic) and Alpine Tethys (Penninic)
Cretaceous synorogenic deposits
Northern Calcareous Alps (Austroalpine Permo-Mesozoic)
Austroalpine Paleozoic and crystalline basement
Southern Alps
Main faults
National boundaries
b) N-S
Langbathseen TS
Höllengebirge TS
Toten-gebirge TS
Dachstein TS
UABT
TF
c) N-S (present-day coordinates)
NCA
Helvetic
Penninic
Austroalpine
Europe
Alpine Tethys
Adria
Meliata Tethys

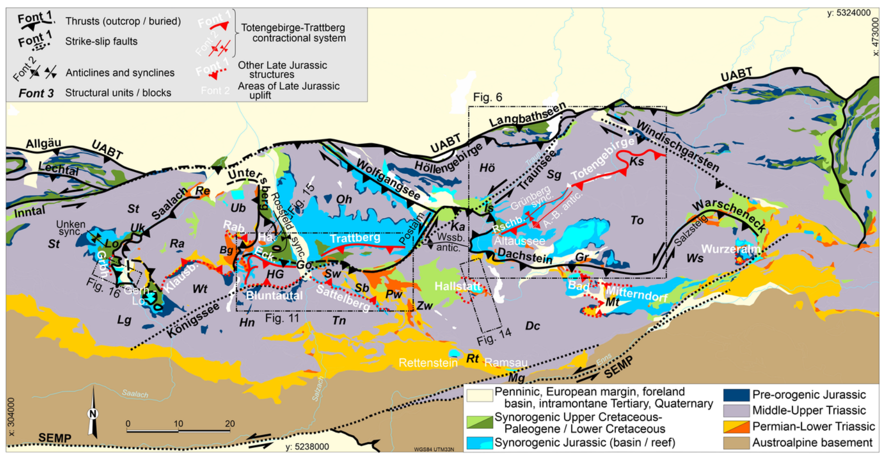
Thrusts (outcrop / buried)
Strike-slip faults
Anticlines and synclines
Structural units / blocks
Totengebirge-Trattberg contractional system
Other Late Jurassic structures
Areas of Late Jurassic uplift
Fig. 6
Fig. 11
Fig. 14
Fig. 16
Trattberg
Dachstein
Hallstatt
Totengebirge
Warscheneck
UABT
SEMP
Penninic, European margin, foreland basin, intramontane Tertiary, Quaternary
Synorogenic Upper Cretaceous-Paleogene / Lower Cretaceous
Synorogenic Jurassic (basin / reef)
Pre-orogenic Jurassic
Middle-Upper Triassic
Permian-Lower Triassic
Austroalpine basement

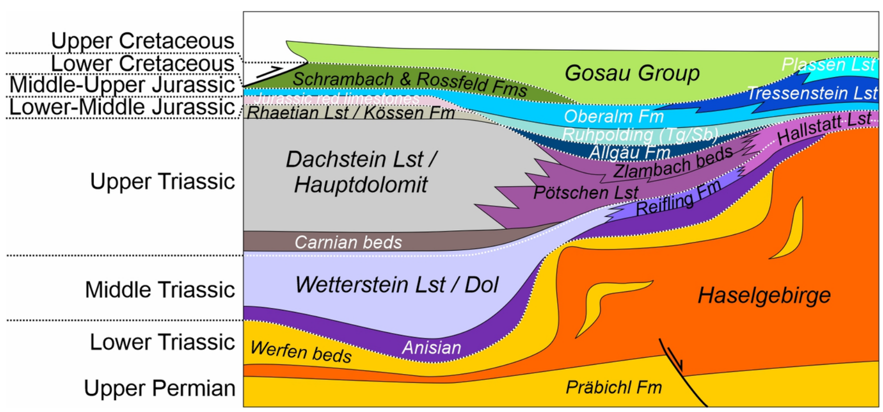
Upper Cretaceous
Lower Cretaceous
Middle-Upper Jurassic
Lower-Middle Jurassic
Upper Triassic
Middle Triassic
Lower Triassic
Upper Permian
Gosau Group
Schrambach & Rossfeld Fms
Plassen Lst
Tressenstein Lst
Oberalm Fm
Jurassic red limestones
Rhaetian Lst / Kössen Fm
Ruhpolding (Tg/Sb)
Allgäu Fm
Hallstatt Lst
Zlambach beds
Dachstein Lst / Hauptdolomit
Pötschen Lst
Reifling Fm
Carnian beds
Wetterstein Lst / Dol
Haselgebirge
Anisian
Werfen beds
Präbichl Fm

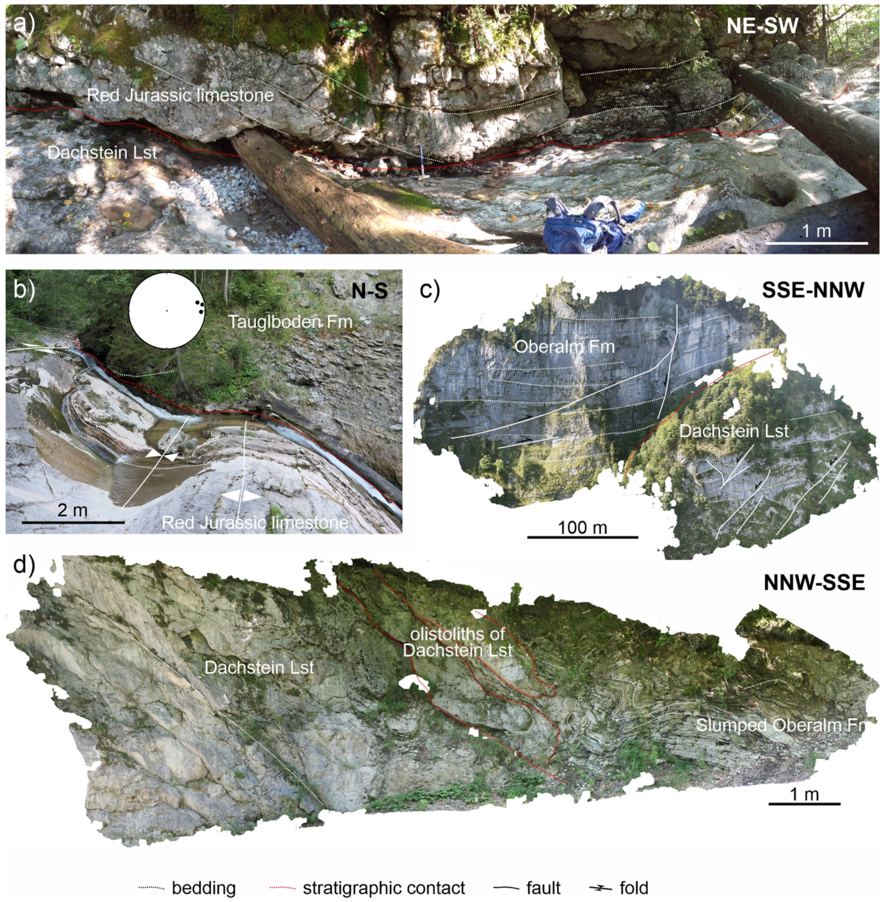
a)
NE-SW
Red Jurassic limestone
Dachstein Lst
1 m
b)
N-S
Tauglboden Fm
2 m
Red Jurassic limestone
c)
SSE-NNW
Oberalm Fm
Dachstein Lst
100 m
d)
NNW-SSE
olistoliths of Dachstein Lst
Dachstein Lst
Slumped Oberalm Fm
1 m
bedding
stratigraphic contact
fault
fold

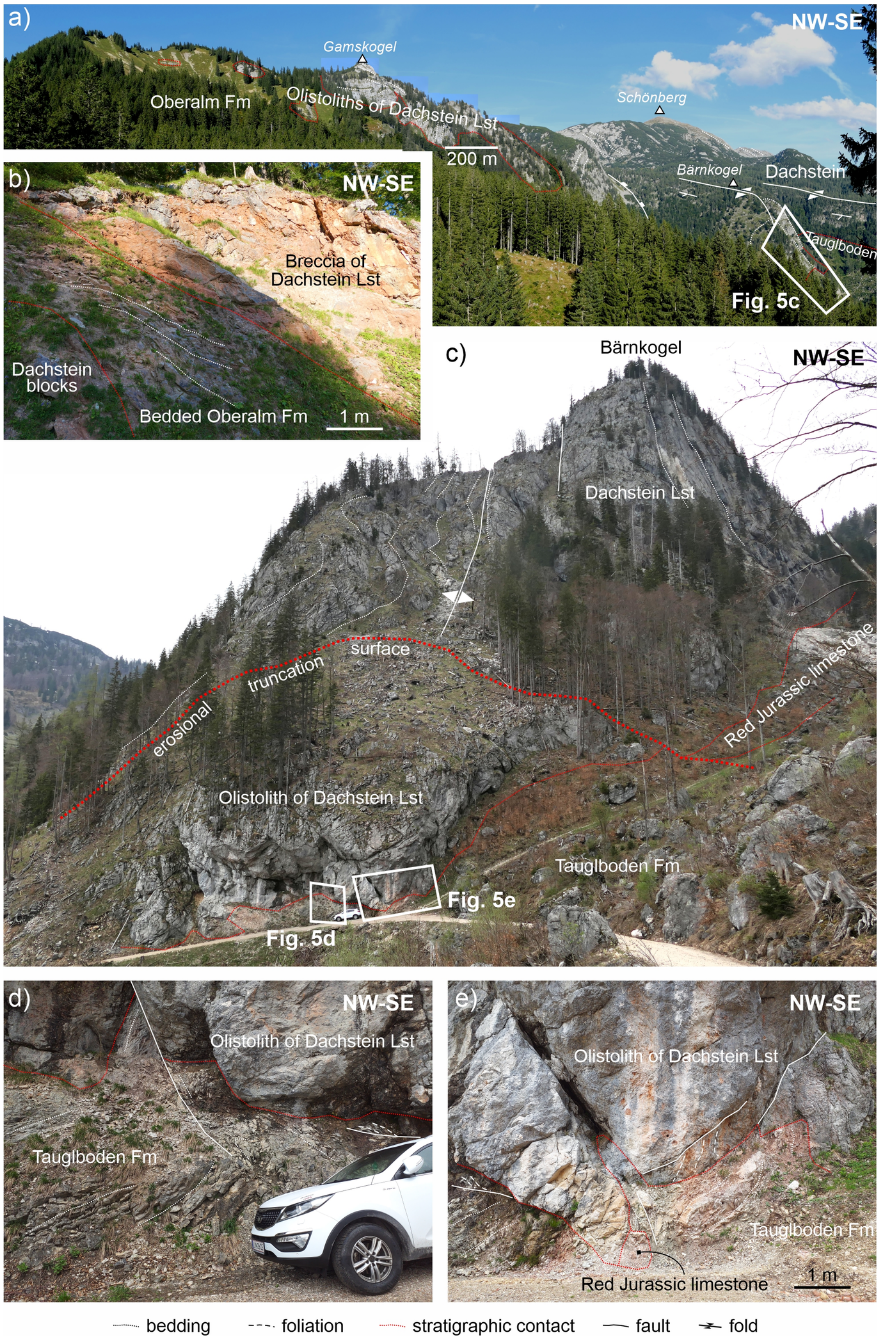
a)
NW-SE
Gamskogel
Oberalm Fm
Olistoliths of Dachstein Lst
200 m
Schönberg
Bärnkogel
Dachstein
Tauglboden
Fig. 5c
b)
NW-SE
Breccia of Dachstein Lst
Dachstein blocks
Bedded Oberalm Fm
1 m
c)
Bärnkogel
NW-SE
Dachstein Lst
erosional truncation surface
Red Jurassic limestone
Olistolith of Dachstein Lst
Tauglboden Fm
Fig. 5e
Fig. 5d
d)
NW-SE
Olistolith of Dachstein Lst
Tauglboden Fm
e)
NW-SE
Olistolith of Dachstein Lst
Tauglboden Fm
Red Jurassic limestone
1 m
bedding
foliation
stratigraphic contact
fault
fold

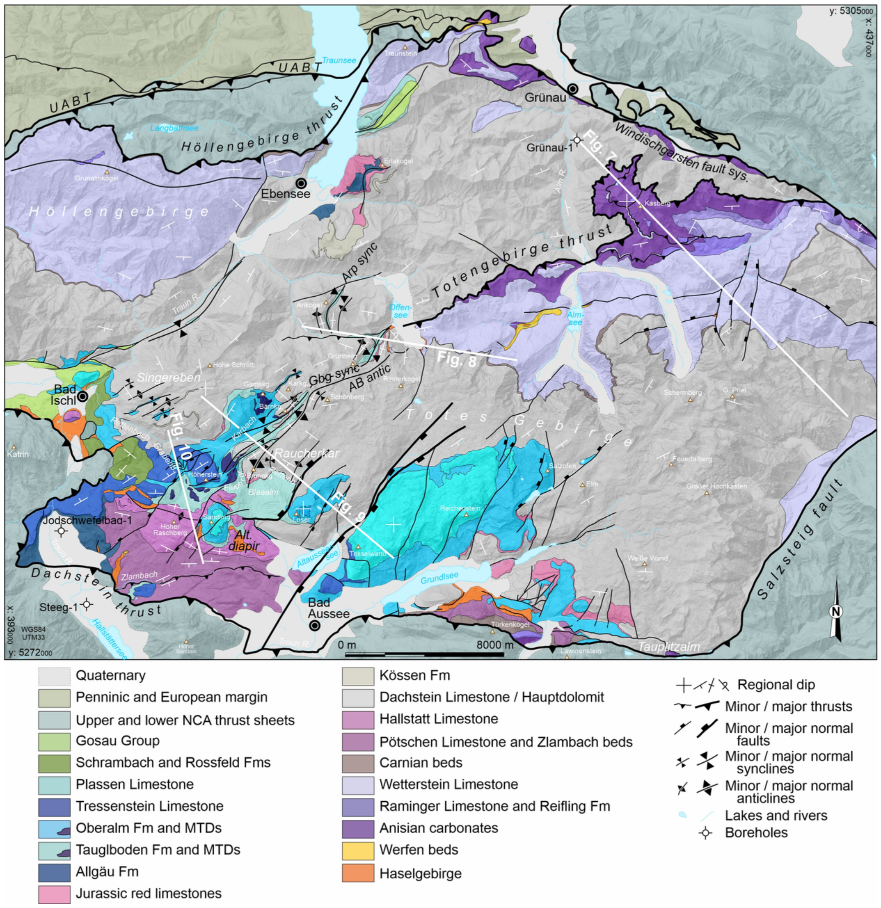
UABT
Höllengebirge thrust
Höllengebirge
Ebensee
Grünau
Grünau-1
Windischgarsten fault sys.
Totengebirge thrust
Arp sync
Fig. 7
Fig. 8
Fig. 9
Fig. 10
Gbg sync
AB antic
Singereben
Bad Ischl
Raucherkar
Totes Gebirge
Alt. diapir
Jodschwefelbad-1
Dachstein thrust
Steeg-1
Zlambach
Bad Aussee
Grundlsee
Salzsteig fault
Tauplitzalm
0 m
8000 m
y: 5305000
x: 437000
x: 393000
y: 5272000
WGS84 UTM33
N
Quaternary
Penninic and European margin
Upper and lower NCA thrust sheets
Gosau Group
Schrambach and Rossfeld Fms
Plassen Limestone
Tressenstein Limestone
Oberalm Fm and MTDs
Tauglboden Fm and MTDs
Allgäu Fm
Jurassic red limestones
Kössen Fm
Dachstein Limestone / Hauptdolomit
Hallstatt Limestone
Pötschen Limestone and Zlambach beds
Carnian beds
Wetterstein Limestone
Raminger Limestone and Reifling Fm
Anisian carbonates
Werfen beds
Haselgebirge
Regional dip
Minor / major thrusts
Minor / major normal faults
Minor / major normal synclines
Minor / major normal anticlines
Lakes and rivers
Boreholes

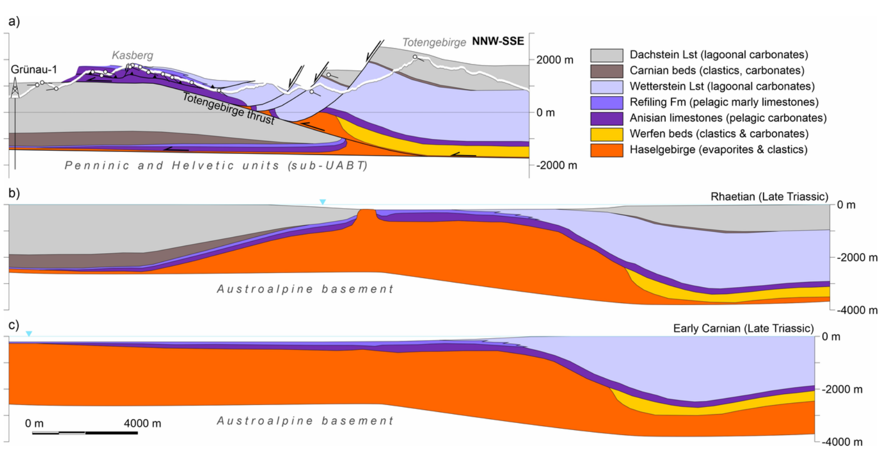
a)
Grünau-1
Kasberg
Totengebirge
NNW-SSE
Totengebirge thrust
Penninic and Helvetic units (sub-UABT)
2000 m
0 m
-2000 m
Dachstein Lst (lagoonal carbonates)
Carnian beds (clastics, carbonates)
Wetterstein Lst (lagoonal carbonates)
Reifling Fm (pelagic marly limestones)
Anisian limestones (pelagic carbonates)
Werfen beds (clastics & carbonates)
Haselgebirge (evaporites & clastics)
b)
Rhaetian (Late Triassic)
Austroalpine basement
0 m
-2000 m
-4000 m
c)
Early Carnian (Late Triassic)
Austroalpine basement
0 m
4000 m
0 m
-2000 m
-4000 m

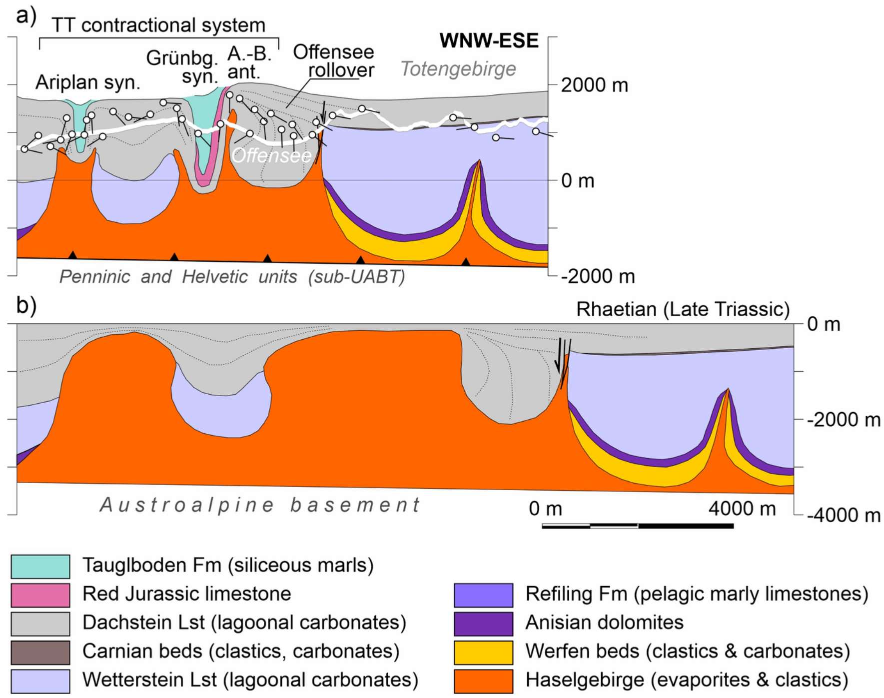

a)
TT contractional system
WNW-ESE
Ariplan syn.
Grünbg. syn.
A.-B. ant.
Offensee rollover
Totengebirge
Offensee
2000 m
0 m
-2000 m
Penninic and Helvetic units (sub-UABT)
b)
Rhaetian (Late Triassic)
0 m
-2000 m
-4000 m
Austroalpine basement
0 m
4000 m
Tauglboden Fm (siliceous marls)
Red Jurassic limestone
Dachstein Lst (lagoonal carbonates)
Carnian beds (clastics, carbonates)
Wetterstein Lst (lagoonal carbonates)
Refiling Fm (pelagic marly limestones)
Anisian dolomites
Werfen beds (clastics & carbonates)
Haselgebirge (evaporites & clastics)

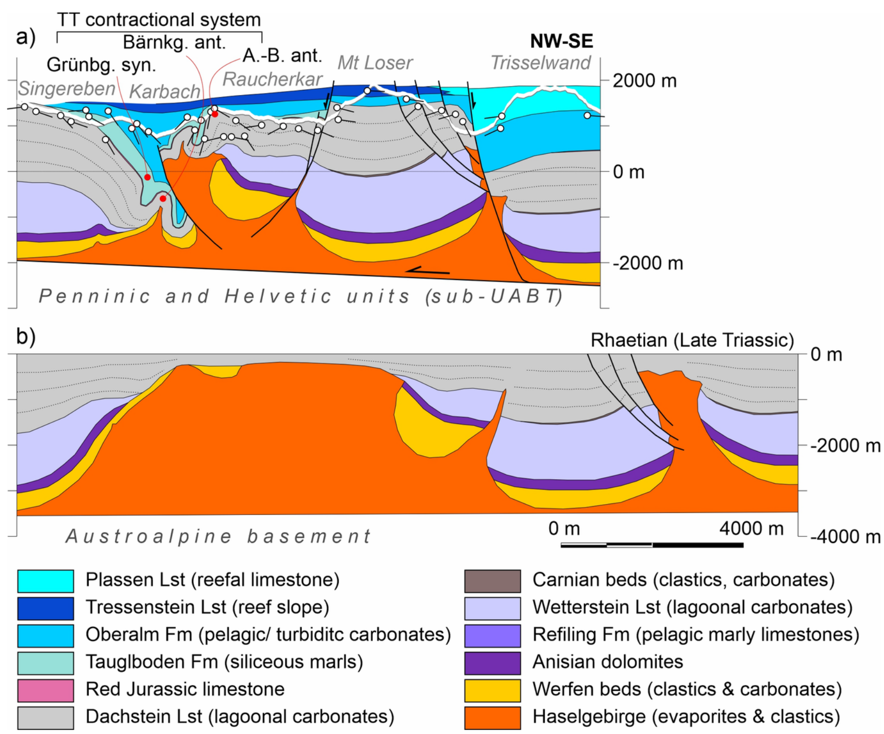

a)
TT contractional system
NW-SE
Bärnkg. ant.
Grünbg. syn.
A.-B. ant.
Mt Loser
Trisselwand
Singereben
Karbach
Raucherkar
2000 m
0 m
-2000 m
Penninic and Helvetic units (sub-UABT)
b)
Rhaetian (Late Triassic)
0 m
-2000 m
-4000 m
Austroalpine basement
0 m
4000 m
Plassen Lst (reefal limestone)
Tressenstein Lst (reef slope)
Oberalm Fm (pelagic/ turbiditc carbonates)
Tauglboden Fm (siliceous marls)
Red Jurassic limestone
Dachstein Lst (lagoonal carbonates)
Carnian beds (clastics, carbonates)
Wetterstein Lst (lagoonal carbonates)
Refiling Fm (pelagic marly limestones)
Anisian dolomites
Werfen beds (clastics & carbonates)
Haselgebirge (evaporites & clastics)

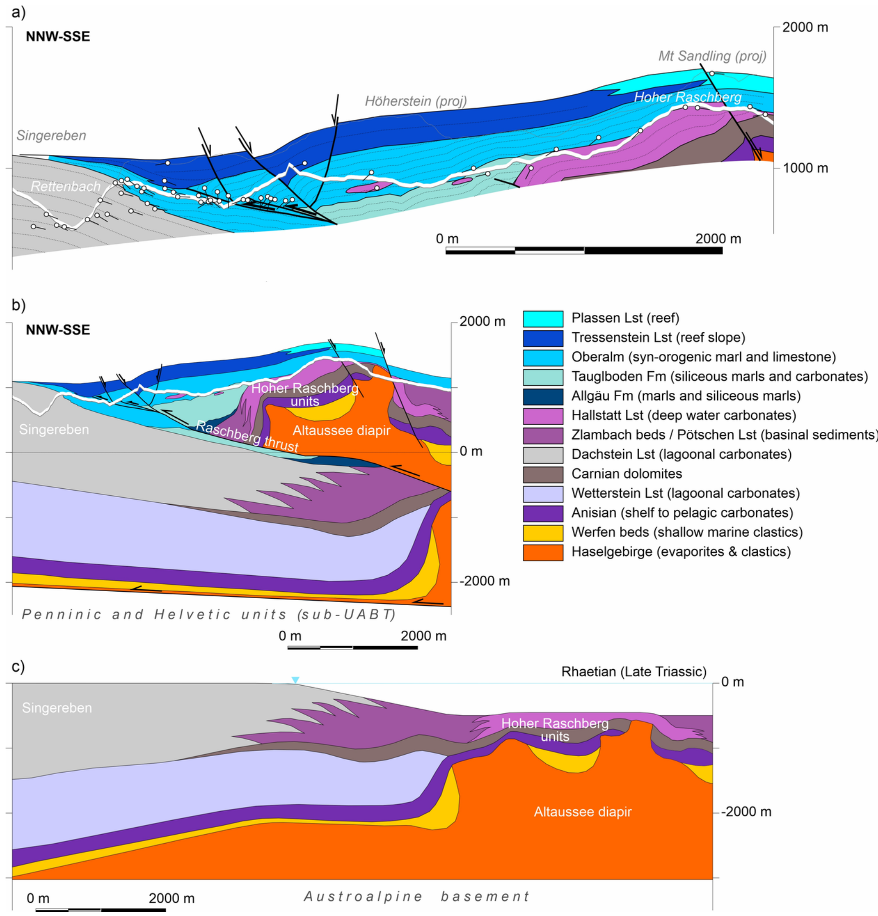
a)
NNW-SSE
2000 m
Mt Sandling (proj)
Höherstein (proj)
Hoher Raschberg
Singereben
Rettenbach
1000 m
0 m
2000 m
b)
NNW-SSE
2000 m
Hoher Raschberg units
Singereben
Raschberg thrust
Altaussee diapir
0 m
-2000 m
Penninic and Helvetic units (sub-UABT)
0 m
2000 m
Plassen Lst (reef)
Tressenstein Lst (reef slope)
Oberalm (syn-orogenic marl and limestone)
Tauglboden Fm (siliceous marls and carbonates)
Allgäu Fm (marls and siliceous marls)
Hallstatt Lst (deep water carbonates)
Zlambach beds / Pötschen Lst (basinal sediments)
Dachstein Lst (lagoonal carbonates)
Carnian dolomites
Wetterstein Lst (lagoonal carbonates)
Anisian (shelf to pelagic carbonates)
Werfen beds (shallow marine clastics)
Haselgebirge (evaporites & clastics)
c)
Rhaetian (Late Triassic)
0 m
Singereben
Hoher Raschberg units
Altaussee diapir
-2000 m
0 m
2000 m
Austroalpine basement

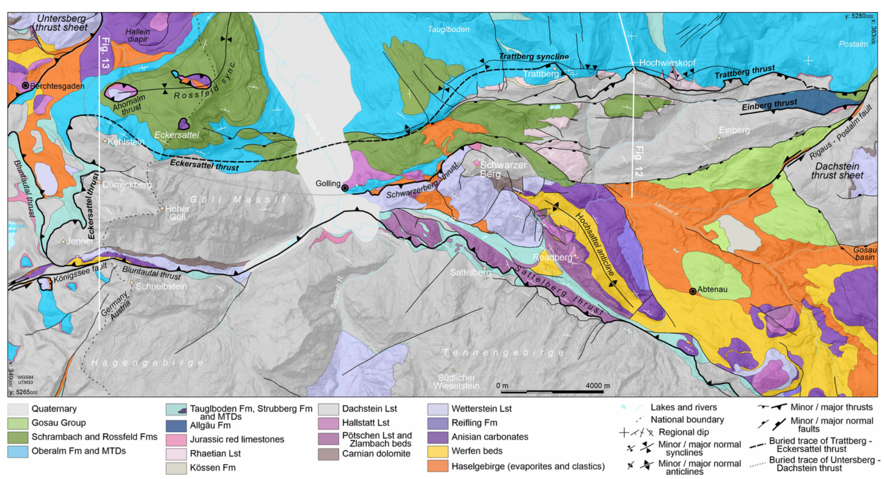
Untersberg thrust sheet
Hallein diapir
Fig. 13
Berchtesgaden
Rossfeld sync.
Eckersattel
Eckersattel thrust
Golling
Göll Massif
Hoher Göll
Königssee fault
Bluntautal thrust
Schneibstein
Germany
Austria
Hagengebirge
Tauglboden
Trattberg syncline
Trattberg
Hochwieskopf
Trattberg thrust
Einberg thrust
Einberg
Fig. 12
Schwarzer Berg
Rigaus - Postalm fault
Dachstein thrust sheet
Gosau basin
Abtenau
Sattelberg
Tennengebirge
Südlicher Wieselstein
0 m
4000 m
Quaternary
Gosau Group
Schrambach and Rossfeld Fms
Oberalm Fm and MTDs
Tauglboden Fm, Strubberg Fm and MTDs
Allgäu Fm
Jurassic red limestones
Rhaetian Lst
Kössen Fm
Dachstein Lst
Hallstatt Lst
Pötschen Lst and Zlambach beds
Carnian dolomite
Wetterstein Lst
Reifling Fm
Anisian carbonates
Werfen beds
Haselgebirge (evaporites and clastics)
Lakes and rivers
National boundary
Regional dip
Minor / major normal synclines
Minor / major normal anticlines
Minor / major thrusts
Minor / major normal faults
Buried trace of Trattberg - Eckersattel thrust
Buried trace of Untersberg - Dachstein thrust

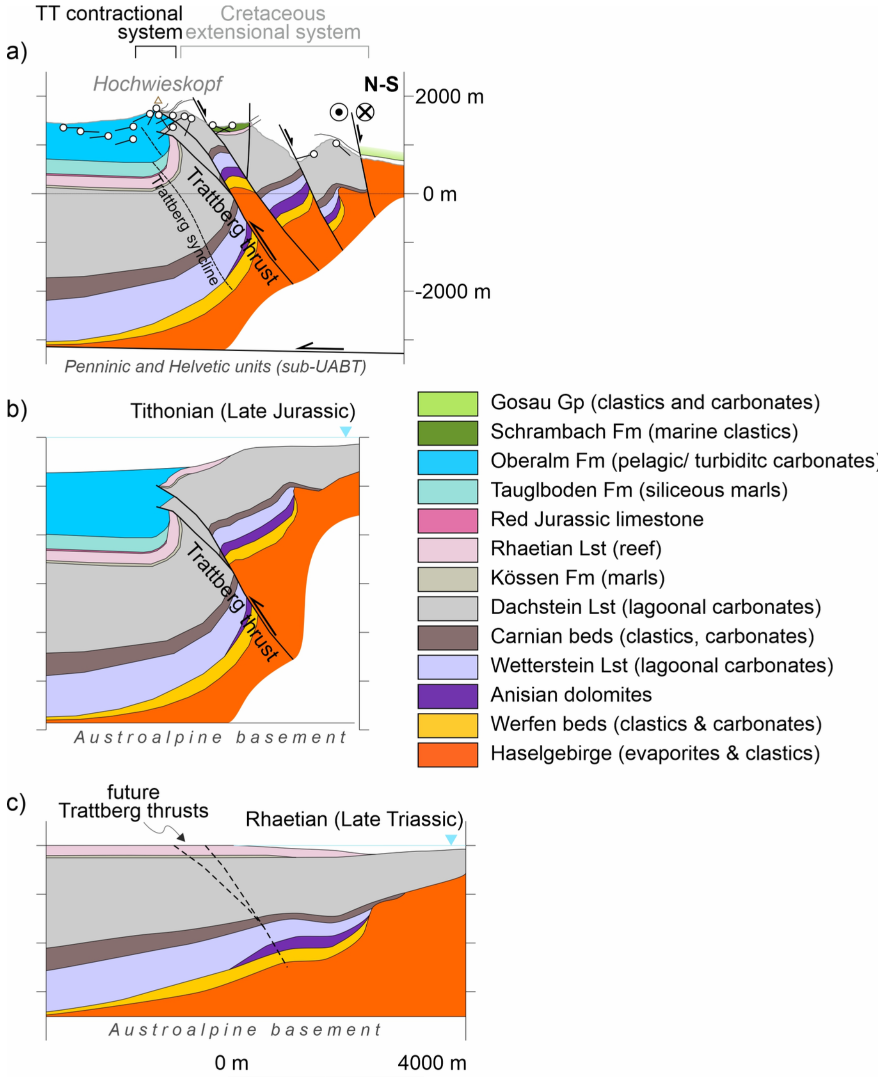
TT contractional system
Cretaceous extensional system
a)
Hochwieskopf
N-S
2000 m
0 m
-2000 m
Trattberg thrust
Trattberg syncline
Penninic and Helvetic units (sub-UABT)
b)
Tithonian (Late Jurassic)
Trattberg thrust
Austroalpine basement
Gosau Gp (clastics and carbonates)
Schrambach Fm (marine clastics)
Oberalm Fm (pelagic/ turbiditc carbonates)
Tauglboden Fm (siliceous marls)
Red Jurassic limestone
Rhaetian Lst (reef)
Kössen Fm (marls)
Dachstein Lst (lagoonal carbonates)
Carnian beds (clastics, carbonates)
Wetterstein Lst (lagoonal carbonates)
Anisian dolomites
Werfen beds (clastics & carbonates)
Haselgebirge (evaporites & clastics)
c)
future Trattberg thrusts
Rhaetian (Late Triassic)
Austroalpine basement
0 m
4000 m

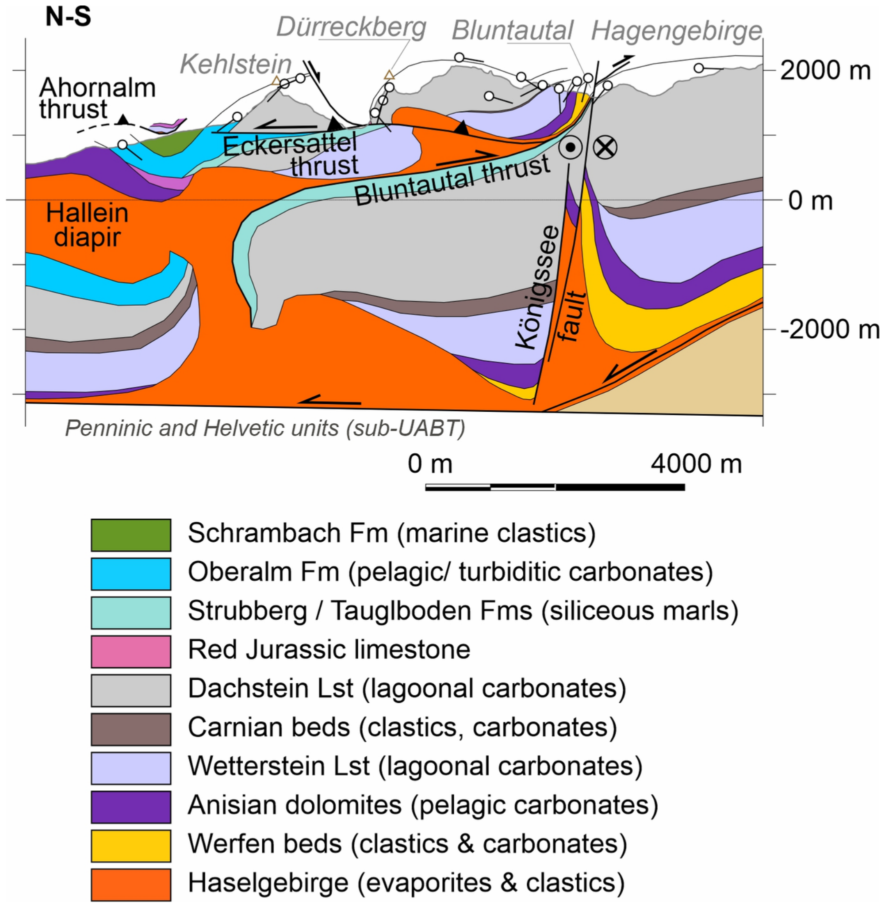
N-S
Dürreckberg
Bluntautal
Hagengebirge
Kehlstein
Ahornalm
thrust
Eckersattel
thrust
Bluntautal thrust
Hallein
diapir
Königssee
fault
2000 m
0 m
-2000 m
Penninic and Helvetic units (sub-UABT)
0 m
4000 m
Schrambach Fm (marine clastics)
Oberalm Fm (pelagic/ turbiditic carbonates)
Strubberg / Tauglboden Fms (siliceous marls)
Red Jurassic limestone
Dachstein Lst (lagoonal carbonates)
Carnian beds (clastics, carbonates)
Wetterstein Lst (lagoonal carbonates)
Anisian dolomites (pelagic carbonates)
Werfen beds (clastics & carbonates)
Haselgebirge (evaporites & clastics)

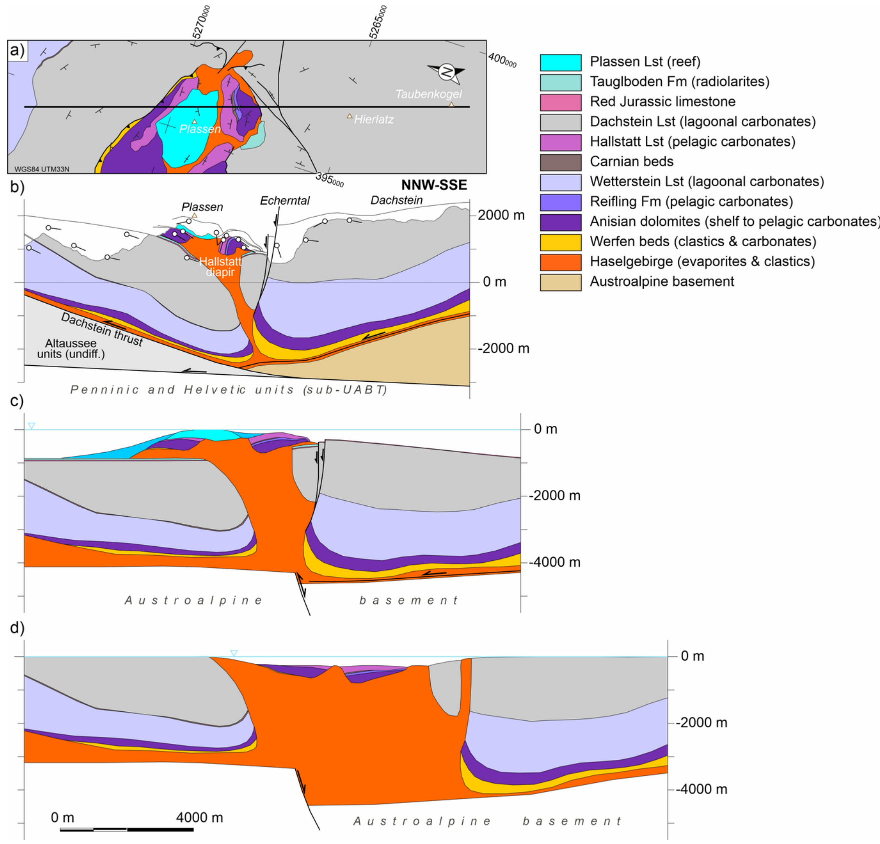
a)
Plassen
Hierlatz
Taubenkogel
WGS84 UTM33N
b)
NNW-SSE
Plassen
Echerntal
Dachstein
Hallstatt diapir
Dachstein thrust
Altaussee units (undiff.)
Penninic and Helvetic units (sub-UABT)
2000 m
0 m
-2000 m
c)
0 m
-2000 m
-4000 m
Austroalpine basement
d)
0 m
-2000 m
-4000 m
0 m
4000 m
Austroalpine basement
Plassen Lst (reef)
Tauglboden Fm (radiolarites)
Red Jurassic limestone
Dachstein Lst (lagoonal carbonates)
Hallstatt Lst (pelagic carbonates)
Carnian beds
Wetterstein Lst (lagoonal carbonates)
Reifling Fm (pelagic carbonates)
Anisian dolomites (shelf to pelagic carbonates)
Werfen beds (clastics & carbonates)
Haselgebirge (evaporites & clastics)
Austroalpine basement

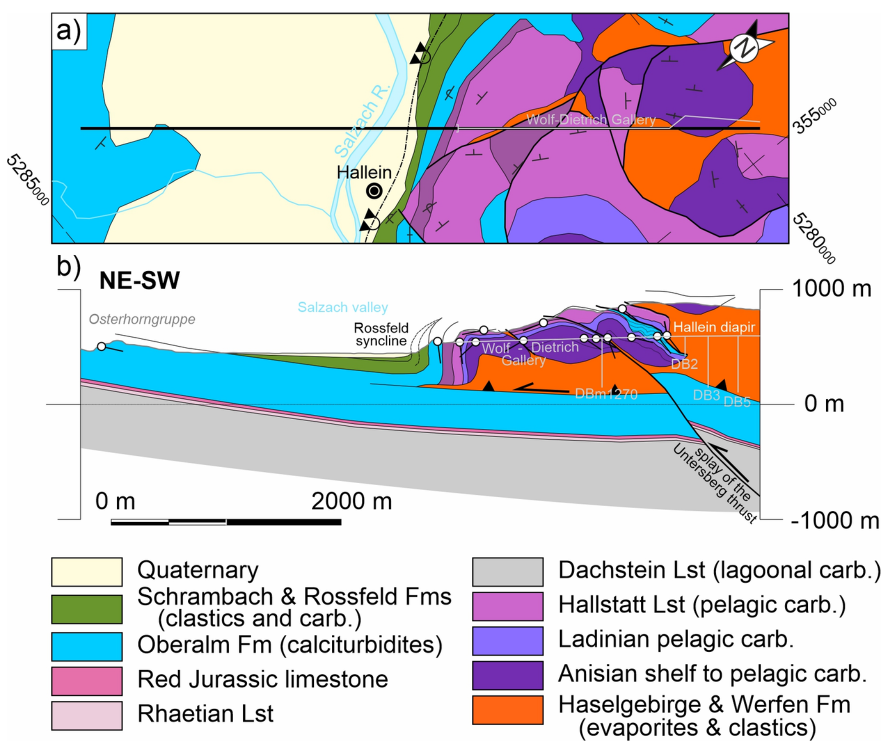
a)
Salzach R.
Hallein
Wolf-Dietrich Gallery
b)
NE-SW
Osterhorngruppe
Salzach valley
Rossfeld syncline
Wolf Dietrich Gallery
Hallein diapir
DB2
DBm1270
DB3
DB5
spray of the Untersberg thrust
1000 m
0 m
-1000 m
0 m
2000 m
Quaternary
Schrambach & Rossfeld Fms (clastics and carb.)
Oberalm Fm (calciturbidites)
Red Jurassic limestone
Rhaetian Lst
Dachstein Lst (lagoonal carb.)
Hallstatt Lst (pelagic carb.)
Ladinian pelagic carb.
Anisian shelf to pelagic carb.
Haselgebirge & Werfen Fm (evaporites & clastics)

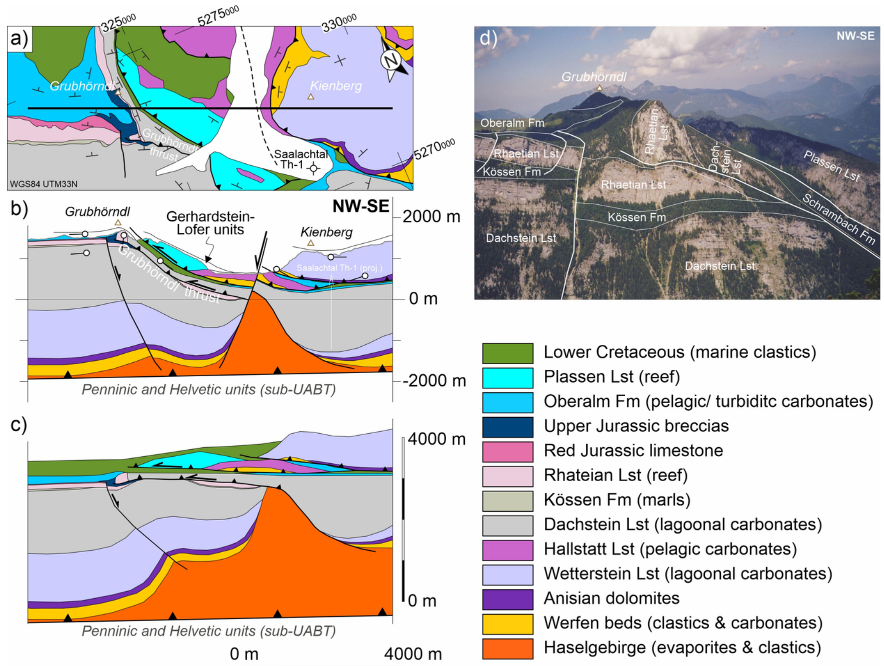
a)
Grubhörndl
Kienberg
Grubhörndl thrust
Saalachtal Th-1
WGS84 UTM33N
b)
NW-SE
Grubhörndl
Gerhardstein-Lofer units
Kienberg
Grubhörndl thrust
2000 m
0 m
-2000 m
Penninic and Helvetic units (sub-UABT)
c)
4000 m
0 m
Penninic and Helvetic units (sub-UABT)
0 m
4000 m
d)
NW-SE
Grubhörndl
Oberalm Fm
Rhaetian Lst
Kössen Fm
Dachstein Lst
Plassen Lst
Schrambach Fm
Lower Cretaceous (marine clastics)
Plassen Lst (reef)
Oberalm Fm (pelagic/ turbiditc carbonates)
Upper Jurassic breccias
Red Jurassic limestone
Rhateian Lst (reef)
Kössen Fm (marls)
Dachstein Lst (lagoonal carbonates)
Hallstatt Lst (pelagic carbonates)
Wetterstein Lst (lagoonal carbonates)
Anisian dolomites
Werfen beds (clastics & carbonates)
Haselgebirge (evaporites & clastics)

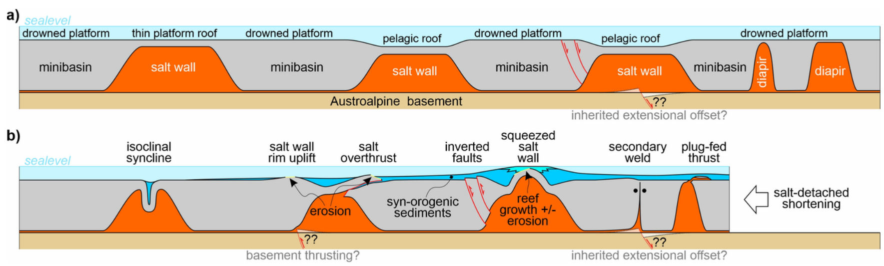
a)
sealevel
drowned platform
thin platform roof
drowned platform
pelagic roof
drowned platform
pelagic roof
drowned platform
minibasin
salt wall
minibasin
salt wall
minibasin
salt wall
minibasin
diapir
diapir
Austroalpine basement
??
inherited extensional offset?
b)
sealevel
isoclinal syncline
salt wall rim uplift
salt overthrust
inverted faults
squeezed salt wall
secondary weld
plug-fed thrust
erosion
syn-orogenic sediments
reef growth +/- erosion
salt-detached shortening
??
basement thrusting?
??
inherited extensional offset?

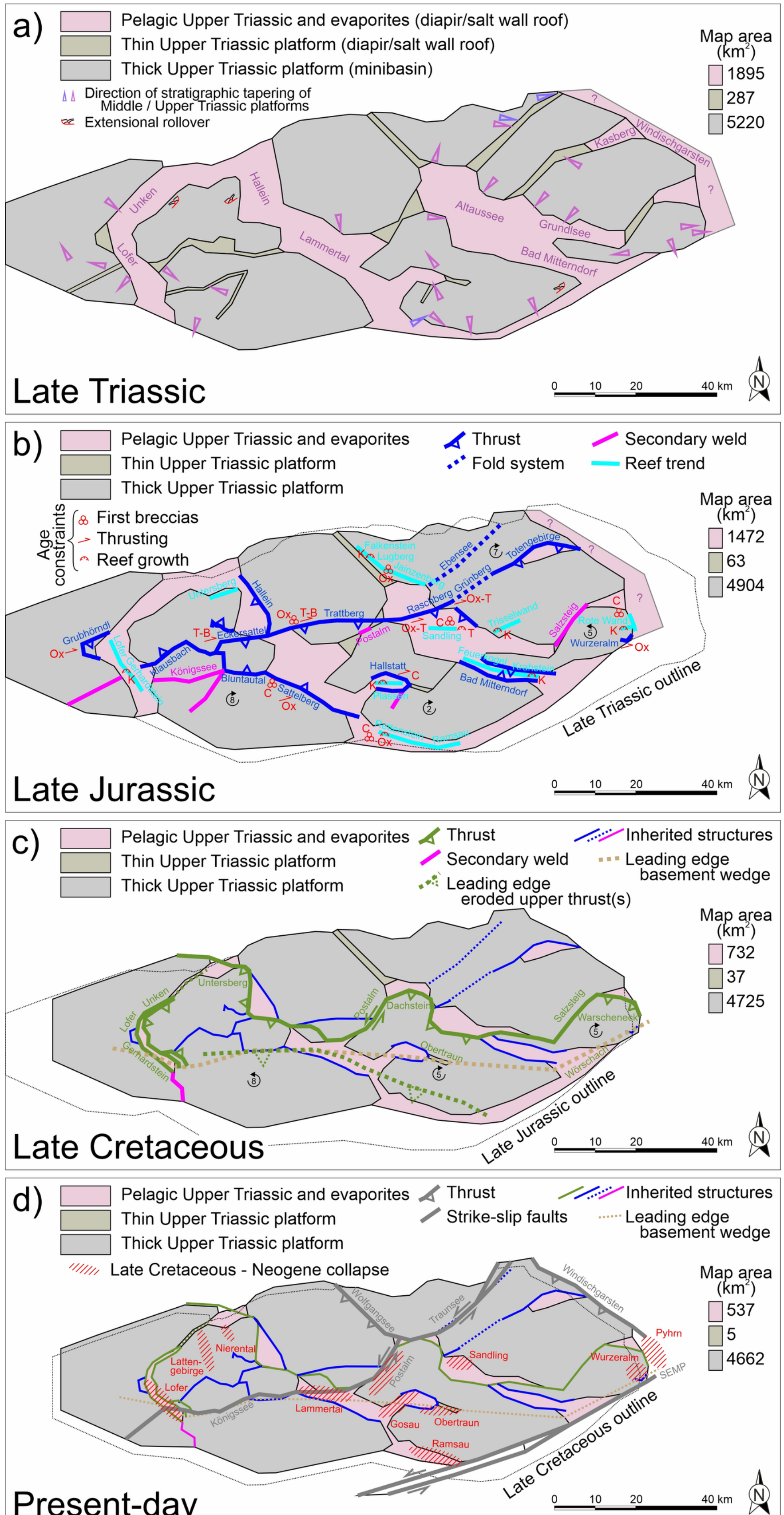
a)
Pelagic Upper Triassic and evaporites (diapir/salt wall roof)
Thin Upper Triassic platform (diapir/salt wall roof)
Thick Upper Triassic platform (minibasin)
Direction of stratigraphic tapering of Middle / Upper Triassic platforms
Extensional rollover
Map area (km²)
1895
287
5220
Unken
Hallein
Lofer
Lammertal
Altaussee
Grundlsee
Bad Mitterndorf
Kasberg
Windischgarsten
Late Triassic
0 10 20 40 km
N
b)
Pelagic Upper Triassic and evaporites
Thin Upper Triassic platform
Thick Upper Triassic platform
Thrust
Fold system
Secondary weld
Reef trend
Age constraints
First breccias
Thrusting
Reef growth
Map area (km²)
1472
63
4904
Late Triassic outline
Late Jurassic
0 10 20 40 km
N
c)
Pelagic Upper Triassic and evaporites
Thin Upper Triassic platform
Thick Upper Triassic platform
Thrust
Secondary weld
Leading edge eroded upper thrust(s)
Inherited structures
Leading edge basement wedge
Map area (km²)
732
37
4725
Late Jurassic outline
Late Cretaceous
0 10 20 40 km
N
d)
Pelagic Upper Triassic and evaporites
Thin Upper Triassic platform
Thick Upper Triassic platform
Late Cretaceous - Neogene collapse
Thrust
Strike-slip faults
Inherited structures
Leading edge basement wedge
Map area (km²)
537
5
4662
Late Cretaceous outline
Present-day
0 10 20 40 km
N

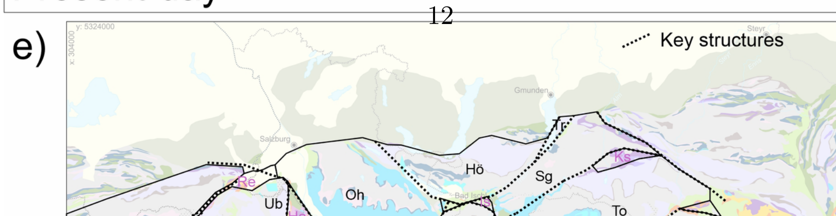
e)
Key structures

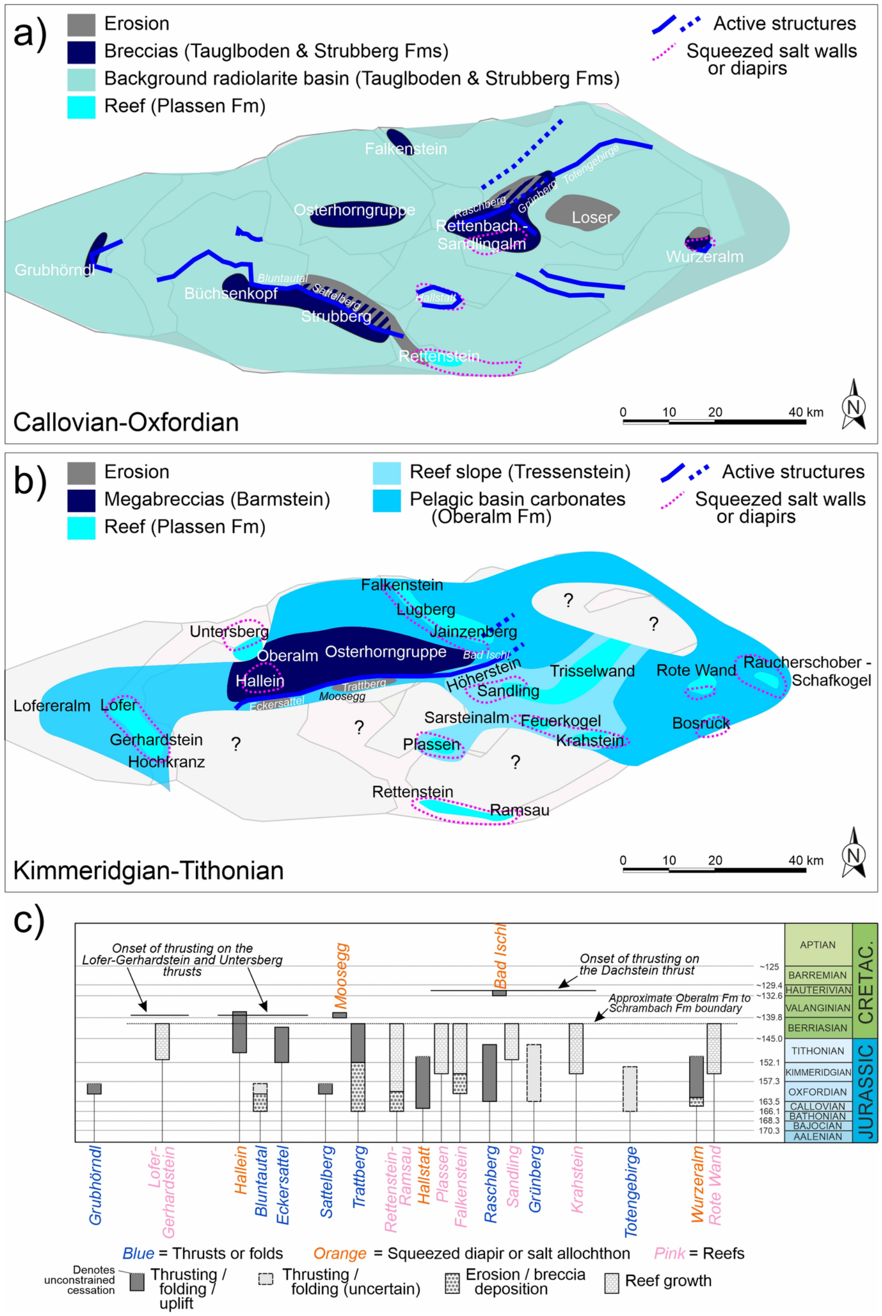
a)
Erosion
Breccias (Tauglboden & Strubberg Fms)
Background radiolarite basin (Tauglboden & Strubberg Fms)
Reef (Plassen Fm)
Active structures
Squeezed salt walls or diapirs
Falkenstein
Osterhorngruppe
Raschberg
Grünberg
Totengebirge
Rettenbach - Sandlingalm
Loser
Wurzeralm
Grubhörndl
Bluntautal
Büchsenkopf
Sattelberg
Strubberg
Rettenstein
Callovian-Oxfordian
0 10 20 40 km
N
b)
Erosion
Megabreccias (Barmstein)
Reef (Plassen Fm)
Reef slope (Tressenstein)
Pelagic basin carbonates (Oberalm Fm)
Active structures
Squeezed salt walls or diapirs
Falkenstein
Lugberg
Jainzenberg
Untersberg
Oberalm
Osterhorngruppe
Bad Ischl
Hallein
Höherstein
Sandling
Trisselwand
Rote Wand
Raucherschober - Schafkogel
Trattberg
Moosegg
Eckersattel
Lofereralm
Lofer
Gerhardstein
Hochkranz
Sarsteinalm
Feuerkogel
Krahstein
Plassen
Bosruck
Rettenstein
Ramsau
?
Kimmeridgian-Tithonian
0 10 20 40 km
N
c)
Onset of thrusting on the Lofer-Gerhardstein and Untersberg thrusts
Moosegg
Bad Ischl
Onset of thrusting on the Dachstein thrust
Approximate Oberalm Fm to Schrambach Fm boundary
~125
~129.4
~132.6
~139.8
~145.0
152.1
157.3
163.5
166.1
168.3
170.3
APTIAN
BARREMIAN
HAUTERIVIAN
VALANGINIAN
BERRIASIAN
TITHONIAN
KIMMERIDGIAN
OXFORDIAN
CALLOVIAN
BATHONIAN
BAJOCIAN
AALENIAN
CRETAC.
JURASSIC
Grubhörndl
Lofer-Gerhardstein
Hallein
Bluntautal
Eckersattel
Sattelberg
Trattberg
Rettenstein-Ramsau
Hallstatt
Plassen
Falkenstein
Raschberg
Sandling
Grünberg
Krahstein
Totengebirge
Wurzeralm
Rote Wand
Blue = Thrusts or folds
Orange = Squeezed diapir or salt allochthon
Pink = Reefs
Denotes unconstrained cessation
Thrusting / folding / uplift
Thrusting / folding (uncertain)
Erosion / breccia deposition
Reef growth

Architecture and Structure of a Fold-and-Thrust Belt During Initial Inversion of a Salt-Bearing Passive Margin (Jurassic of the Eastern Alps, Austria)

O. Fernandez[1] H. Ortner[2], W. E. H. Munday[3], M. Moser[4], D. Sanders[5], B. Grasemann[6], and T. Leitner[7]

[1] Dept. of Geology, Univ. of Vienna, Josef-Holaubek Platz 2, 1090 Vienna, Austria.

[2] Dept. of Geology, Univ. of Innsbruck, Innrain 52, 6020 Innsbruck, Austria.

[3] Dept. of Geology, Univ. of Vienna, Josef-Holaubek Platz 2, 1090 Vienna, Austria.

[4] Dept. of Geology, Univ. of Vienna, Josef-Holaubek Platz 2, 1090 Vienna, Austria.

[5] Dept. of Geology, Univ. of Innsbruck, Innrain 52, 6020 Innsbruck, Austria.

[6] Dept. of Geology, Univ. of Vienna, Josef-Holaubek Platz 2, 1090 Vienna, Austria.

[7] Salinen AG, Altaussee 139, 8992 Altaussee, AUSTRIA

Corresponding author: Oscar Fernandez (oscar.fernandez.bellon@univie.ac.at), ORCID: 0000-0003-1584-2684

Keywords:

Salt tectonics, Fold-and-thrust belt, Inversion, Passive margin, Eastern Alps

Key Points:

- Salt structures controlled the location of initial, Late Jurassic inversion of the salt-bearing Austroalpine margin.
- The style of deformation was controlled by supra-salt stratigraphic thickness and the lateral linkage of structures.
- Thrusting and squeezing of salt structures exerted a major control on the distribution of Late Jurassic depositional environments.

Abstract

Inversion of the Austroalpine Triassic salt-bearing passive margin, represented by the Northern Calcareous Alps (Eastern Alps), started in the Late Jurassic. Subsequent deformation during the Cretaceous and Cenozoic mostly preserved the Late Jurassic deformation fabric in the central Northern Calcareous Alps, making it an outstanding location to understand the early history of inversion of salt-bearing margins. Thrusting and folding in the central NCA during the Late Jurassic were strongly conditioned by the distribution of Triassic salt structures, the thickness of supra-salt stratigraphy, the lateral propagation of deformation, and the possible influence of sub-salt basement faults. Syn-orogenic sediments make it possible to reliably reconstruct the timing of structural inversion. The description of Late Jurassic structures presented here indicates that initial inversion of the Northern Calcareous Alps led to the development of coherent deformation systems that accumulated limited amounts of shortening, totaling few tens of kilometers. This differs from previous interpretations of Late Jurassic deformation of the area, that involve major amounts of allochthony (many tens of kilometers). As a specific example of coherent structural development, we present here an 80 km long linked system of thrusts and folds (the

Totengebirge–Trattberg contractional system), whose outstanding continuity has gone previously unrecognized. The anatomy of this system and its temporal evolution are described in detail and discussed in the framework of the Jurassic to recent evolution of the Eastern Alps.

Plain Language Summary

The Eastern Alps (Austria) are a mountain chain with a protracted history. Sedimentary rocks deposited in marine environments in the Northern Calcareous Alps (along the northern Eastern Alps) recorded the initial phases of mountain-building during the Jurassic, at a time that this area lay hundreds of meters below sea level. Multiple instances of submarine landslides preserved in rocks of Late Jurassic age (approximately 150 to 165 million years old) are the first indication of active faults and relief building in this area. As deformation and uplift progressed, the seafloor reached depths shallow enough for the development of reefs (that need sunlight to grow). This early phase of Alpine history was strongly controlled by the presence of salt diapirs (underground accumulations of rock salt and other evaporitic minerals), which determined what areas experienced the greatest uplift. Although indirect evidence for this phase of Alpine growth evolution has been previously put forward by other authors, this is the first time that specific structures relating to mountain-building are documented, and will require a rewriting of the history of the Alpine mountain chain.

1 Introduction

The impact of evaporite sequences (referred here onwards as *salt*) on the structural development of contractional systems has generated extensive research in recent years. Studies include analyses of the impact of pre-existing salt structures during shortening (e.g., Callot et al., 2012; Célini et al., 2020; Duffy et al., 2018; 2021; Rowan & Vendeville, 2006; Santolaria et al., 2021), the influence of salt detachment or sedimentary cover thickness on thrust development (Cotton & Koyi, 2000; Storti et al., 2007; Santolaria, Harris, et al., 2022), or the dynamics of salt in inverted rifts or passive margins (e.g., Ferrer et al., 2023; Granado et al., 2021; Santolaria, Granado, Wilson, et al., 2022). Some of these studies explore the 3D (cross-section and map pattern) expression of salt influence during contractional deformation, particularly using analog models (e.g., examples and references within Jackson & Hudec, 2017; or Célini et al., 2020; Cotton & Koyi, 2000; Duffy et al., 2018, 2020; Santolaria, Harris et al., 2022). In this contribution we explore the initial inversion of salt structures formed in a passive margin setting in the central Northern Calcareous Alps of the Eastern Alps (Austria).

The Northern Calcareous Alps (NCA) are a north-directed fold-and-thrust belt developed from Late Jurassic to recent times, related to the closing of the Meliata and Alpine Tethyan oceans (Fig. 1). Although the earliest published record of widespread subduction-related metamorphism in the Eastern Alps is of Late Cretaceous age (e.g., Miladinova et al., 2022), there is abundant evidence in the sedimentary record in the central NCA, in the form of breccias and mass transport deposits (MTDs), for significant convergence-related tectonism since the Middle to Late Jurassic (e.g., Faupl & Wagreich, 2000; Frisch & Gawlick, 2003; Gawlick et al. 1999, 2009; Gawlick & Missoni, 2015, 2019; Mandl, 2000; Missoni & Gawlick, 2011; Tollmann, 1987). Late Jurassic tectonics are also associated with rapid and very local shallowing of depositional environments led to the development of, mostly isolated, reefs (Mandl, 2000; Mandl et al., 2012; Tollmann, 1987). Late Jurassic deformation in the NCA is interpreted to relate to intra-oceanic subduction followed by obduction, documented hundreds of kilometers to the east in the Dinarides (Plašienka, 2018, Schmid et al., 2008).

It has been previously interpreted that Late Jurassic tectonics in the central NCA are associated to the gravitational emplacement of kilometer-sized bodies of Triassic limestones (known locally as *Gleitschollen*, or down-glided plates) onto deepwater Upper Jurassic sediments in the central NCA. These *Gleitschollen* have been interpreted to be olistoliths or MTDs (e.g., Tollmann, 1987; Braun, 1998; Mandl, 2000; Ortner et al., 2008) or part of an accretionary prism (e.g., Gawlick & Missoni, 2019) and in general requiring large amounts of displacement. Recently, however, Fernandez et al. (2024) and Kurz et al. (2023) have proposed a tectonic interpretation (as thrust sheets or salt allochthons) for some of these units, but description of these Late Jurassic structures remains patchy.

In this contribution we show that Late Jurassic tectonic structures are indeed widespread in the central NCA, and that they form structurally coherent shortening systems. We focus on an 80 km long structure that developed during this time, and whose regional character and age of development have not been previously fully recognized. Besides its outstanding length, comparable in size to that of major structures in other fold-and-thrust belts, this structure presents striking variations in structural style along its length that relate to the influence of pre-contractional salt structures and stratigraphic thickness variations.

This article aims to document this exceptionally well-preserved early Alpine structure and its associated syn-tectonic sedimentary record. Beyond the unique nature of this salt-related contractional structure, we document other Late Jurassic structures that conform coherent contractional systems of similar dimensions. Furthermore, we comprehensively document, for the first time, Late Jurassic tectonic contractional deformation in the Eastern Alps.

2 Geological setting

The Northern Calcareous Alps (NCA) are a morphotectonic unit of the Eastern Alps comprising Permo-Mesozoic stratigraphy. The NCA are almost entirely decoupled from their Austroalpine (Adria) basement and are imbricated and thrust northwards on the UABT (Upper Austroalpine Basal Thrust) onto imbricated Penninic ocean and European margin units (Fig. 1). The NCA stratigraphy developed initially on a Tethys-facing passive margin, up to the Middle Jurassic. From the late Middle Jurassic, the NCA were involved in Alpine orogenesis, which reached its peak in the Cretaceous to Cenozoic. Of particular interest in this contribution are the central segment of the NCA (Fig. 2), an area characterized by widespread Jurassic basins that provide a tectono-sedimentary record for the earliest stage of Alpine orogenesis (Gawlick et al., 1999, 2009).

2.1 Structure

The central NCA are internally imbricated into 4 main thrust-bounded units. From north to south (and footwall to hangingwall) these are the Langbathsee, the Höllengebirge, the Totengebirge and the Dachstein thrust sheets (Figs. 1b, 2) (Fernandez et al., 2024). These thrust sheets correlate to tectonic units traditionally referred to as the Bajuvaric (Langbathsee), Tirolic (Höllengebirge–Totengebirge) and Juvavic (Dachstein) thrust systems (e.g., Tollmann, 1976; Mandl, 2000). Herein, the individual thrust sheet names are used.

Internal imbrication along the Dachstein and Höllengebirge low-angle thrusts during Cretaceous to Paleocene times has been previously documented and discussed (e.g., Fernandez et al., 2024; Levi, 2023; Mandl, 2000; Ortner & Kilian, 2022; Strauss et al., 2023). The Paleogene and older structures in the central NCA are partly offset by younger (Neogene) strike-slip faults and high-angle thrusts (e.g., Königssee, Traunssee, Wolfgangsee, Windischgarsten) (Linzer et al., 1995;

Peresson & Decker, 1997). Although the Cretaceous to Neogene structures locally accumulate many kilometers of displacement, they have not significantly distorted the Late Jurassic structure of the central NCA (Fernandez et al., 2024).

Jurassic structures in the central NCA have been documented to date as isolated features: the Trattberg (Ortner, 2017), the Sattelberg, Raschberg and Bad Mitterndorf thrusts (Fernandez et al., 2024), the Wurzeralm allochthon (Kurz et al., 2023) (Fig. 2). However, map-scale blocks of Triassic rocks that rest on Middle to Upper Jurassic sediments, previously interpreted to have a non-tectonic origin (as *Gleitschollen*), are widespread (e.g., the Hoher Göll, Schwarzer Berg, Sattelberg, Gerhardstein, Altaussee; Fig. 2) (Braun, 1998; Gawlick & Missoni, 2015, 2019; Mandl, 1982, 2000; Mandl et al., 2012; Plöchinger, 1997; Tollmann, 1987). The re-interpretation of some of these *Gleitschollen* as tectonic salt-related structures (Fernandez et al., 2024) underscores the need for a comprehensive review of Jurassic tectonics in the area.

Likewise, one of the key structures in the central NCA, the Totengebirge thrust (Fig. 2), has been interpreted to be Cretaceous in age (Linzer et al., 1995) based purely on geodynamic assumptions. This thrust, however, correlates along strike with the Grünberg syncline and Ahornkogel-Brunnkogel anticline (Spengler, 1924; Ganss, 1937; Mandl, 2013; Tollmann, 1976; 1985) (Fig. 2), two structures that are associated to a major Late Jurassic depocenter (Gawlick et al., 2007; Mandl et al., 2012).

2.2 Tectonostratigarphy

The stratigraphy in the NCA, from Permian to Cretaceous, is summarized by Faupl and Wagreich (1992), Gawlick et al. (2009) and Mandl (2000), and its nomenclature synthesized by Piller et al. (2004). It is illustrated schematically in Fig. 3 and described below.

The oldest strata in the central NCA are a thick succession of Permian to Lower Triassic clastics (Präbichl Fm and Werfen beds) and evaporites (Haselgebirge). This succession, in particular the evaporitic member, was many hundreds of meters thick, allowing for the widespread development of salt-related structures (Leitner & Spötl, 2017; Strauss et al., 2023; Fernandez et al., 2024). The Lower Triassic is followed by a Middle Triassic succession of relatively thin (under 200 m, locally absent) Anisian limestones and dolomites (Gutenstein and Steinalm Fms) above which developed the Ladinian to Carnian Wetterstein Limestone (Lst) platform (up to 1500 m). Carbonate production was greatly reduced during the Carnian pluvial event (Schlager & Schöllnberger, 1974). Deposits during this period are relatively thin (under 200 m, often absent) and include clastics, evaporites and shallow water carbonates. During the Late Carnian, carbonate platform development restarted, leading to the deposition of the thick Carnian to Norian Dachstein Lst and Hauptdolomit lagoonal and reefal carbonates (up to 1500 m). Platform development is capped by the development of intra-platform Kössen Fm basins and isolated carbonate platforms and reefs of Rhaetian age, that were drowned at the end of the Triassic (Gawlick et al., 1999; Schlager & Schöllnberger, 1974).

Synchronous with Triassic platform growth, subsiding diapiric structures within the NCA platform domain (cored by Haselgebirge) led to the localized development of deeper (pelagic) water conditions (Fernandez et al., 2024; Strauss et al., 2021). In these areas deep water equivalents of the Ladinian-Rhaetian platforms deposited: allodapic slope limestones (Ladinian Raming Lst and Norian Pötschen Lst) and pelagic marls, limestones, and marly limestones (Ladinian Reifling Fm and Norian Hallstatt Lst). The Norian Hallstatt and Pötschen Lsts interfingered with the carbonatic turbidites and marls of the Zlambach beds, whose deposition stretched into the Rhaetian. The Triassic basinal successions are significantly thinner than their platform equivalents, reaching a total maximum thickness of around 500 m.

The Zlambach beds grade upwards into the Lower Jurassic Allgäu Fm (Mandl et al., 2012). Coevally and lasting into the Middle Jurassic, condensed red limestones (Hierlatz Lst, Adnet Fm and Klaus Fm, meters to few tens of meters thick) deposited on the drowned Triassic platforms and represent a marked deepening of the NCA basin. Breccias, syn-faulting sediments, and slope instability, likely related to the opening of the Alpine Tethys, are documented locally in the central NCA (Böhm et al., 1995; Garrison & Fischer, 1969; Krainer et al., 1994).

A major change occurs in the late Middle Jurassic, with the onset of radiolaritic deposition (Gawlick et al., 1999; 2009). Siliceous limestones and marls, cherty limestones, cherts, breccias and MTDs with a radiolaritic matrix conform the Tauglboden and Strubberg Fms (Gawlick et al., 2007; Mandl, 2013). Gawlick et al. (2009) (in contrast to Piller et al., 2004) grouped the Tauglboden and Strubberg Fms under the Ruhpolding Radiolarite. This unit grades upwards into or is unconformably overlain by the Upper Jurassic Oberalm Fm (Gawlick et al., 2007; Mandl et al. 2012; Mandl, 2013; Ortner et al., 2008). The Oberalm Fm is a succession of pelagic marls and limestones, calciturbidites, and thick banks of resedimented carbonates (the Barmstein Limestone) (Garrison, 1967; Gawlick et al., 2005). In the shallower waters of the Upper Jurassic basin, reefs of the Plassen Lst developed coeval with the Oberalm Fm. The Oberalm Fm in the study area is capped in its more proximal domain by relatively thick (meters to tens of meters), relief-forming banks of allodapic carbonates that are referred to here informally as the Tressenstein Lst (Mandl, 2013; Schäffer, 1982). The entire Middle to Upper Jurassic succession varies from being absent to up to nearly 1000 meters thick.

Deposition of the Plassen Lst and Oberalm Fm lasted into the earliest Cretaceous and was gradually replaced by the deep-water, marl-dominated Berriasian to Hauterivian Schrambach Fm (Decker et al., 1987; Faupl & Wagreich, 1992; Rasser et al., 2003). This unit is overlain by the Rossfeld Fm, a succession of turbiditic sandstones, polymictic breccias and shales whose deposition lasted into the Aptian (Decker et al., 1987; Faupl & Wagreich, 1992; Krische et al., 2014). The Schrambach and Rossfeld Fms and their temporal equivalents record the imbrication of the Dachstein, Höllengebirge and Langbathsee thrusts. This deformation is partly sealed by strata of the Upper Cretaceous to Paleogene Gosau Gp, a thick assemblage of continental to marine sediments that infilled pre-existing topography (Wagreich & Faupl, 1994; Sanders, 1998). The Gosau Gp itself deposited in a complex tectonic setting as the NCA units decoupled from their underlying basement and thrust forwards, leading to complex subsidence patterns with ongoing deformation (Ortner, 2001; Ortner et al., 2016; Wagreich & Decker, 2001; Wagreich & Faupl, 1994).

There is a very limited sedimentary record of final stages of Alpine deformation (Neogene) in the central NCA.

3 Middle to Late Jurassic deformation in the central NCA

As stated above, Middle to Late Jurassic structures have been previously documented in the central NCA. We therefore do not aim to describe most of these structures in detail but will focus on the criteria for determining the ages of the structures, the nature of syn-tectonic sedimentation, and, most importantly, on understanding the relationships between these structures.

3.1 Stratigraphic record of Jurassic deformation

The onset of convergence-related deformation in the central NCA can be documented locally to coincide with the onset of deposition of the Middle to Upper Jurassic Tauglboden and Strubberg Fms based on onlapping relationships (Fig. 4b). Below them, the Lower Jurassic mainly infilled pre-contractional topography at the top of the Triassic platform (Fig. 4a) or is interpreted to have deposited in an extension-dominated system (Böhm et al., 1995; Krainer et al., 1994). Erosion of the Triassic platforms underlying the Tauglboden or Strubberg Fms was commonplace and leads to the frequent omission of significant portions of Jurassic and Triassic stratigraphy (Fig. 4c,d). Erosion of the Triassic platforms and Lower Jurassic sediments resulted in the frequent emplacement of deca- to hectometric-sized olistoliths and breccias within the Middle to Upper Jurassic Strubberg, Tauglboden and Oberalm Fms (Fig. 5). The contact at the base of multiple olistoliths (placing Triassic rocks on Jurassic rocks) have been previously documented by several authors (Braun, 1998; Fernandez et al., 2024; Garrison & Fischer, 1969; Gawlick & Missoni, 2015, 2019; Mandl, 1982, 2013). The abundance of olistoliths have led some authors to interpret all of the Triassic-on-Jurassic contacts to be of sedimentary nature, including those relating to map-scale blocks of Triassic (interperted to be *Gleitschollen*). However, many instances of Triassic blocks overlying Jurassic are in fact due to thrusting, as will be discussed below (see also discussion in Fernandez et al., 2024).

3.2 The Totengebirge–Trattberg (TT) contractional system

The main focus of this paper is a system of structures that extends from the Totengebirge in the east, to the Trattberg and Hoher Göll in the west (Fig. 2). The structures in this system, the Totengebirge–Trattberg (TT) system, run roughly parallel to and south of an E-W trending depocenter of Middle to Upper Jurassic syn-orogenic Tauglboden and Oberalm Fms. This makes the TT system and ideal set of structures for analyzing syn-tectonic relationships.

The TT system can be subdivided into two segments based on their interruption in outcrop by the Dachstein thrust sheet (Fig. 2) that was thrust onto the TT system in the Early Cretaceous (Fernandez et al., 2024; Levi, 2023). The eastern segment of the TT system runs from the Windischgarsten fault system to the Altaussee area. The western segment runs along the Trattberg and west, to the Hoher Göll.

3.2.1 Structure of the eastern segment of the TT contractional system

A detailed geological map of the eastern segment of the TT contractional system can be seen in Figure 6. In this segment, the system changes from being a major E-W trending thrust along its NE half (from the Windischgarsten fault system to the Offensee) to a system of NE-SW trending anticlines and synclines along its SW half (from the Offensee to the Dachstein thrust).

The easternmost part of the TT contractional system is represented by the Totengebirge thrust (Fig. 6). This thrust terminates in the east in the Windischgarsten fault system (of Tertiary age) and has no known continuation beyond that fault system (Linzer et al., 1995; Peresson & Decker, 1997; Tollman, 1976). The Totengebirge thrust is best exposed in the Kasberg (Fig. 7). Here the thrust places the Gutenstein Fm on the uppermost Hauptdolomit (equivalent of the Dachstein Lst) in a flat-on-flat configuration. Transport on the Totengebirge thrust at Kasberg has been interpreted to be NW-directed based on fault striations (Linzer et al., 1995). In this direction, shortening on the thrust is over 10 km. However, shortening estimated on a N-S cross-section yields only 7 km of shortening (Fernandez et al., 2024). Although no direct indications for north-directed thrusting in the form of kinematic indicators have been documented, the footwall ramp of the Totengebirge thrust strikes roughly E-W to ENE-WSW (Fig. S2), possibly implying that thrusting was indeed north-directed. NW-directed oblique thrusting above such a ramp might be expected to generate greater internal deformation (in the form of tear-faulting) in the hanging wall than is observed in the field (Fig. 6).

The Reifling Fm in the hanging wall of the Totengebirge thrust at Kasberg is under 200 m thick, in strong contrast to the nearly 2000 m thick equivalent Wetterstein Lst to the south (Fig. 7a). The Upper Triassic above the Reifling Fm of the Kasberg is completely absent, due to erosion, but potentially was also thin and represented by basinal facies as Middle and Upper Triassic basins often coincide in the central NCA (Fernandez et al., 2024; Mandl, 2000). Below the Totengebirge thrust, the Hauptdolomit (Dachstein Lst) is the youngest unit, implying a post-Triassic age for thrusting.

The Totengebirge thrust extends westward to the Offensee, where it terminates (Fig. 6, Fig. S3a). Shy of its termination, east of the Offensee, the Totengebirge thrust brings the Wetterstein to rest on the Hauptdolomit, in a ramp-on-ramp configuration (Fig. S3a). This ramp-on-ramp configuration implies the displacement on the thrust has not exceeded the stratigraphic thickness of the Wetterstein–Hauptdolomit succession (less than 4 km in the Totengebirge unit; Fig. 8a). Across the Offensee, shortening related to the Totengebirge thrust is relayed into a system of two vertical isoclinal synclines, the Ariplan and Grünberg synclines (Ganss, 1937; Spengler, 1924). Both synclines are cored by Upper Jurassic Tauglboden Fm overlying the Lower Jurassic and a highly thinned Dachstein Lst (under 200 m thick) (Fig. 8a) (Fig. S4a,c). Flanking the Grünberg syncline on the southeast, the Ahornkogel–Brunnkogel anticline presents a major stratigraphic expansion in the Dachstein Lst associated to a salt-floored extensional rollover (Fig. 8, Fig. S4a,b). The extensional rollover is at present strongly overturned, in part due to contractional deformation. Shortening in the Offensee area is estimated to be slightly over 4 km (Fig. 8b).

The Grünberg syncline and the Ahornkogel–Brunnkogel anticline can be followed from the Offensee southwestward (Mandl, 2013) (Fig. 6). The Grünberg syncline broadens progressively to the SW and is infilled by Upper Jurassic sediments (Tauglboden and Oberalm Fms) (Fig. 9a). At the Karbach (Figs. 6, 9a), the TT contractional system is formed by a set of isoclinal anticlines and synclines (Figs. 5c, 9a) (Fig. S4a,b) similar to those in the Offensee. There is no evidence for units older than the Dachstein Lst being involved in folding. Within the folds, the Dachstein Lst is observed to be significantly thinner than in the surrounding areas, going from around 1500 m in the Raucherkar and Singereben down to under 200 m of thickness in the Karbach (Fig. 9a). Along the Raucherkar, folding in the Dachstein Lst is gentler and the Dachstein Lst dips steeply to the SW (Fig. S4c), plunging in under a major Upper Jurassic depocenter that is partly fault-bounded (Fig. 6, Fig. 9a, Fig. S4a,b). Shortening across the TT system in the Karbach is estimated to be around 4 km (Fig. 9b), although uncertainty in the interpretation at depth imply this value could be up to 1 km greater or smaller.

The structure south of the TT contractional system and the Raucherkar folds is dominated by extensional faults that bound the Mt Loser block (Fig. 9a) (Fig. S4a,b). Some faults on the southern side of the Mt Loser are originally of Triassic age (Fig. 9b) and are associated to deepening of the depositional water depth in their hanging wall (Fig. S4d). These faults were re-activated during the Jurassic, causing tilting of the Dachstein Lst (Fig. 9a) (Fig. S4e) and generating accommodation space in the Trisselwand (Fig. 9a).

Southwest of the Karbach–Raucherkar, isoclinal folding of the Dachstein Lst is replaced by thrusting of the pelagic Upper Triassic Hallstatt Lst onto the lagoonal Dachstein Lst (Fig. 10b). At this location, the TT contractional system becomes mostly buried by syn-tectonic Upper Jurassic sediments (Fig. 10a,b). North-directed thrusts transport vertically dipping Oberalm Fm

(Upper Jurassic) in their hanging wall (Fig. 10a) (Fig. S5). The thrusts are sealed by the Tressenstein Lst (uppermost Upper Jurassic) that also discordantly overlies the vertical hanging wall strata (Fig. S5). These thrusts dip to the south and are interpreted to merge into a single thrust (called here the Raschberg thrust) that is rooted in the Altaussee diapir and carries in its hanging wall a condensed Triassic basinal succession (Fig. 10b). The Middle to Upper Jurassic Tauglboden and Oberalm Fms onlap the uplifted basinal units of the Hoher Raschberg (Fig. 10a,b). Thrust-related uplift and folding raised the Hoher Raschberg units from their original deep-water setting during the Late Triassic and Early Jurassic (Fig. 10c) into the photic zone, allowing for the development of the Mt Sandling Plassen Lst reef.

The position of the footwall cutoff to the Raschberg thrust is not observed in outcrop or in mine galleries. However, the contrast in facies between the hanging wall Upper Triassic Hallstatt Lst and its footwall equivalent, the lagoonal Dachsetin Lst, provides a minimum constraint for displacement. Kenter and Schlager (2009) documented that the transition between lagoonal Dachstein Lst and Hallstatt Lst requires in the order of 2 km horizontal distance, which would be an absolute minimum for offset on the Raschberg thrust. The interpretation in Figure 10 implies roughly 4 km of total shortening.

3.2.2 Structure of the western segment of the TT contractional system

West of the Hoher Raschberg, the TT contractional system was thrust over by the Dachstein thrust sheet in Early Cretaceous times (Fernandez et al. 2024; Levi, 2023). The Dachstein thrust sheet rests in a flat-on-flat situation on the underlying Tressenstein Lst (that seals deformation of the TT contractional system). The Jodschwefelbad borehole (Fig. 6; Mandl et al., 2012) shows that syn-TT Upper Jurassic sediments are thin in the footwall of the Dachstein thrust, indicating that the Upper Triassic experienced Late Jurassic uplift in the current footwall of the Dachstein thrust sheet.

The Dachstein thrust sheet and its footwall collapsed along the NW-SE trending Postalm fault (Figs. 2, 11). The age for this collapse post-dates the Early Cretaceous emplacement of the Dachstein thrust sheet, and most likely occurred due to the evacuation of Permo-Triassic evaporites (as proposed for the Gosau basin by Fernandez et al., 2022). The TT contractional system resurfaces in the footwall of the Postalm fault (to its west).

A detailed geological map of the western segment of the TT contractional system can be seen in Figure 11. The western segment of the TT contractional system can further sub-divided into two segments, as the system is partly displaced by the Cretaceous Untersberg–Dachstein thrust (Fig. 11). In the east, along the Trattberg portion, the the TT system is dominated by high angle reverse faulting (Ortner, 2017) (Fig. 12) (Fig. S6). The structure is dominated by the highly continuous Trattberg thrust whose growth is recorded by progressive unconformities in the footwall Oberalm Fm and mass wasting of the Triassic limestones in the hanging wall (Ortner, 2017) (Fig. 12). The thrust of the Trattberg has been reworked, at least partially, as an extensional fault during the Cretaceous but has mostly retained its reverse throw (Fernandez et al., 2024; Ortner, 2017) (Fig. 12). Even though the Triassic succession in the area thins to the south (Fig. 12) (Fernandez et al., 2024), deformation of the TT system concentrated on the Trattberg thrust, that cuts through a relatively thick portion of the Triassic succession. This contrasts with the Raschberg and Totengebirge thrusts (Figs. 7, 10) that cut through areas of relatively thin Triassic stratigraphy. One possible explanation for this difference could be that the Trattberg thrust is an inversion structure, reactivating a syn-depositional extensional fault. Syn-depositional Triassic faults in the carbonate platforms are observed south of the Mt Loser (Fig. 9b) and, possibly, south of the Trattberg (Fig. S9).

Along the eastern segment of the Trattberg thrust (presumably extending under the Dachstein thrust sheet) Jurassic shortening is also taken up by the Einberg thrust (Fig. 11). Towards the west, the Trattberg thrust is buried by the syn-orogenic Oberalm Fm, which is folded above it (Ortner, 2017) (Fig. 11). It is possible that Jurassic shortening in this direction is also partly taken up by the Schwarzerberg thrust (Fig. 11), as indicated by deformation structures within the Oberalm Fm in its footwall (Plöchinger, 1979).

Uplift related to the Trattberg thrust reappears west of the Salzach river valley. Here, the Eckersattel thrust (Fernandez et al., 2024), was responsible for uplifting the Dachstein Lst of the Hoher Göll mountain (Figs. 11, 13) (Fig. S7). Uplift is recorded by the erosive truncation of the Dachstein Lst in the northern flank of the Hoher Göll and its onlap by beds of the Oberalm Fm (Fig. S7) (Braun, 1998; Fernandez et al., 2024). At present, the Dachstein Lst of the Hoher Göll is tilted to the north due to the entire block being also partially backthrust along the Bluntautal thrust (Fig. 13) and deformation related to the Untersberg–Dachstein thrust. The Bluntautal backthrust places the entire Triassic stratigraphy of the Hoher Göll onto a north-dipping panel of Triassic and Middle Jurassic stratigraphy (the Hagengebirge block, Fig. 13). The Hagengebirge block in the footwall of the Bluntautal thrust is cross-cut by the left-lateral Königssee fault (Decker et al., 1994), a structure that has its origin as a Triassic-age salt structure (Fernandez et al., 2024).

To the west, both the backthrust of the Bluntautal and the (blind) Eckersattel thrust come together along the western margin of the Hoher Göll mountain (Fig. 11) (Fig. S7). Here, the Triassic of the Hoher Göll is observed to have been emplaced onto the Oberalm and Strubberg

Fms (Fig. 11) (Fig. S7). Along this western margin of the Hoher Göll, a north-dipping panel of Triassic is offset by a roughly E-W trending extensional fault (Fig. 13) that likely developed above a pre-existing diapir prior to or synchronous with Jurassic thrusting.

3.3 Other Jurassic contractional structures in the central NCA

Although this contribution lays particular emphasis on the TT contractional system, this is not the only Late Jurassic contractional feature documented in the area. South of the TT system, Late Jurassic structures span the entire study area from west to east (Fig. 2).

Contraction-driven allochthony of salt in the Hallstatt and Wurzeralm diapirs and in the Bad Mitterndorf area has been documented by Fernandez et al. (2021), Kurz et al. (2023), and Fernandez et al. (2024). The Hallstatt diapir recorded approximately 4 km of N-S shortening (Fig. 14), the Bad Mitterndorf structures are estimated to have shortened by around 10 km (Fernandez et al., 2024), and the Wurzeralm is interpreted to have experienced much more limited amounts of shortening (in the order of 1-2 km based on the work of Kurz et al., 2023).

Despite the disparity in shortening magnitudes, shortening in the three cases involved the salt-related uplift of condensed Triassic stratigraphy and the build-up of isolated Upper Jurassic (Plassen Lst) reefs atop the squeezed diapirs, similar to the reef developed above the Altaussee diapir (Fig. 10). After widespread deepening of the NCA during the Early to Middle Jurassic, Jurassic shortening of salt structures was required to locally raise the seafloor into the photic zone and allow for isolated reef development (Kurz et al., 2023; Tollmann, 1987).

In analogous manner, the Upper Jurassic reefs of the Rettenstein (Auer et al., 2009; Neubauer & Moser, 2022), Ramsau (Mandl & Matura, 1995; Mandl et al., 2014) (Fig. 2) (Figs. S8, S9), and of the Gerhardstein-Lofer (Mosna, 2010; Pavlik, 2006; Sanders et al., 2007) (Fig. 2) are interpreted to mark the presence of salt walls also shortened in the Late Jurassic.

The Hallein diapir, which lies north of the TT contractional system (Figs. 2, 11), also experienced salt allochthony in the Late Jurassic, with Haselgebirge evaporites at present resting sandwiched within beds of the Oberalm Fm (Plöchinger, 1977, 1984, 1990; Schauberger, 1972) (Fig. 15). The direction of Jurassic allochthonous salt emplacement in this case is less well constrained as in the previous examples as the precise location of the feeding salt stock is unknown, but was likely N to E directed. Posterior deformation of the allochthonous salt during the Early Cretaceous was east directed to northeast, as inferred from folding of the Oberalm Fm and growth geometries in the Schrambach and Rossfeld Fms (Figs. 11, 13). Immediately west of the Hallein diapir, Jurassic shortening also led to the development of the south-directed Rabenstein thrusts (Fig. 2) (Fig. S10).

In the westernmost part of the study area a further isolated Jurassic thrust (the Grubhörndl thrust) is present (Figs. 2, 16). The Grubhörndl thrust, previously interpreted as an olistolith (Ortner et al., 2008), is interpreted here as a thrust transporting a thin (supra-diapir) Upper Triassic in its hanging wall. The origin of this unit as an olistolith, as proposed by Ortner et al. (2008), requires the presence of a major W-facing extensional fault of Late Jurassic age with exposed footwall (Ortner et al., 2008) which hasn’t been documented to date (despite the presence of extensional Early and Late Jurassic faults in the area; Krainer et al., 1994; Ortner et al., 2008). Jurassic breccias constrain the time of emplacement of this thrust sheet (Ortner et al., 2008). This unit was posteriorly thrust over in the Early Cretaceous by the Gerhardstein units (Fig. 16c) and later collapsed in extension into its present-day geometry (Fig. 16b).

As opposed to the isolated nature of the structures described above, the Klausbach–Bluntautal–Sattelberg thrusts (Fig. 2), running along the western half of the study area and south of the TT contractional system, represent a second hard-linked contractional system. At its westernmost end, this system is represented by the Klausbach thrust (Fig. 2), which placed the Triassic platform of the Reiteralm southeastward onto that of the Watzmann (Fig. S10). The Klausbach thrust transitions eastward into the Bluntautal thrust (Fig. S10). The Bluntautal backthrust can in turn be correlated eastward to the Sattelberg backthrust (Fernandez et al., 2024) (Figs. 2, 11). The Sattelberg thrust sheet (Fig. S11) and other, associated, minor imbricates have been interpreted by some authors to represent olistoliths and breccias re-sedimented during Jurassic tectonism (Gawlick and Missoni, 2015, 2019). Although the dimensions of the bodies are compatible with those of large slides (Woodcock, 1979), the overall coherent arrangement (i.e., along-strike continuity of the structures for over 10 km with stratigraphically upright bedding) and the consistent indications for south-directed emplacement (Cornelius and Plöchinger, 1952; Fernandez et al., 2024; Häusler, 1979; Tollmann, 1975) make their interpretation as south-directed thrusts the most reasonable interpretation. Fernandez et al. (2024) provide an estimate of over 5 km of N-S shortening on these structures.

The Sattelberg backthrust has only been traced to the eastern end of the Tennengebirge (Fig. 2). There it enters an area dominated by the outcrop of the Lower Triassic Werfen beds and Anisian carbonates (Fig. 2) deformed by north-directed thrusts and north-vergent folds (Mostler & Roßner, 1977; Neubauer & Genser, 2018; Roßner, 1972). It is unclear if backthrusting on the Sattelberg thrust is relayed into these structures or dies out in this direction.

4 Discussion

4.1 Early inversion of a salt-bearing rifted margin

Jurassic contractional structures in the central NCA are the result of the initial inversion of the Triassic Austroalpine rifted margin (Fig. 17). Jurassic structures nucleated along pre-existing Triassic-age salt structures, whose initial layout can be mapped based on the presence of thickness and facies changes in the Middle to Upper Triassic succession (Fernandez et al., 2024). The NCA at Late Triassic times comprised minibasins developed above evacuating Permo-Triassic salt and that accumulated 2-4 km thick platform carbonates (Wetterstein and Dachstein–Hauptdolomit platforms). The minibasins were areas of shallow water separated by embayments in which coeval condensed pelagic carbonates (<500 m thick) deposited above subsiding salt walls or diapirs (Fig. 17a). Some salt walls (e.g., Figs. 8, 9) were covered in the Late Triassic by thin platform carbonate rooves (<200 m in thickness) (Fig. 17a). The Triassic margin subsided significantly in the Early Jurassic, drowning out platform growth (Schlager & Schöllnberger, 1974) and leaving the seafloor hundreds or over a thousand meters deep (as illustrated in Fig. 17a) (see Kurz et al., 2023 for a discussion on water depth estimates.

Jurassic shortening structures conform a complex system of thrusts, folds, and squeezed salt walls, that spans the entire central NCA from west to east (Fig. 18). The Jurassic-age structures occur both as hard-linked systems (the TT and Klausbach–Bluntautal–Sattelberg systems) and as more isolated features. All Jurassic structures developed along pre-existing salt structures (diapirs and walls) or areas of thin (<0.5 km) Triassic stratigraphy, except for the Eckersattel and Trattberg thrusts, which cut across relatively thick (>1 km) Triassic. The initial phase of Jurassic inversion led to the re-activation (at least partial) of all the existing salt features in the area (Fig. 18b).

The structures that developed during the initial stage of inversion (Figs. 17b, 18b) can be grouped into 6 main types:

1) Salt overthrusts (*sensu* Jackson & Hudec, 2017), where salt walls were shortened and displaced along with their rooves into thrusts travelling multiple kilometers (Totengebirge, Raschberg, Eckersattel, Bluntautal, Sattelberg, Bad Mitterndorf, and Grubhörndl thrusts; Figs. 7, 10, 13, 16; Fig. S11).
2) High-angle thrusts, likely re-activating Triassic-age extensional faults (Trattberg thrust, Schönau thrust, Kuchlberg fault; Fig. 12; Figs. S10, S11).
3) Systems of synclines and anticlines developed in thin Triassic successions that originally overlay salt walls (Grünberg and Ariplan synclines, and Bärnkogel and Ahornkogel-Brunnkogel anticlines; Figs. 8, 9).
4) Plug-fed thrusts (*sensu* Jackson & Hudec, 2017), where salt extruded from diapirs transporting their rooves passively (Hallstatt, Hallein, Wurzeralm; Figs. 14, 15; Kurz et al., 2023).
5) Squeezed salt walls for which no salt allochthony is known but uplift was sufficient to raise the bathymetry into the photic zone as recorded by the growth of Upper Jurassic reefs (Gerhardstein-Lofer, Rettenstein, Ramsau; Figs. S8, S9). In some instances, squeezing of the salt wall led to the uplift of the flanking minibasin margin (rim uplift), such that the reef developed on the minibasin margin as well as above the rising salt stock/wall (Kurz et al., 2023) (Wurzeralm, Lugberg, Falkenstein; Fig. 17b).
6) Secondary welds (welds of salt walls or diapirs) without the development of significant bathymetric relief (or at least with a lack of recorded uplift). An example of such a weld

is the Echerntal weld documented by Fernandez et al. (2021) near Hallstatt and Königssee weld (discussed by Fernandez et al., 2024).

Many of these structures are associated to the rapid and localized uplift of the seafloor from bathyal depths into the photic zone which enabled the growth of Upper Jurassic reefs (e.g., Fernandez et al., 2021; Kurz et al., 2023). The isolated nature of Upper Jurassic reefs across the entire central NCA (Fig. 18b) indicates that bathymetry remained mostly sub-neritic away from the growing structures, indicating no widespread uplift or stacking of tectonic units occurred. The development of isolated structures without the growth of a well-developed orogenic wedge can be explained by the presence of a well-connected and highly efficient basal detachment in the Permo-Triassic salt. Analogue models indicate that contractional systems can develop with a very subdued taper geometry (in cross-section) and fast forelandward propagation of the deformation in the presence of continuous evaporite detachments (Pla et al., 2019; Santolaria, Granado, Carrera, et al., 2022; Santolaria, Granado, Wilson, et al., 2022). Notwithstanding the low taper angle, significant coeval uplift and unroofing occurring in more southerly (?) positions is required to account for the inflow of detrital ophiolitic material in the Late Jurassic (e.g., Steiner et al., 2021; Drvoderic et al., 2023).

Sliding of the Triassic Wetterstein–Dachstein minibasins along the evaporitic basal detachment are interpreted to have led to the vertical-axis rotation of some minibasins (Fig. 18b), a feature indicative of a thick basal detachment during shortening (Duffy et al., 2021; Santolaria, Granado, Carrera, et al., 2022). The amounts of vertical-axis rotation required for the map restoration (Fig. 18) are well within the magnitude range documented for younger block rotations by Pueyo et al. (2007).

Finally, but importantly, even though Jurassic shortening re-activated all salt structures, it did not progress to the point of closing or welding them, thus leaving a remaining potential for subsequent deformation stages (Figs. 16c,d). This incomplete inversion or welding of the central NCA salt structures could be due to either a limited amount of shortening or to the blocking of deformation by some mechanism. In this sense, the possible presence of basement faults offsetting the Permo-Triassic salt could have hindered the propagation of deformation (Granado et al., 2021). Fernandez et al. (2024) proposed that syn-rift basement faults that offset the Permo-Triassic evaporites were inverted completely during the Late Jurassic. This inversion might, however, not have always been total, as inferred, for instance, for the Hallstatt diapir (Fig. 14; Fernandez et al., 2021).

Remarkably, the Jurassic shortening spared the closure of two broad salt-floored areas, Altaussee and Hallein, flanking the Untersberg–Hoher Göll and the Dachstein–Kasberg blocks (Fig. 18b). These were subsequently thrust over in the Early Cretaceous (Fig. 18c). The reason for this could relate to the interplay of the supra-salt cover with sub-salt basement faults, that could have hindered greater closure during the Late Jurassic.

4.2 Architecture of the Totengebirge–Trattberg system

A particularly prominent element of the Jurassic inversion system is the TT contractional system. This system is a hard-linked system of thrusts and folds that spans 80 km from west to east across the study area. This dimension implies it involved multiple minibasins during deformation. Deformation along the TT system appears to have propagated from east to west (Table 1).

Deformation in the TT system can be dated based on its relationship with the Oberalm Fm and Tressenstein Lst (both Tithonian to Berriasian) (Gawlick et al., 2005, 2007; Steiger, 1981). In the Eckersattel and the Trattberg thrusting is coeval with and sealed by the Oberalm Fm (Fig. S7a; Ortner, 2017), indicating a Tithonian to Berriasan age. Uplift along the Trattberg prior to the Tithonian is further recorded by erosion of Upper Triassic units under the Tauglboden Fm in the footwall of the Trattberg thrust (Fig. 12; Ortner, 2017), whose initial deformation likely led to the development of a gentle anticline with many tens of meters in relief. This uplift, albeit limited in relief when compared to that generated by the Trattberg thrust, accounts for the difference in facies of the Strubberg and Tauglboden Fms in the area (Trattberg Rise of Gawlick & Firsch, 2003) and can therefore be inferred to have an Oxfordian onset.

Further east, the Raschberg thrust involves the Oberalm Fm but is sealed by the base of the Tressenstein Lst (Fig. 10) locally dated as Tithonian (Gawlick et al., 2007). In this same area, Jurassic stratigraphy records northward onlap of the syn-orogenic succession onto the Triassic-Middle Jurassic carbonates in the footwall of the Raschberg thrust: the oldest syn-orogenic sediments are Callovian in the south (under the Sandling) and Oxfordian in the north (under the Höherstein) (Fig. 10) (Gawlick et al., 2007). This indicates that structures in the area developed from Oxfordian to Tithonian, ending somewhat earlier than in the western TT system. The precise age of the Totengebirge thrust, at the eastern end of the system, is unconstrained due to the absence of preserved Jurassic (or younger) sediments in the area. However, the fact that sediments of the Tithonian Oberalm Fm are widespread in the area (Fig. 19b; Fenninger & Holzer, 1970) and yet absent under the Totengebirge thrust (Fig. 7) may be due to its pre-Tithonian emplacement.

Segment	Map length (km)	Shortening (km)	Hanging wall thickness (m)	Type of structure	Age constraints
Totengebirge	19	7-10	400-5000	plug-fed thrust	--
Grünbach	12	4-5	150-250	synclines-anticlines	? – Tithonian
Raschberg	7	4	500-1000	plug-fed thrust	Oxfordian(?) – Tithonian
sub-Dachstein (Einberg thrust)	14	?	>500m[1](?)	thrust(?)	--
Trattberg	21	2-3	>2000	inverted normal fault	Tithonian – Berriasian (antiform from Oxfordian)
Eckersattel	12	3	>1000	plug-fed thrust	Tithonian – Berriasian

[1] Thickness based on Jodschwefelbad borehole (Mandl et al., 2012)

Table 1. Characteristics of the segments of the Totengebirge–Trattberg (TT) contractional system.

This timing implies that the TT contractional system grew by lateral propagation rather than by linkage of smaller structures. It is therefore not surprising that the TT contractional system does not display the arcuate shape for thrusts discussed by Elliot (1976) nor does it display its maximum displacement in its center, as could also be expected for linked systems (Kim & Sanderson, 2005). Maximum displacement on the TT system occurs at its eastern end, along the Totengebirge, where displacement is in the order of 7-11 km. This represents 8-13% of total structure length, somewhat higher than the average value of 7-10% displacement-length value quoted by Kim & Sanderson (2005).

The TT contractional dies out into the Neogene Windischgarsten fault system (Fig. 6) and no equivalent Jurassic-age structures have been documented to the east. The Windischgarsten fault system developed along a pre-existing salt-floored Triassic embayment (Fig. 18a) (Eggerth, 2023). This zone of abundant salt would have represented a “loose-end” for the TT contractional system during Jurassic shortening (Fig. 18b), potentially explaining the anomalous pattern with maximum throw at the eastern tip of the contractional system.

Another interesting feature in the TT contractional system is the variability in its structure, that includes low-angle salt overthrusts, syncline–anticline systems, and inverted extensional faults. These changes occur despite the structures having very similar orientations. It is possible that the thickness of the deformed supra-salt Triassic stratigraphy played an important role in defining the structural style. The syncline–anticline system of the Grünberg segment, for instance, developed in the only area where supra-salt stratigraphy was under 250 m thick. In areas of thicker supra-salt stratigraphy, thrusting is the dominant structural style. In the case of the Trattberg segment, it is further surprising that thrusting developed through a thick supra-salt cover, as opposed to through the Lammertal area of thin basinal deposits to the south. In this case this could relate to the fact that the Trattberg thrust developed once the Sattelberg thrust to its south had already been emplaced and shortened the Lammertal salt wall (see Section 4.3) in combination with the presence of Triassic-age extensional faults, as discussed above.

4.3 Timing of Jurassic deformation in the central NCA

The onset of deformation in the area, based on the first generalized appearance of re-sedimented Upper Triassic rocks, is Early Callovian (latest Middle Jurassic) in the southern half of the study area (Sattelberg, Rettenstein, and Sandlingalm areas) (Auer et al., 2009; Gawlick et al., 2002; Gawlick et al., 2003; Gawlick & Frisch, 2003) (Fig. 19a). Along the eastern margin of the study area (Wurzeralm and to the east, Fig. 19a), the earliest breccias are dated to be Mid-Callovian to Oxfordian (Drvoderic et al., 2023; Ottner, 1990). Deformation progressed northwards, with the earliest re-sedimented Triassic rocks occurring in the Oxfordian (earliest Late Jurassic) in the basins along and north of the TT contractional system (Rettenbach, Osterhorngruppe, Flankenstein; Fig. 19a) (Gawlick & Frisch, 2003; Kügler et al., 2003). This northward gradient in the age of breccias is also observed locally, as discussed for the Raschberg thrust above (Rettenbach–Sandlingalm area).

The development of specific structures follows a similar pattern. The oldest structure in the central NCA is the salt allochthon of the Hallstatt diapir, where evaporites override Callovian age radiolarites (Suzuki & Gawlick, 2009). Deformation then spread west to the Sattelberg thrust, in the Oxfordian (its youngest footwall sediments are Oxfordian; Gawlick et al., 2002), as well as to the Grubhörndl thrust farther west (this thrust is emplaced on and sealed by Oxfordian breccias; Ortner et al., 2008). Likewise, salt allochthony at the eastern end of the study area occurred in the Wurzeralm in the Oxfordian (salt extruded onto radiolarites of that age; Hiebl, 2011; Kurz et al., 2023; Ottner, 1990). Deformation subsequently propagated north, to the eastern segment of the TT contractional system, active from Oxfordian to Tithonian times, and finally to the western segment of the TT contractional system. The Trattberg and Eckersattel thrusts (Tithonian–Berriasian), represent the youngest Jurassic thrusts. Although dating has not been established in detail, allochthony in the Hallein diapir is potentially of equivalent age, as it occurred synchronous with deposition of the youngest Oberalm Fm (Fig. 15).

During advanced phases of deformation on individual structures, the growth of isolated Upper Jurassic reefs marks the shallowing of the seafloor from bathyal depths to within the photic zone. Just as deformation follows a northward propagation, the age of Upper Jurassic reefs also becomes younger in that direction. The Rettenstein (Fig. 19a) stands out as the location where shortening-related uplift first brought the Jurassic seafloor into the photic zone and enabled the growth of the first Upper Jurassic reef in the area (Late Oxfordian) (Auer et al., 2008, 2009).

Further north, the reefs of the Plassen, the Krahstein, the Trisselwand, the Rote Wand, Falkenstein (Fig. 19b), are dated as starting in the Kimmeridgian (Gawlick et al., 2003; Gawlick et al., 2009; Hiebl, 2011; Kügler et al., 2003; Schlagintweit et al., 2003; Schlagintweit & Ebli, 1999; Steiner et al., 2021). Reef development in the Mt Sandling and the Lofer-Gerhardstein (Fig. 19b) started in the Tithonian (Gawlick et al., 2007; Sanders et al., 2007).

The inversion of the NCA salt-bearing margin led to a transition from depositional environments starved in carbonates in the Middle to earliest Late Jurassic (Fig. 19a) to a setting rich in carbonates during the latest Late Jurassic (Fig. 19b). Two carbonate sources appeared during the Middle to Late Jurassic to explain this transition. Initially submarine erosion of uplifted Triassic carbonates along incipient Jurassic structures fed locally sourced breccia bodies (Gawlick et al., 2002, 2007; Gawlick & Missoni, 2015; Mandl, 2013). Breccias related to uplift and erosion continued to deposit throughout the entire Late Jurassic (Gawlick et al., 2005; Ortner, 2017; Steiger, 1981). Once inversion had progressed sufficiently, the seafloor above some squeezed diapirs and salt walls reached neritic depths, allowing for reefs to grow on their tops, or on the uplifted flanking minibasins. Reefs became an additional source of carbonatic material in the basin.

In contrast to the other reefs in the area, the Trisselwand reef did not grow on a squeezed diapir but above a minibasin of Triassic platform carbonates that is in the hanging wall of an extensional fault (Figs. 9, 19b). Paradoxically, the footwall of the extensional fault accumulated reef slope deposits (Fig. 9). This counter-intuitive arrangement could have resulted from either: a rotation of the underlying Triassic minibasins around horizontal axes as they interacted with fault related steps in the sub-salt; or extensional faulting being the result of post-Jurassic extension (see Section 4.4).

4.4 Post-Jurassic deformation

Analyzing deformation after the Jurassic is beyond the scope of this article. However, the map restoration presented in Fig. 18 required modelling Cretaceous to Neogene deformation to understand the Triassic and Jurassic configuration of the central NCA (Fig. S11). Two key stages of deformation were modelled: a phase of Early Cretaceous thrusting, in which the Untersberg–Dachstein–Warscheneck thrust sheet was transported to the NE (Fernandez et al., 2024) (Fig. 18c); and a phase of Neogene strike-slip that offset the pre-existing structures (Linzer et al., 1995; Peresson & Decker, 1997) (Fig. 18d).

Shortening during the Early Cretaceous was variable along strike. The Dachstein thrust accumulated approximately 8 km of displacement, whereas its along-strike equivalents (the Untersberg and Warscheneck thrusts) have been interpreted to have had more limited displacement (5 and 3 km). Displacement on the Dachstein thrust is constrained as its footwall cutoff is known to lie SW of the Steeg-1 borehole (Levi, 2023; Mandl et al., 2012). Displacement on the other two thrust segments are estimates derived by reducing block overlaps in the palinspastic restoration.

Thrusting during this stage occurred, as in the Jurassic, by decoupling along the basal Permo-Triassic salt, a décollement observed at the base of the Triassic stratigraphy of the Tennengebirge and Dachstein minibasins (Roßner, 1972). This stage of thrusting significantly contracted the salt structures remaining after Jurassic shortening.

Coeval with thrusting of the Untersberg–Dachstein–Warscheneck, a set of structurally higher thrust sheets was emplaced above the southern margin of the NCA. There are no preserved remnants of these structural units, but their presence is inferred based on Early Cretaceous metamorphism (Fernandez et al., 2024; Frank & Schlager, 2006). The location of the leading edge of these upper thrust sheets, estimated based on the distribution of Early Cretaceous metamorphism (Frank & Schlager, 2006; Kralik et al., 1987), is indicated in Fig. 18c. During the Late Cretaceous, thrusting also involved the Austroalpine basement in the trailing edge of the NCA. This basement forms a wedge (in section view) whose leading edge has also been represented in Fig. 18c.

From Late Cretaceous through to Neogene times, a system of extensional collapse structures developed across the area (Fig. 18d). Whereas the Gosau basin is documented to have developed by extension in the Late Cretaceous (Wagreich & Decker, 2001), the age of collapse in other areas is Eocene or younger (Lattengebirge; Herm, 1962; Risch, 1993). In many other locations, timing of collapse is only constrained to be post-Jurassic (e.g., Lofer–Gerhardstein, Lammertal, Sandling, Obertraun, Ramsau, Wurzeralm) (Fernandez et al., 2022, 2024; Kurz et al., 2023).

Finally, during the Neogene (Fig. 18d), pre-existing salt structures were further re-activated in thrusting (Wolfgangsee, Windischgarsten) or in strike-slip (Königssee, Postalm, Traunsee). Throw on the Traunsee fault is estimated to be 3 km at its southwestern end (Decker et al., 1994) and a similar 3 km at its northeastern end (Egger, 2007) and acted mainly as a relay structure between the Wolfgangsee and Windischgarsten thrusts. Further to the southwest, a limited amount of displacement (1-2 km) has been interpreted along the Königssee and Postalm faults. Evidence for any greater offset along the Königssee fault is lacking, as the criterion previously used to determine throw (offset of map contacts; Decker et al., 1994) can be explained as an inherited geometry in the Triassic minibasins (the Königssee fault is an inherited salt structure; Fernandez et al., 2024).

Similarly, the Mandlingzug fault (Fig. S9), a branch of the SEMP (Salzach-Ennstal-Mariazell-Puchberg) fault (Fig. 2), re-activates a pre-existing Triassic salt structure in its shallowest portions. The possible re-activation of salt structures along the SEMP fault itself has not yet been explored.

Despite the significant magnitudes of vertical-axis rotation documented for this time in the area (Pueyo et al., 2007; Thöny et al., 2006), there is no evidence in the field or from the map restoration (Fig. 18, Fig. S11) that any segments of the central NCA experienced any significant vertical-axis rotation. Frisch & Gawlick (2003) came up with a similar result in an earlier attempt at a map restoration of the same area.

4.5 Regional tectonic transport directions

The local tectonic transport direction in most of the Jurassic structures documented here is roughly dip-slip, with directions including NW-, N-, NE, SE, and S-directed transport. At a more regional scale, and based on the palinspastic reconstruction presented, it is observed that during the Late Jurassic the study area shortened in both N-S and E-W directions (Fig. 18b). The overall direction of Jurassic tectonic transport is however not certain. Thrusting along the Trattberg is NE directed (Ortner, 2017) (Fig. S6), whereas thrusting at the eastern end of the Totengebirge thrust is NW directed (Linzer et al., 1995). These both could correspond to a regional N-S directed shortening direction, but further observations are required to support this assumption.

An analogous situation is found in the Early Cretaceous. During this time, the area is also observed to experience shortening in the N-S and E-W directions (Fig. 18c). NE-directed thrusting in the study area is the one that best explains the structural configuration of the Untersberg–Dachstein–Warscheneck system, with the Postalm and Salzsteig acting as lateral faults (Fig. 2; see also Fernandez et al., 2024). However, this contrasts with NW-directed shortening documented in the western NCA (Ortner & Kilian, 2022). N-directed regional shortening, with divergence occurring in the western and central NCA, potentially due to the role of the Permo-Triassic detachment, could provide a satisfactory explanation.

Posterior thrusting events, in the Late Cretaceous to Paleogene, are not captured in the restoration as during this stage the entire central NCA were transported mostly passively northwards, with very limited internal deformation (Fernandez et al., 2024). Evidence from the Austroalpine basement south of the study area (Ratschbacher & Neubauer, 1989) and from the western NCA (Ortner & Kilian, 2022) points to W- or NW-directed transport during this time. Finally, the NCA experienced Neogene left-lateral transpression (Linzer et al., 1995, 2002; Peresson & Decker, 1997) that caused the reactivation of pre-existing structures with relatively minor magnitudes of displacement (Fernandez et al., 2024) (Fig. 17d).

4.6 Salt volume balance

Shortening from Late Jurassic to present-day led to the major and continued re-activation of salt structures. In the central NCA, salt structures during the Triassic were dominantly subsiding diapirs and salt walls covered by pelagic carbonates or thin platform carbonate rooves (Figs. 17a, 18a; Fernandez et al., 2024). Tracking the map area of the pelagic carbonates and areas of thin carbonate platforms (supra-salt-wall or supra-diapir carbonates) therefore provides a proxy to estimate the magnitude of evaporite volume loss during deformation. The comparison of the map areas in Figs. 18a and 18d indicates that supra-diapir carbonates in the central NCA at present cover an area that is around 30% of their extent at Late Triassic times. Assuming a 1:1 relationship between the original (Late Triassic) map area of supra-diapir carbonates with the map area of salt walls and diapirs (as a first approximation), a loss of 70% of supra-diapir carbonate outcrop area would imply that around 70% of the original evaporite volume has been lost. This value is consistent with the estimate of Fernandez et al. (2021) for the Hallstatt diapir and of Santolaria, Granado, & Wilson (2022) for analogue models of the neighboring eastern NCA.

At present, the Permo-Triassic evaporites in the salt diapirs in the central NCA have contents of halite ranging from 50 to 65% (Leitner & Mayr, 2017). If the 70% of volume loss is assumed to have mostly removed halite (the most soluble component in the Haselgebirge), then the original composition can be estimated to have contained 85-90% of halite (most likely including other highly soluble constituents, such as potash salts). This composition would be comparable to that in the Zechstein or South Atlantic salt basins (e.g., Fiduk & Rowan, 2012; Jackson & Stewart, 2017; Szatmari et al., 2021).

5 Conclusions

The central NCA is an outstanding example to study the inversion of salt-dominated margins. Its structural and geomorphologic configuration, with Triassic minibasins preserved in sub-horizontal position and the preserved syn-tectonic strata, make it feasible to reconstruct the temporal evolution of this province since Triassic times. This contribution presents the first systematic analysis of the evolution of Late Jurassic to Cretaceous inversion of this salt-dominated margin.

Unsurprisingly, Triassic-age salt structures strongly controlled the location of the earliest inverted structures during the Late Jurassic. All salt structures that persisted into the Late Triassic were inverted, even if only partially, during the initial Late Jurassic deformation stage. Deformation during the Late Jurassic did not, however, succeed in completely squeezing all salt structures. The possible interaction of the supra-salt cover with sub-salt basement faults could help explain this pattern.

The same Triassic salt structures continued to play a key role during the later inversion of the margin (Early Cretaceous) and during its partial dismemberment under transpression during the Neogene.

Remarkably, the Totengebirge–Trattberg contractional system, that formed during the early inversion of the margin, during the Late Jurassic, presents uncommon features. It exhibits outstanding continuity (it is over 80 km in length) with strong along-strike variability in structural style (including low-angle, high-angle faulting, or isoclinal folding) and is postulated to have developed by along-strike propagation rather than by linkage of smaller structures. The variability in structural style of the Totengebirge–Trattberg contractional system and its peculiarities in growth and displacement patterns can be traced back to the key role exerted by salt structures and the supra-diapir stratigraphy.

Acknowledgments

The authors declare no conflict of interest. Research by W. Munday, O. Fernandez, and M. Moser, H. Ortner, D. Sanders, and B. Grasemann is supported by FFG and Salinen AG through the FFG-Bridge Project ETAPAS (FO999888049). Research by O. Fernandez and B. Grasemann is further supported by FWF Project POLARIS (I 5399-N) and Structure and Deformation of Salt-bearing Rifted Margins (SABREM), PID2020-117598GB-I00, funded by MCIN/ AEI /10.13039/501100011033. Petex Inc provided academic licenses of Move, that has been used for cross-section construction and restoration. The authors wish to thank J.A. Muñoz, J.-C. Ringenbach, and M. Rowan for enriching discussions.

Open research

Data archiving of field dip data and revised geological maps compiled by the authors and presented in this contribution is in process (repository PANGAEA).

References

Auer, M., Gawlick, H.-J., & Schlagintweit, F. (2008). An extensional allochthon at the southern rim of the central Northern Calcareous Alps - the isolated Jurassic occurrence of Mount Rettenstein near Filzmoos. *Journal of Alpine Geology*, 49, 4-5.

Auer, M., Gawlick, H.-J., Suzuki, H., & Schlagintweit, F. (2009). Spatial and temporal development of siliceous basin and shallow-water carbonate sedimentation in Oxfordian Northern Calcareous Alps. *Facies*, 55, 63–87. doi: 10.1007/s10347-008-0155-3

Böhm, F., Dommergues, J.-L., & Meister, C. (1995). Breccias of the Adnet Formation: indicators of a Mid-Liassic tectonic event in the Northern Calcareous Alps (Salzburg/Austria). *Geologische Rundschau*, 84, 272–286.

Braun, R. (1998). *Die Geologie des Hohen Gölls.* Nationalpark Berchtsegaden Forschungsbericht 40/1998. Berchtsegaden, Germany: Nationalparkverwaltung Berchtesgaden.

Callot, J.-P., Trocmé, V., Letouzey, J., Albouy, E., Jahani, S., & Sherkati, S. (2012). Pre-existing salt structures and the folding of the Zagros Mountains. In: Alsop, G. I., Archer, S. G., Hartley, A. J., Grant, N. T., & Hodgkinson, R. (Eds.) *Salt Tectonics, SedimentsandProspectivity*. Geological Society, London, Special Publications, 363, 545–561. doi: 10.1144/SP363.27

Célini, N., Callot, J.-P., Ringenbach, J.-C., & Graham, R. (2020). Jurassic Salt Tectonics in the SW Sub-Alpine Fold-and-Thrust Belt. *Tectonics*, 39, e2020TC006107. doi: https://doi.org/10.1029/2020TC006107

Cornelius, H.P., & Plöchinger, B. (1952). Der Tennengebirgs-N-Rand mit seinen Manganerzen und die Berge im Bereich des Lammertales. *Jahrbuch der Geologischen Bundesanstalt*, 95, 145–225.

Cotton, J. T., & Koyi, H. A. (2000), Modeling of thrust fronts above ductile and frictional detachments: Application to structures in the Salt Range and Potwar Plateau, Pakistan. *GSA Bulletin*, 112(3), 351–363. doi: 10.1130/0016-7606(2000)112<351:MOTFAD>2.0.CO;2

Decker, K., Faupl, P., & Müller, A. (1987). Synorogenic sedimentation on the Northern Calcareous Alps during the Early Cretaceous. In: Flügel, H. W. & Faupl, P. (Eds.) *Geodynamics of the Eastern Alps*. Vienna (AUT): Deuticke, 112–125.

Decker, K., Peresson, H. & Faupl, P. (1994). Die miozäne Tektonik der östlichen Kalkalpen: Kinematic, Paläospannungen und Deformationsaufteilung während der “lateralen Extrusion” der Zentralalpen. *Jahrbuch der Geologischen Bundesanstalt*, 137, 5–18.

Drvoderic, S.P., Gawlick, H.-J., Suzuki, H., & Schlagintweit, F. (2023). Suprasubduction ophiolite (SSZ) components in a middle to lower upper Jurassic Hallstatt Mélange in the Northern Calcareous Alps (Raucherschober/Schafkogel area). *Geosystems and Geoenvironment*, 2, 100174. doi: 10.1016/j.geogeo.2022.100174

Duffy, O. B., Dooley, T. P., Hudec, M. R., Fernandez, N., Jackson, C. A.-L., & Soto, J. I. (2021). Principles of shortening in salt basins containing isolated minibasins. *Basin Research*, 33, 2089–2117. doi: 10.1111/bre.12550

Duffy, O. B., Dooley, T. P., Hudec, M. R., Jackson, M. P. A., Fernandez, N., Jackson, C. A.-L., et al. (2018). Structural evolution of salt-influenced fold-and-thrust belts: A synthesis and new insights from basins containing isolated salt diapirs. *Journal of Structural Geology*, 114, 206–221. doi: 10.1016/j.jsg.2018.06.024

Egger, H. (Ed.) (1996). Blatt 66 Gmunden 1:50,000. In: *Geologische Karte der Republik Österreich 1:50,000*, Nr. 66. Vienna (AUT): Verlag der Geologischen Bundesanstalt.

Egger, H. (Ed.) (2007). *Erläuterungen zu Blatt 66 Gmunden*. Vienna (AUT): Verlag der Geologischen Bundesanstalt.

Egger, H., & van Husen, D. (Eds.) (2007). Blatt 67 Grünau 1:50,000. In: *Geologische Karte der Republik Österreich 1:50,000*, Nr. 67. Vienna (AUT): Verlag der Geologischen Bundesanstalt.

Eggerth, L. (2023). *3D-structural modelling approach to explore the link between syn-sedimentary deformation of the Lofermauern and salt tectonics (Wurzeralm)* (master's thesis). Vienna (AUT): University of Vienna.

Elliot, D. (1976). The energy balance and deformation mechanisms of thrust sheets. *Philosophical Transactions of the Royal Society of London Series A*, 283, 289-312

Elster, E., Goldbrunner, J., Wessely, G., Niederbacher, P., Schubert, G., Berka, R., et al. (2016). Erläuterungen zur geologischen Themenkarte 1:500,000 Thermalwässer in Österreich. Vienna (AUT): Verlag der Geologischen Bundesanstalt.

Faupl, R., & Wagreich, M. (1992). Cretaceous flysch and pelagic sequences of the Eastern Alps: correlations, heavy minerals, and paleogeographic implications. *Cretaceous Research*, 13, 387–403. doi: 10.1016/0195-6671(92)90006-C

Faupl, P., & Wagreich, M. (2000). Late Jurassic to Eocene paleogeography and geodynamic evolution of the Eastern Alps. *Mitteilungen der Österreichischen Geologischen Gesellschaft*, 92, 79-94.

Fenninger, A., & Holzer, H.-L. (1970). Fazies und Paläogeographie des oberostalpinen Malm. *Mitteilungen der Geologischen Gesellschaft in Wien*, 63, 52-141.

Fernandez, O., Grasemann, B. & Sanders, D. (2022). Deformation of the Dachstein Limestone in the Dachstein thrust sheet (Eastern Alps, Austria). *Austrian Journal of Earth* Sciences, 115, 167–190. doi: 10.17738/ajes.2022.0008

Fernandez, O., Habermüller, M. & Grasemann, B. (2021). Hooked on salt: Rethinking Alpine tectonics in Hallstatt (Eastern Alps, Austria). *Geology*, 49, 325-329. doi: 10.1130/G47981.1

Fernandez, O., Ortner, H., Sanders, D., Grasemann, B., & Leitner, T. (2024). Salt-rich versus salt-poor structural scenarios in the central Northern Calcareous Alps: implications for the Hallstatt facies and early Alpine tectonic evolution (Eastern Alps, Austria). *International Journal of Earth Sciences*. doi: 10.1007/s00531-023-02377-4

Ferrer, O., Carola, E., & McClay, K. (2023). Structural control of inherited salt structures during inversion of a domino basement-fault system from an analogue modelling approach. *Solid Earth*, 14, 517–589. doi: 10.5194/se-14-571-2023

Fiduk, J.C., & Rowan, M.G., (2012). Analysis of folding and deformation within layered evaporites in Blocks BM-S-8 & -9, Santos Basin, Brazil. In: Alsop, G.I., Archer, S.G., Hartley, A.J. ,Grant, N.T. & Hodgkinson, R. (Eds.), *Salt Tectonics, Sediments and Prospectivity*. Geological Society, London, Special Publications, 363, 471-487. doi: 10.1144/SP363.22

Frank, W., & Schlager, W. (2006). Jurassic strike slip versus subduction in the Eastern Alps. *International Journal of Earth Sciences*, 95, 431–450. doi: 10.1007/s00531-005-0045-7

Frisch, W., & Gawlick, H.-J. (2003). The nappe structure of the central Northern Calcareous Alps and its disintegration during Miocene tectonic extrusion — a contribution to understanding the orogenic evolution of the Eastern Alps. *International Journal of Earth Sciences*, 92, 712–727. doi: 10.1007/s00531-003-0357-4

Ganss, O. (1937). Zur Geologie des westlichen Toten Gebirges. *Jahrbuch der Geologischen Bundesanstalt*, 87, 331–374.

Garrison, R. E. (1967). Pelagic limestones of the Oberalm beds (Upper Jurassic – Lower Cretaceous), Austrian Alps. *Bulletin of Canadian Petroleum Geology*, 15, 21–49.

Garrison, R. E., & Fischer, A. (1969). Deep-water limestones and radiolarites of the Alpine Jurassic. In: Friedman, G. M. (Ed.) *Depositional Environments in Carbonate Rocks*. SEPM Special Publication 14, 20–56.

Gawlick, H.-J., & Frisch, W. (2003). The Middle to Late Jurassic carbonate clastic radiolaritic flysch sediments in the Northern Calcareous Alps: sedimentology, basin evolution, and tectonics - an overview. *Neues Jahrbuch für Geologie und Paläontolgie – Abhandlungen*, 230, 163-213. doi: 10.1127/njgpa/230/2003/163

Gawlick, H.-J., Frisch, W., Missoni, S., & Suzuki, H. (2002). Middle to Late Jurassic radiolarite basins in the central part of the Northern Calcareous Alps as a key for the reconstruction of their early tectonic history – an overview. *Memorie della Società Geologica Italiana*, 57, 123-132.

Gawlick, H.-J., Frisch, W., Vecsei, A., Steiger, T., & Böhm, F. (1999). The change from rifting to thrusting in the Northern Calcareous Alps as recorded in Jurassic sediments. *Geologische Rundschau*, 87, 644–657. doi: 10.1007/s005310050237

Gawlick, H.-J., & Lein, R. (1997). Neue stratigraphische und fazielle Daten aus dem Jakobberg- und Wolfdietrichstollen des Hallein-Bad Dürrnberger Salzberges und ihre Bedeutung für die Interpretation der geologischen Verhältnisse im Bereich der Hallein - Berchtesgadener Schollenregion. *Geologisch-Paläontologische Mitteilungen Innsbruck*, 22, 199-225.

Gawlick, H.-J., Missoni, S., Schlagintweit, F., Suzuki, H., Frisch, W., Krystyn, L., et al. (2009). Jurassic tectonostratigraphy of the Austroalpine Domain. *Journal of Alpine Geology*, 50, 1–152.

Gawlick, H.-J., & Missoni, S. (2015). Middle Triassic radiolarite pebbles in the Middle Jurassic Hallstatt Mélange of the Eastern Alps: implications for Triassic–Jurassic geodynamic and paleogeographic reconstructions of the western Tethyan realm. *Facies*, 61, 13. doi: 10.1007/s10347-015-0439-3

Gawlick, H.-J., & Missoni, S. (2019). Middle-Late Jurassic sedimentary mélange formation related to ophiolite obduction in the Alpine-Carpathian-Dinaridic Mountain Range. *Gondwana Research*, 74, 144–172. doi: 10.1016/j.gr.2019.03.003

Gawlick, H.-J., Schlagintweit, F., Ebli, O., & Suzuki, H. (2003). Die Plassen-Formation (Kimmeridgium) des Krahstein (Steirisches Salzkammergut, Österreich) und ihre Unterlagerung: neue Daten zur Fazies, Biostratigraphie und Sedimentologie. *Zentralblatt für Geologie und Paläontologie – Teil I*, 3-4, 295-334.

Gawlick, H.-J., Schlagintweit, F., & Missoni, S. (2005). Die Barmsteinkalke der Typlokalität nordwestlich Hallein (hohes Tithonium bis tieferes Berriasium; Salzburger Kalkalpen) – Sedimentologie, Mikrofazies, Stratigraphie und Mikropaläontologie: neue Aspekte zur Interpretation der Entwicklungsgeschichte der Ober-Jura-Karbonatplattform und der tektonischen Interpretation der Hallstätter Zone von Hallein – Bad Dürrnberg. *Neues Jahrbuch für Geologie und Paläontologie – Abhandlungen*, 236(3), 351–421.

Gawlick, H.-J., Schlagintweit, F., & Suzuki, H. (2007). Die Ober-Jura bis Unter-Kreide Schichtfolge des Gebiets Höherstein-Sandling (Salzkammergut, Österreich) – Implikationen zur Rekonstruktion des Block-Puzzles der zentralen Nördlichen Kalkalpen, der Gliederung der Radiolaritflyschbecken und der Plassen-Karbonatplattform. *Neues Jahrbuch für Geologie und Paläontologie – Abhandlungen*, 243, 1–70.

Granado, P., Ruh, J. B., Santolaria, P., Strauss, P., & Muñoz, J. A. (2021). Stretching and contraction of extensional basins with pre-rift salt: a numerical modeling approach. *Frontiers in Earth Sciences*, 9, 648937. doi: 10.3389/feart.2021.648937

Griesmeier, G.E.U., & Hornung, T. (Eds.) (2023). Blatt 68 Kirchdorf a.d. Krems 1:50,000. In: *Zusammenstellung ausgewählter Archivunterlagen der GeoSphere Austria GEOFAST 1:50,000*, Nr. 68. Vienna (AUT): Verlag der Geologischen Bundesanstalt.

Häusler, H. (1979). Zur Geologie und Tektonik der Hallstätter Zone im Bereich des Lammertales zwischen Golling und Abtenau (Sbg.). *Jahrbuch der Geologischen Bundesanstalt*, 122(1), 75–141.

Herm, D. (1962). Stratigraphische und mikropaläontologische Untersuchungen der Oberkreide im Lattengebirge und im Nierental. *Bayerische Akademie der Wissenschaften: Mathematisch-Naturwissenschaftliche Klasse, Abhandlungen Neue Folge*, 10, 9-119.

Hiebl, R. (2011). *Mikrofazies, Stratigraphie und Bewertung von Massenbewegungen der Mittel- bis Ober-Jura – Sedimente im Gebiet Wurzerkampl – Rote Wand – Mitterberg (Oberösterreich, Österreich)* (master's thesis). Leoben (AUT): Montanuniversität Leoben.

Jackson, C.A.L., & Stewart, S. (2017). Composition, tectonics, and hydrocarbon significance of Zechstein Supergroup salt on the United Kingdom and Norwegian continental shelves: A review. In: Soto, J. I., Flinch, J. F., & Tari, G. (Eds.), *Permo-Triassic Salt Provinces of Europe, North Africa and the Atlantic Margins*. Amsterdam (NL): Elsevier, 175-201. doi: 10.1016/B978-0-12-809417-4.00009-4

Jackson, M. P. A., & Hudec, M. R. (2017). *Salt Tectonics: Principles and Practice*. Cambridge, UK: Cambridge University Press.

Kellerbauer, S. (1996). Geologie und Geomechanik der Salzlagerstätte Berchtesgaden. *Münchner Geologische Hefte Reihe B: Angewandte Geologie*, 2, 1–101.

Kenter, J. A. M., & Schalger, W. (2009). Slope angle and basin depth of the Triassic platform-basin transition at the Gosaukamm, Austria. *Austrian Journal of Earth* Sciences, 102, 15–22.

Kim, Y.-S., Sanderson, D.J. (2005). The relationship between displacement and length of faults: a review. *Earth-Science Reviews*, 68, 317-334.

Krainer, K., Mostler, H., & Haditsch, J. G. (1994). Jurassische Beckenbildung in den Nördlichen Kalkalpen bei Lofer (Salzburg) unter besonderer Berücksichtigung der Manganerz-Genese. *Abhandlungen der Geologischen Bundesanstalt*, 50, 257–293.

Kralik, M., Krumm, H., & Schramm, J.M. (1987). Low grade and very low grade metamorphism in the Northern Calcareous Alps and in the Greywacke Zone: Illite-crystallinity data and isotopic ages. In: Flügel, H.W., & Faupl, P. (Eds.) *Geodynamics of the Eastern Alps*. Vienna (AUT): Franz Deuticke, 164–178.

Krenmayr, H. G. (2005). *Geologische Karte von Salzburg 1:200,000*. Vienna (AUT): Geologische Bundesanstalt.

Krenmayr, H. G., & Schnabel, H.-J. (2006). *Geologische Karte von Oberösterreich 1:200,000*. Vienna (AUT): Geologische Bundesanstalt.

Krische, O., Goričan, Š., & Gawlick, H.-J. (2014). Erosion of a Jurassic ophiolitic nappe-stack as indicated by exotic components in the Lower Cretaceous Rossfeld Formation of the Northern Calcareous Alps (Austria). *Geologica Carpathica*, 65, 3-24. doi: 10.2478/geoca-2014-0001

Kügler, U., Schlagintweit, F., Suzuki, H., & Gawlick, H.-J. (2003). Stratigraphie und Fazies des Höheren Mittel- bis Ober-Jura im Bereich des Falkensteinzuges am Wolfgangsee, Salzkammergut (Österreich) mit besonderer Berücksichtigung der Plassen-Formation (Kimmeridgium). *Gmundner Geo-Studien*, 2, 97-106.

Kurz, M., Fernandez, O., Eggerth, L., Grasemann, B. & Strauss, P. (2023). Emplacement and associated sedimentary record of the Jurassic submarine salt allochthon of the Wurzeralm (Eastern Alps, Austria). *Terra Nova*, 35(6), 524–532. doi: 10.1111/ter.12675

Leitner, T., & Mayr, M. (2017). Die Salinen Austria AG und die Geologie ihrer Salzlagerstätten im Salzkammergut. In: Wimmer-Frey, I., Römer, A., & Janda, C. (Eds.) *Arbeitstagung 2017 Bad Ischl, Hallstatt, Gmunden*. Vienna (AUT): Geologische Bundesanstalt, 80–85.

Leitner, C., & Spötl, C. (2017). The Eastern Alps: Multistage development of extremely deformed evaporites. In: Soto, J. I., Flinch, J. F., & Tari, G. (Eds.), *Permo-Triassic Salt Provinces of Europe, North Africa and the Atlantic Margins*. Amsterdam (NL): Elsevier, 467-482. doi: 0.1016/B978-0-12-809417-4.00022-7

Levi, N. (2023). Polyphase tectonics in the central Salzkammergut (Northern Calcareous Alps, Austria): An updated interpretation. *Journal of Geodynamics*, 156, 101793. doi: 10.1016/j.jog.2023.101973

Linzer, H.-G., Ratschbacher, L. & Frisch, W. (1995). Transpressional collision structures in the upper crust: the fold-thrust belt of the Northern Calcareous Alps. *Tectonophysics*, 242, 41–61. doi: 10.1016/0040-1951(94)00152-Y

Linzer, H.-G., Decker, K., Peresson, H., Dell'Mour, R., & Frisch, W. (2002). Balancing lateral orogenic float of the Eastern Alps. *Tectonophysics*, 354, 211–237.

Mandl, G. W. (1982). Jurassische Gleittektonik im Bereich der Hallstätter Zone zwischen Bad Ischl und Bad Aussee (Salzkammergut, Österreich). *Mitteilungen der Gesellschaft der Geologie- und Bergbaustudenten in Österreich*, 28, 55-76.

Mandl, G. W. (2000). The Alpine sector of the Tethyan shelf — Examples of Triassic to Jurassic sedimentation and deformation from the North Calcareous Alps. *Mitteilungen der Österreichischen Geologischen Gesellschaft*, 92, 61–77.

Mandl., G. W. (2013). Zur Geologie des Raumes Hütteneckalm–Sandlingalm–Blaa-Alm (Salzkammergut, Österreich) mit kritischen Anmerkungen zur Sandlingalm-Formation. *Jahrbuch der Geologischen Bundesanstalt*, 153, 33–74.

Mandl, G.W., Hejl, E., & van Husen, D. (2014). Erläuterungen zu Blatt 127 Schladming. Vienna (AUT): Geologische Bundesanstalt.

Mandl, G. W., van Husen, D., & Lobitzer, H. (Eds.) (2012). Erläuterung zu Blatt 96 Bad Ischl. Vienna (AUT): Geologische Bundesanstalt.

Mandl, G.W., & Matura, A. (Eds.) (1995). Blatt 127 Schladming 1:50,000. In: *Geologische Karte der Republik Österreich 1:50,000*, Nr. 127. Vienna (AU): Verlag der Geologischen Bundesanstalt.

Medwenitsch, W. (1960). Zur Geologie des Halleiner Salzberges. Die Profile des Jakobberg- und Wolfdietrichstollens. *Mitteilungen der Geologischen Gesellschaft in Wien*, 51, 197–218.

Miladinova, I., Froitzheim, N., Nagel, T. J., Janák, M., Fonseca, R. O. C., Sprung, P., & Münker, C. (2022). Constraining the process of intracontinental subduction in the Austroalpine Nappes: Implications from petrology and Lu-Hf geochronology of eclogites. *Journal of Metamorphic Geology*, 40(3), 423–456. doi: 10.1111/jmg.12634

Missoni, S., & Gawlick, H.-J. (2011). Evidence for Jurassic subduction from the Northern Calcareous Alps (Berchtesgaden; Austroalpine, Germany). *International Journal of Earth Sciences*, 100, 1605–1631. doi: 10.1007/s00531-010-0552-z

Moser, M., & Moshammer, B. (2018). Die Mitteltrias-Schichtfolge des Kasberg-Gebietes in Oberösterreich (Totengebirgsdecke) und deren Bedeutung für die Mitteltrias Stratigrafie der Nördlichen Kalkalpen. *Geo.Alp*, 15, 37–59.

Mosna, D. (2010). *Die Lärchberg-Schichten im Gebiet des Gerhardsteins nahe Lofer* (master's thesis). Innsburck (AUT): University of Innsbruck.

Mostler, H., & Roßner, R. (1977). Stratigraphisch-fazielle und tektonische Betrachtungen zu Aufschlüssen in skyth-anisischen Grenzschichten im Bereich der Annaberger Senke (Salzburg, Österreich). *Geologisch-Paläontologische Mitteilungen Innsbruck*, 6, 1–44.

Neubauer, F., & Genser, J. (2018). Field Trip Post-EX-1 – Transect across the Eastern Alps. *Berichte der Geologischen Bundesanstalt (Österreich)*, 126, 137–222.

Neubauer, F., & Moser, M. (Eds.) (2022). Blatt 126 Radstadt 1:50,000. In: *Zusammenstellung ausgewählter Archivunterlagen der GeoSphere Austria GEOFAST 1:50,000*, Nr. 126. Vienna (AUT): Verlag der Geologischen Bundesanstalt.

Ortner, H. (2001). Growing folds and sedimentation of the Gosau Group, Muttekopf, Northern Calcareous Alps, Austria. *International Journal of Earth Sciences*, 90, 727–739. doi: 10.1007/s005310000182

Ortner, H. (2017). Geometry of growth strata in wrench-dominated transpression: 3D-model of the Upper Jurassic Trattberg rise, Northern Calcareous Alps, Austria. *Geophysical Research Abstracts*, 19, EGU2017-9222.

Ortner, H., & Kilian, S. (2022). Thrust tectonics in the Wetterstein and Mieming mountains, and a new tectonic subdivision of the Northern Calcareous Alps of Western Austria and Southern Germany. *International Journal of Earth Sciences*, 11, 543–571. doi: 10.1007/s00531-021-02128-3

Ortner, H., Kositz, A., Willingshofer, E. & Sokoutis, D. (2016). Geometry of growth strata in a transpressive fold belt in field and analogue model: Gosau Group at Muttekopf, Northern Calcareous Alps, Austria. *Basin Research*, 28 (6), 731–751. doi: 10.1111/bre.12129

Ortner, H., Ustaszewski, M., & Rittner, M. (2008). Late Jurassic tectonics and sedimentation: breccias in the Unken syncline, central Northern Calcareous Alps. *Swiss Journal of Geosciences*, 101(S1), S55–S71. doi: 10.1007/s00015-008-1282-0

Ottner, F. (1990). Zur Geologie der Wurzer Deckenscholle und deren Rahmen im Bereich des Warschenecks (OÖ). *Mitteliungen der Gesellschaft der Geologie- und Bergbaustudenten Österreichs*, 36, 101–145.

Pavlik, W. (Ed.) (2006). Blatt 92 Lofer 1:50,000. In: *Provisorische Geologische Karte der Republik Österreich GEOFAST 1:50,000*, Nr. 92. Vienna (AUT): Verlag der Geologischen Bundesanstalt.

Pavlik, W. (Ed.) (2007). Blatt 93 Bad Reichenall 1:50,000. In: *Zusammenstellung ausgewählter Archivsunterlagen der Geologischen Bundesanstalt GEOFAST 1:50,000*, Nr. 93. Vienna (AUT): Verlag der Geologischen Bundesanstalt.

Peresson, H., & Decker, K. (1997). The Tertiary dynamics of the northeastern Eastern Alps (Austria): changing paleostresses in a collisional plate boundary. *Tectonophysics*, 272, 125–157. doi: 10.1016/S0040-1951(96)00255-7

Piller, W.E., Egger, H., Erhart, C.W., Gross, M., Harzhauser, M., Hubmann, B., et al. (2004). *Die stratigraphische Tabelle von Österreich 2004 (sedimentäre Schichtfolgen)*. Vienna (AUT): Österreichische Stratigraphische Komission.

Pla, O., Roca, E., Xie, H., Izquierdo-Lavall, E., Muñoz, J.A., Rowan, M.G., et al. (2019). Influence of Syntectonic Sedimentation and Décollement Rheology on the Geometry and Evolution of Orogenic Wedges: Analog Modeling of the Kuqa Fold-and-Thrust Belt (NW China). *Tectonics*, 38, 2727–2755. doi: 10.1029/2018TC005386

Plašienka, D. (2018). Continuity and episodicity in the early Alpine tectonic evolution of the Western Carpathians: how large-scale processes are expressed by the orogenic architecture and rock record data. *Tectonics*, 37, 2029–2079. doi: 10.1029/2017TC004779

Plöchinger, B. (1977). Die Untersuchungsbohrung Gutrathsberg BI südlich St. Leonhard im Salzachtal (Salzburg). *Verhandlungen der Geologischen Bundesanstalt*, 1977, 3–11.

Plöchinger, B. (1979). Argumente für die intramalmische Eingleitung von Hallstätter Schollen bei Golling (Salzburg). *Verhandlungen der Geologischen Bundesanstalt*, 1979, 181–194.

Plöchinger, B. (Ed.) (1982). Blatt 95 Sankt Wolfgang 1:50,000. In: *Geologische Karte der Republik Österreich 1:50,000*, Nr. 95. Vienna (AU): Verlag der Geologischen Bundesanstalt.

Plöchinger, B. (1984). Zum Nachweis jurassisch-kretazischer Eingleitungen von Hallstätter Gesteinsmassen beiderseits des Salzach-Quertales (Salzburg). *Geologische Rundschau*, 73, 293–306.

Plöchinger, B. (Ed.) (1987). Blatt 94 Hallein 1:50,000. In: *Geologische Karte der Republik Österreich 1:50,000*, Nr. 94. Vienna (AU): Verlag der Geologischen Bundesanstalt.

Plöchinger, B. (Ed.) (1990). *Erläuterungen zu Blatt 94 Hallein*. Vienna (AU): Verlag der Geologischen Bundesanstalt.

Pueyo, E.L., Mauritsch, H.J., Gawlick, H.-J., Scholger, R., & Frisch, W. (2007), New evidence for block and thrust sheet rotations in the central northern Calcareous Alps deduced from two pervasive remagnetization events. *Tectonics*, 26, TC5011. doi:10.1029/2006TC001965

Rasser, M. W., Vasicek, Z., Skupien, P., Lobitzer, H. & Boorova, D. (2003). Die Schrambach-Formation an ihrer Typuslokalität (Unter-Kreide, Nördliche Kalkalpen, Salzburg): Lithostratigraphische Formalisierung und "historische" Irrtümer. In: Piller, W. E. (Ed.)

Stratigraphia Austriaca, 193–216. Schriftenreihe der Erdwissenschaftlichen Kommission Österreichische Akademie der Wissenschaften, Vienna (AUT): ÖAK.

Ratschbacher, L., & Neubauer, F. (1989). West-directed decollement of Austro-Alpine cover nappes in the eastern Alps: geometrical and rheological considerations. In: Coward, M.P., Dietrich, D., & Parker, R.G. (Eds.) *Alpine Tectonics*. London (UK): Geological Society, London, Special Publication 45, 243–262.

Risch, H. (Ed.) (1993). *Erläuterungen zum Blatt Nr. 8343 Berchtesgaden West*. München (DEU), Bayerisches Geologisches Landesamt.

Roßner, R. (1972). Die Geologie des nordwestlichen St. Martiner Schuppenlandes am Südostrand des Tennengebirges (Oberostalpin). *Erlanger geologische Abhandlungen*, 89, 1-57.

Rowan, M. G., & Vendeville, B. C. (2006). Foldbelts with early salt withdrawal and diapirism: Physical model and examples from the northern Gulf of Mexico and the Flinders Ranges, Australia. *Marine and Petroleum Geology*, 23, 871–891. doi: 10.1016/j.marpetgeo.2006.08.003

Sanders, D. (1998). Tectonically controlled Late Cretaceous terrestrial to neritic deposition (Northern Calcareous Alps, Tyrol, Austria). *Facies*, 39, 139–177. doi: 10.1007/BF02537015

Sanders, D., Lukesch, M., Rasser, M., & Skelton, P. (2007). Shell beds of diceratid rudists ahead of a low-energy gravelly beach (Tithonian, Northern Calcareous Alps, Austria): Palaeoecology and Taphonomy. *Austrian Journal of Earth Sciences*, 100, 186-199.

Santolaria, P., Ferrer, O., Rowan, M. G., Snidero, M., Carrera, N., Granado, P., et al. (2021). Influence of preexisting salt diapirs during thrust wedge evolution and secondary welding: Insights from analog modeling. *Journal of Structural Geology*, 149, 104374. doi: 10.1016/j.jsg.2021.104374

Santolaria, P., Granado, P., Carrera, N., Schneider, C.L., Ferrer, O., Snidero, M., et al. (2022). From downbuilding to contractional reactivation of salt-sediment systems: Insights from analog modeling. *Tectonophysics*, 819, 229078. doi: 10.1016/j.tecto.2021.229078

Santolaria, P., Granado, P., Wilson, E., de Matteis, M., Ferrer, O., Strauss. P., et al. (2022). From salt-bearing rifted margins to fold-and-thrust belts. Insights from analog modeling and Northern Calcareous Alps case study. *Tectonics*, 41, e2022TC007503. doi: 10.1029/2022TC007503

Santolaria, P., Harris, L. B., Casas, A. M., & Soto, R. (2022). Influence of *décollement*-cover thickness variations in fold-and-thrust belts: Insights from centrifuge analog modeling. *Journal of Structural Geology*, 163, 104704. doi: 10.1016/j.jsg.2022.104704

Schäffer, G. (Ed.) (1982). Blatt 96 Bad Ischl 1:50,000. In: *Geologische Karte der Republik Österreich 1:50,000*, Nr. 96. Vienna (AU): Verlag der Geologischen Bundesanstalt.

Schauberger, O. (1972). *Längsprofil durch den Salzstock von Hallein-Dürrenberg in der Achse der Wolfdietrichstollens* (internal report). Altaussee (AUT): Österreichische Salinen AG.

Schlager, W., & Schöllnberger, W. (1974). Das Prinzip stratigraphischer Wende in der Schichtfolge der Nördlichen Kalkalpen. *Mitteilungen der Geologischen Gesellschaft Wien*, 66/67, 165–193.

Schlagintweit, F., & Ebli, O. (1999). New Results on Microfacies, Biostratigraphy and Sedimentology of Late Jurassic - Early Cretaceous platform carbonates of the Northern Calcareous Alps – Part I: Tressenstein Limestone, Plassen Formation. *Abhandlungen der Geologischen Bundesanstalt*, 56, 379-418.

Schlagintweit, F., Gawlick, H.-J., & Lein, R. (2003). Die Plassen-Formation der Typlokalität (Salzkammergut, Österreich) – neue Daten zu Fazies, Sedimentologie und Stratigraphie. *Mitteilungen der Gesellschaft Geologie- und Bergbaustudenten Österreichs*, 46, 1-34.

Schmid, S.M., Bernoulli, D., Fügenschuh, B., Matenco, L., Schefer, S., Schuster, R., et al. (2008). The Alpine-Carpathian-Dinaridic orogenic system: correlation and evolution of tectonic units. *Swiss Journal of Geoscience*, 101, 139-183. doi: 10.1007/s00015-008-1247-3

Schuster, R., Egger, H., Krenmayr, H.-G., Linner, M., Mandl, G. W., Matura, A., et al. (2013). Geologische Übersichtskarte der Republik Österreich 1:1 500 000 (ohne Quartär). In: Schuster, R., Daurer, A., Krenmayr, H.-G., Linner, M., Mandl, G. W., Pestal, G. & Reitner, J. M. (Eds.) *Rocky Austria – Geologie von Österreich – kurz und bunt*. Vienna (AU): Geologische Bundesanstalt.

Spengler, E. (1924). Zur Frage des “Almenfensters” in der Grünauer Voralpen. *Verhandlungen der Geologischen Bundesanstalt*, 9, 157–164.

Steiger, T. (1981). Kalkturbidite im Oberjura der Nördlichen Kalkalpen (Barmsteinkalke, Salzburg, Österreich). *Facies*, 4, 215–347. doi: 10.1007/BF02536589

Steiner, T.M.C., Gawlick, H.-J., Melcher, F., & Schlagintweit, F. (2021). Ophiolite derived material as parent rocks for Late Jurassic bauxite: evidence for Tithonian unroofing in the Northern Calcareous Alps (Eastern Alps, Austria). *International Journal of Earth Sciences*, 110, 1847-1862. doi: 10.1007/s00531-021-02044-6

Strauss, P., Granado, P., & Muñoz, J. A (2021). Subsidence analysis of salt tectonics-driven carbonate minibasins (Northern Calcareous Alps, Austria). *Basin Research*, 33, 968-990. doi: 10.1111/bre.12500

Storti, F., Soto Marín, R., Rosetti, F., & Casas, A. M. (2007). Evolution of experimental thrust wedges accreted from along-strike tapered, silicone-floored multilayers. *Journal of the Geological Society*, 164(1), 73–85. doi: 10.1144/0016-76492005-186

Strauss, P., Granado, P., Muñoz, J.A., Böhm, K. & Schuster, R. (2023). The Northern Calcareous Alps revisited: Formation of a hyperextended margin and mantle exhumation in the Northern Calcareous Alps sector of the Neo-Tethys (Eastern Alps, Austria). *Earth-Science Reviews*, 243, 104488. doi: 10.1016/j.earscirev.2023.104488

Suzuki, H., & Gawlick, H.-J. (2009). Jurassic radiolarians from cherty limestones below the Hallstatt salt mine (Northern Calcareous Alps, Austria). *Neues Jahrbuch für Geologie und Paläontologie – Abhandlungen*, 251, 155-197. doi: 10.1127/0077-7749/2009/0251-0155

Szatmari, P., Moré de Lima, C., Fontaneta, G., de Melo Lima, M., Zambonato, E., Menezes, M.R., et al. (2021). Petrography, geochemistry and origin of South Atlantic evaporites: The Brazilian side. *Marine and Petroleum Geology,* 127, 104805. doi: 10.1016/j.marpetgeo.2020.104805

Thöny, W., Ortner, H. & Scholger, R. (2006). Paleomagnetic evidence for large en-bloc rotations in the Eastern Alps during Neogene orogeny. *Tectonophysics*, 414, 169-189. doi: 10.1016/j.tecto.2005.10.021

Tollmann, A. (1975). Zur Frage der Parautochthonie der Lammereinheit in der Salzburger Hallstätter Zone. *Sitzungsberichte der Akademie der Wissenschaften, mathematisch-naturwissenschaftliche Klasse, Abteilung 1*, 184, 237–257.

Tollmann, A. (1976). *Der Bau der Nördlichen Kalkalpen: Orogene Stellung und regionale Tektonik*. Vienna (AU): Franz Deuticke.

Tollmann, A. (1985). *Geologie von Österreich, Band II: Außerzentralalpiner Anteil*. Vienna (AU): Franz Deuticke.

Tollmann, A. (1987). Late Jurassic/Neocomian gravitational tectonics in the Northern Calcareous Alps in Austria. In: Flügel, H. W. & Faupl, P. (Eds.) *Geodynamics of the Eastern Alps*. Deuticke, Vienna, 112–125.

Wagreich, M., & Decker, K. (2001). Sedimentary tectonics and subsidence modelling of the type Upper Cretaceous Gosau basin (Northern Calcareous Alps, Austria). *International Journal of Earth Sciences*, 90, 714–726. doi: 10.1007/s005310000181

Wagreich, M., & Faupl, P. (1994). Palaeogeography and geodynamic evolution of the Gosau Group of the Northern Calcareous Alps (Late Cretaceous, Eastern Alps, Austria). *Palaeogeography, Palaeoclimatology, Palaeoecology*, 110, 235–254.

Walker, J.D., & Geissman, J.W., (Eds.) (2022). *Geologic Time Scale v. 6.0*. Geological Society of America. doi: 10.1130/2022.CTS006C

Woodcock, N.H. (1979). Sizes of submarine slides and their significance. *Journal of Structural Geology*, 1(2), 137–142.

Figure 1. (a) Simplified geological map of the Eastern Alps (modified from Schuster et al., 2013). See inset for location. Abbreviations: Apenn.: Apennines, Dinar.: Dinarides, E.: East, W.: West. **(b)** Simplified cross-section through the central Northern Calcareous Alps (NCA). TF: Traunsee fault, UABT: Basal Thrust of the Upper Austroalpine, TS: thrust sheet. **(c)** Schematic section showing the paleogeographic domains of the Eastern Alps.

Figure 2. Simplified structural framework of the central NCA. Structures with Jurassic tectonic activity are highlighted with names in white. The map is simplified from Krenmayr (2005) and Krenmayr and Schnabel (2006). Structures are drawn, and partly simplified, from Tollmann (1976), Braun (1998), Linzer et al. (1995), Ortner and Kilian (2022) and Fernandez et al. (2024). Abbrevations for structures: A.-B.: Ahornkogel-Brunnkogel; Eck.: Eckersattel; Gerh.-Lo.: Gerhardstein-Lofer; Grbh: Grubhörndl; Ha.: Hallein; Klausb.: Klausbach; Rab.: Rabenstein; Rschb.: Raschberg; SEMP: Salzach-Enns-Mariazell-Puchberg fault system; UABT: Basal thrust of the Upper Austroalpine; Wssb.: Weissenbach; sync.: syncline; antic.: anticline. Abbreviations for structural units: Bg: Berchtesgaden; Dc: Dachstein; Go: Golling; Gr: Grundlsee; Ha: Hallein; HG: Hoher Göll; Hn: Hagengebirge; Hö: Höllengebirge; Is: Bad Ischl; Ka: Katrin; Ks: Kasberg; Lg: Leoganger Steinberge; Mg: Mandlingzug; Mt: Bad Mitterndorf; Oh: Osterhorngruppe; Pw: Pailwand; Ra: Reiteralm; Re: Bad Reichenhall; Rt: Rettenstein; Sb: Sattelberg; Sg: Singereben; St: Steinplatte; Sw: Schwarzer Berg; Tn: Tennengebirge; To: Totengebirge; Ub: Untersberg; Uk: Unken; Ws: Warscheneck. Zw: Zwieselalm.

Figure 3. Synthetic Permo-Mesozoic stratigraphy of the central NCA. Jurassic unit names are highlighted in white. A variety of condensed red limestones of Early to Middle Jurassic age are grouped informally under “Jurassic red limestones”. The Ruhpolding Radiolarite includes the Tauglboden (Tg) and Strubberg (Sb) Fms. The Middle-Upper Jurassic and Cretaceous units are syn-orogenic in nature and can exhibit onlap relationships on a variety of older units. After Fernandez et al. (2024).

Figure 4: (a) Unconformable contact between red Jurassic limestone (of Lower to Middle Jurassic age) on the underlying Triassic Dachstein Fm. Outcrop location: x403930 y5283470. **(b)** The limestone in (**a**) is folded into gentle E-W trending anticlines that are onlapped by Middle to Upper Jurassic Tauglboden Fm beds. **(a)** and **(b)** are under 300 m apart. Outcrop location: x403730 y5283235. **(c) (d)** Unconformable contact of the Upper Jurassic Oberalm Fm on the Triassic Dachstein Lst. Note that beds of both the Dachstein Lst and Oberalm Fm are oblique to the contact and both the Lower Jurassic and parts of the Dachstein Lst have been eroded. Reworked blocks of Dachstein Lst are sometimes contained in the Oberalm Fm (**c**). Both images are orthophotos generated with photogrammetry out of handheld and airborne photographs. Both outcrops are approximately 100 m apart across a valley (note opposing orientations) and 2500 m west of the outcrop in (**a**). Outcrop (**c**) is located at x401400 y5282100 and (**d**) is located at x401355 y5282365. All coordinates are in WGS84 UTM33N and all outcrops are located between the sections in Figs. 9 and 10 (see Fig. 6 for location).

Figure 5: (a) Composite panorama view showing olistoliths of Dachstein Lst within the Oberalm Fm on the flank of the Gamskogel mountain (labelled Gamskg. in Fig. 6). An approximate scale bar is provided for the main body of olistoliths. Photos taken from x404915 y5284585. **(b)** Detail of breccias of Dachstein Lst with interbedded Oberalm Fm. Outcrop location: x405615 y 5285000. **(c)** Erosional truncation of a tight anticline in the Dachstein Lst (Bärnkogel anticline) overlain by an olistolith of Dachstein Lst. The car in the photo is roughly 5 m long. **(d) (e)** Detailed pictures of the contact between the Dachstein Lst olistolith and the underlying Tauglboden Fm. Note strong folding and development of foliation in the Tauglboden Fm. The car in (**c**, **d**) was parked in front of the outcrop by a third party and does not obstruct any key structures. Outcrop location: x406720 y5284215. All coordinates are in WGS84 UTM33N and all outcrops are within 2 km of the section in Fig. 9 (see Fig. 6 for location).

Figure 6. Map of the eastern segment of the Totengebirge–Trattberg contractional system and surrounding areas. AB antic: Arikogel–Brunnkogel anticline; Alt. diapir: Altaussee diapir; Arp sync: Ariplan syncline; Gbg sync: Grünberg syncline; Fludergr.: Fludergraben; Rettenb.: Rettenbach; peak names with ending *kg.: *kogel; R.: River; sys.: system. This map is based on fieldwork by the authors and previously published 1:50,000 scale geological mapping (Egger, 1996; Egger & van Husen, 2007; Griesmeier & Hornung, 2023; Moser & Moshammer, 2018; Plöchinger, 1982; Schäffer, 1982).

Figure 7. a) Cross-section of the Totengebirge thrust at the Kasberg. See Fig. 6 for location. **b)** Restoration of the section in (**a**) to Late Triassic times. **c)** Restoration of the section in (**a**) to early Late Triassic times.

Figure 8. a) Cross-section of the TT contractional system in the area of the Offensee. The TT structure here is dominated by two isoclinal synclines involving the Dachstein Lst and Jurassic units: the Ariplan and Grünberg synclines (Grünbg. syn.). In contrast to the highly reduced thickness of the Dachstein Lst in the synclines, the eastern flank of the Ahornkogel–Brunnkogel anticline (A.-B. ant.) presents a major stratigraphic expansion of the Dachstein Lst associated to an extensional roll-over. See Fig. 6 for location and Fig. S3 for accompanying field observations. **b)** Restoration of the section in (**a**) to Late Triassic times.

Figure 9. a) Cross-section of the TT contractional system between the Singereben and the Trisselwand. The TT structure is dominated in the Karbach area by a train of isoclinal folds, potentially thrusted. Grünbg. syn.: Grünberg syncline; Bärnkg. ant.: Bärnkogel anticline; A.-B. ant.: Ahornkogel-Brunnkogel anticline. See Fig. 6 for location and Fig. S4 for accompanying field observations. **b)** Restoration of the section in (**a**) to Late Triassic times.

Figure 10. a) Detailed surface cross-section of the TT contractional system between the Singereben and the Hoher Raschberg, near its plunging below the Dachstein thrust sheet. The TT contractional system is here mainly conformed by north-directed low angle

thrusts, sealed by the uppermost Upper Jurassic Tressenstein Lst. Thrusts were re-activated in extension in the Late Cretaceous. The topography of the Höherstein and Mt Sandling (immediately east of the profile location) have been projected for reference. See Fig. 6 for location. **b)** Cross-section corresponding to (**a**) interpreted at depth. Note that the contrast in facies in the Upper Triassic (basinal vs platform carbonates) requires the presence of a lateral transition at depth. **c)** Cross-section in (**b**) restored to Late Triassic times.

Figure 11. Map of the western segment of the TT contractional system. This map is based on fieldwork by the authors and previously published 1:50,000 scale geological mapping (Pavlik, 2007; Plöchinger, 1982, 1987).

Figure 12. a) Cross-section of the TT contractional system immediately west of the Trattberg. Thrusting of Jurassic age along the Trattberg thrust is partly inverted in extension along a set of Cretaceous (?) extensional faults. See Fig. 11 for location. **b)** Restoration of the section in (**a**) to Late Jurassic times. Uplift on the Trattberg thrust was accompanied by erosion of its hanging wall, as evidenced by the local absence of the uppermost Triassic (Rhaetian reefal limestone) under the Upper Jurassic Oberalm Fm. **c)** Restoration of the section in (**a**) to Late Triassic times.

Figure 13. a) Cross-section of the Hoher Göll area with the Eckersattel and Bluntautal thrusts. The Eckersattel thrust places the Hoher Göll unit onto the margin of the Hallein diapir and the Bluntautal backthrust places it onto the Hagengebirge block. The

Bluntautal thrust is disturbed by the Neogene left-lateral motion along the Königssee fault. The base of the Hallein diapir is known to lie below sea level based on data from exploratory boreholes in the Hallein and Berchtesgaden salt mines (Kellerbauer, 1996; Medwenitsch, 1960; Schauberger, 1972) but is otherwise unconstrained. The Untersberg thrust relays with the Dachstein thrust in the subsurface across the Hallein diapir (structure not shown), and the Ahornalm thrust is a shallow splay of the Untersberg thrust. See Fig. 11 for location.

Figure 14. a) Geological map along a transect crossing the Hallstatt diapir. Map based on mapping by the authors and Schäffer (1982). See Fig. 2 for location. **b)** Cross-section of the Hallstatt diapir, updated from Fernandez et al. (2021). **c)** Restoration of the section in **(b)** to Late Jurassic times. This interpretation contrasts with that in Fernandez et al. (2021) because of the revised dating and structural analysis of the southern flank of the Hallstatt diapir presented by Fernandez et al. (2022). **d)** Restoration of the section in **(b)** to Late Triassic times.

Figure 15. a) Geological map along a transect crossing the eastern portion of the Hallein diapir. Map based on mapping by Plöchinger (1987) and Pavlik (2007). See Fig. 2 for location. **b)** Cross-section of the Hallein diapir along the Wolf-Dietrich Gallery of the Hallein salt mine. Four deep boreholes (DB) constrain the interpretation at depth (Medwenistch, 1960; Schauberger, 1972). Biostratigraphy along the Wolf-Dietrich Gallery is based on the work of Gawlick & Lein (1997).

Figure 16. a) Geological map along a transect crossing the Grubhörndl thrust. Map based on mapping by Ortner et al. (2008) and Pavlik (2006). See Fig. 2 for location. **b)** Cross-section of the Grubhörndl thrust. The Grubhörndl thrust is sealed by Jurassic breccias in its leading edge and is overthrust by thrust sheets of the Gerhardstein-Lofer system (Early Cretaceous in age). The entire area experienced Late Cretaceous (?) extensional collapse. The wellbore Saalachtal Th-1 drilled a 1600 m thick Dachstein Lst with 35-40° dips (Elster et al., 2016). **c)** Restoration of the section in **(b)** to Early Cretaceous times. Thrusting in the area is interpreted to be dominantly out of the section plane and therefore no balance is expected. Jurassic and Cretaceous age thrusting are further expected to have variable transport directions.

Figure 17. a) Schematic structure of the central NCA at Early Jurassic times. The margin was configured in minibasins with thick carbonate platform deposits separated by salt walls. Some salt walls were rooved by thin platform carbonates whereas others had subsided and were the loci of pelagic carbonate deposition. **b)** Shortening in the Middle to Late Jurassic led to the development of shortening structures above the salt walls. The Middle to Late Jurassic basin was starved, with the major thickness of sediments relating to the presence of Late Jurassic reefs and the erosion and re-deposition of uplifted Triassic carbonates. The presence of inherited or inverted basement structures, or structures newly formed during the Late Jurassic is uncertain.

Figure 18. Palinspastic reconstruction of the central NCA from Late Triassic to present-day through key time stages: **a)** Late Triassic; **b)** Late Jurassic; **c)** Late Cretaceous; **d)**

present-day. For the restoration, the structure of the central NCA has been subdivided into domains of thick Upper Triassic carbonate platforms (minibasin domains in the Late Triassic), areas of thin Upper Triassic deposition in shallow water settings (thin Upper Triassic rooves of salt walls), and areas dominated by Upper Triassic pelagic carbonate deposition (rooves of subsiding diapirs and salt walls). The map in **(b)** further shows age constraints on deformation indicators, including thrusts, breccias and reef growth. Ages for these are abbreviated: C: Callovian; Ox: Oxfordian; K: Kimmeridgian; T: Tithonian; B: Berriasian. The map in **(e)** shows an overlay of the domains used in the restoration with the present-day geology (cf. Fig. 2). The map restoration is based on the exercise shown in Fig. S11. The restored location of the Mandlingzug block is highly unconstrained (cf. Frisch & Gawlick, 2003) and has therefore not been incorporated in this figure. Platform domain abbreviations (black lettering): Dc: Dachstein; Gb: Grubhörndl; HG: Hoher Göll; Hn: Hagengebirge; Hö: Höllengebirge; Ka: Katrin; Lg: Leoganger Steinberge; Mg: Mandlingzug; Oh: Osterhorngruppe; Ra: Reiteralm; Sg: Singereben; St: Steinplatte; Sw: Schwarzer Berg; Tn: Tennengebirge; To: Totengebirge; Tr: Traunstein; Tt: Trattberg; Ub: Untersberg; Ws: Warscheneck. Pelagic domain abbreviations (purple lettering): As: Altaussee; Gh: Gerhardstein; Go: Golling; Gr: Grundlsee; Ha: Hallein; Ht: Hallstatt; Is: Bad Ischl; Ks: Kasberg; Lo: Lofer; Mt: Bad Mitterndorf; Pw: Pailwand; Re: Bad Reichenhall; Rt: Rettenstein; Sb: Sattelberg; Uk: Unken; Zw: Zwieselalm.

Figure 19. Proposed paleogeography of the central NCA at: **a)** early Late Jurassic; **b)** late Late Jurassic. Names for Jurassic outcrop localities are shown on both maps. The

configuration of Triassic minibasins from Fig. 18b is shown in the background. Structures interpreted to be active at each stage are shown. Both maps are based on observations by the authors and on the map of Fenninger & Holzer (1970). **c)** Chronologic chart of structure activity and sedimentary record of structure growth (erosion and reef growth). Structures and features are located in their relative W-E location. Chronostratigraphic ages are from Walker and Geissman (2022).

Figure 1.


a)
10º W
11º
12º
13º
14º
15º
16º
48º N
47º
Alps
E.Alps
W.Carp.
Dinar.
Apenn.
250km
Munich
Vienna
Fig. 2
Salzburg
Fig. 1b
Innsbruck
Graz
50km
Cenozoic basin deposits
European basement
European margin (Helvetic) and Alpine Tethys (Penninic)
Cretaceous synorogenic deposits
Northern Calcareous Alps (Austroalpine Permo-Mesozoic)
Austroalpine Paleozoic and crystalline basement
Southern Alps
Main faults
National boundaries
b)
N-S
Langbathseen TS
Höllengebirge TS
Toten-gebirge TS
Dachstein TS
0
5 km
TF
UABT
UABT
0
10
20 km
c)
N-S (present-day coordinates)
NCA
Helvetic
Penninic
Austroalpine
Europe
Alpine Tethys
Adria
Meliata Tethys

Figure 2.

Font 1 Thrusts (outcrop / buried)
Font 1 Strike-slip faults
Font 2 Anticlines and synclines
Font 3 Structural units / blocks
Font 1 Font 2 Totengebirge-Trattberg contractional system
Font 1 Other Late Jurassic structures
Font 2 Areas of Late Jurassic uplift
y: 5324000
x: 473000
Fig. 6
Langbathseen
UABT
Allgäu
Lechtal
Inntal
Höllengebirge
Hö
Traunsee
Sg
Totengebirge
Ks
Windischgarsten
Wolfgangsee
Untersberg
Re
Saalach
St
Ub
Rossfeld sync.
Fig. 15
Oh
Grünberg sync.
A.-B. antic.
Is
Rschb.
Altaussee
To
Warscheneck
Salzsteig
Wurzeralm
Ws
Unken sync.
Uk
Lo
Rab
Ha
Ra
Bg
Eck.
Trattberg
Postalm
Ka
Wssb. antic.
Dachstein
Gr
Grbh.
Klausb.
HG
Go
Sw
Sb
Pw
Fig. 16
Gerh.-Lo.
Wt
Bluntautal
Sattelberg
Hallstatt
Bad
Mitterndorf
Mt
Zw
Lg
Königssee
Hn
Fig. 11
Tn
Fig. 14
Dc
Rettenstein
Rt
Ramsau
Mg
SEMP
Enns
Saalach
Salzach
Traun
Alm
Steyr
N
0 10 20
x: 304000
y: 5238000
WGS84 UTM33N
Penninic, European margin, foreland basin, intramontane Tertiary, Quaternary
Synorogenic Upper Cretaceous-Paleogene / Lower Cretaceous
Synorogenic Jurassic (basin / reef)
Pre-orogenic Jurassic
Middle-Upper Triassic
Permian-Lower Triassic
Austroalpine basement

Figure 3.

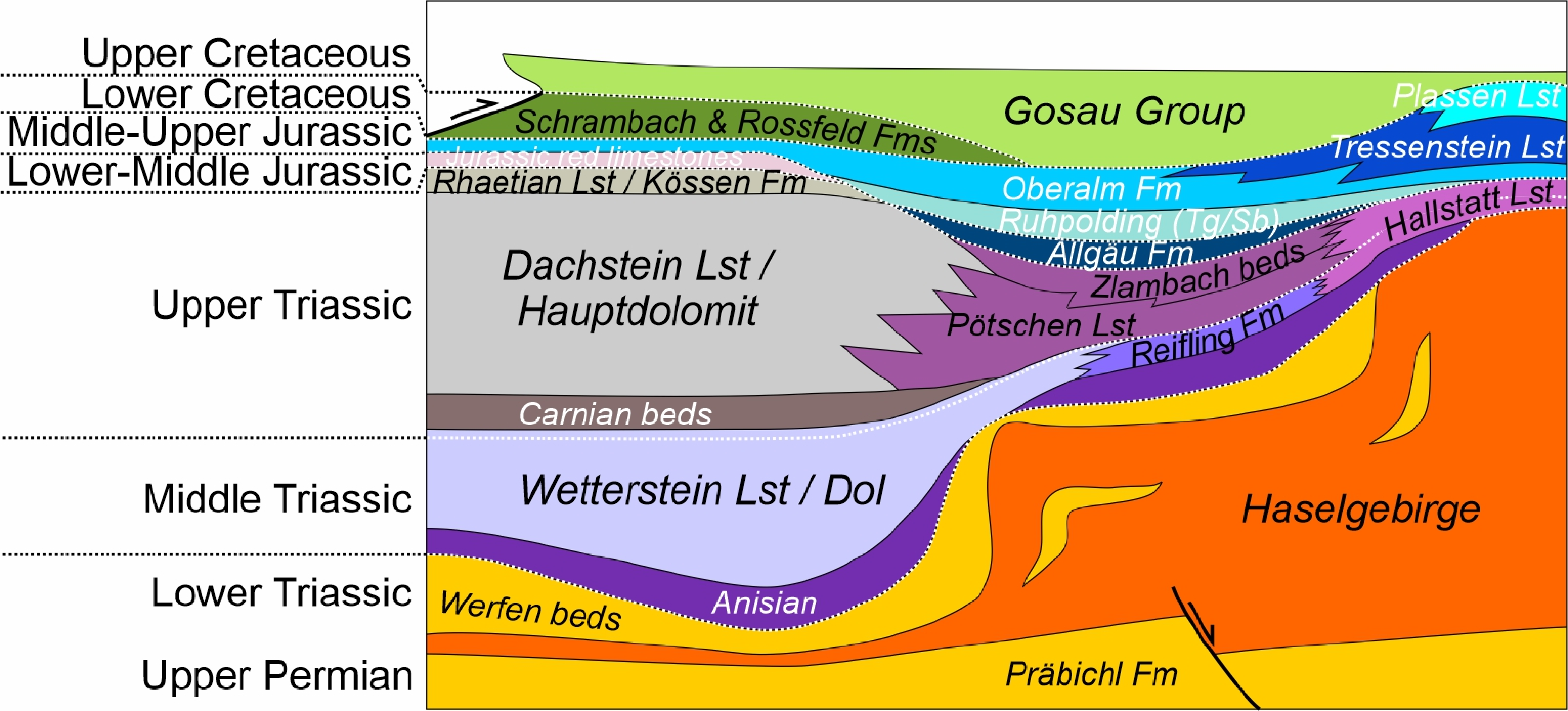
Upper Cretaceous
Lower Cretaceous
Middle-Upper Jurassic
Lower-Middle Jurassic
Upper Triassic
Middle Triassic
Lower Triassic
Upper Permian
Gosau Group
Plassen Lst
Schrambach & Rossfeld Fms
Tressenstein Lst
Jurassic red limestones
Rhaetian Lst / Kössen Fm
Oberalm Fm
Hallstatt Lst
Ruhpolding (Tg/Sb)
Allgäu Fm
Dachstein Lst / Hauptdolomit
Zlambach beds
Pötschen Lst
Reifling Fm
Carnian beds
Wetterstein Lst / Dol
Haselgebirge
Anisian
Werfen beds
Präbichl Fm

Figure 4.

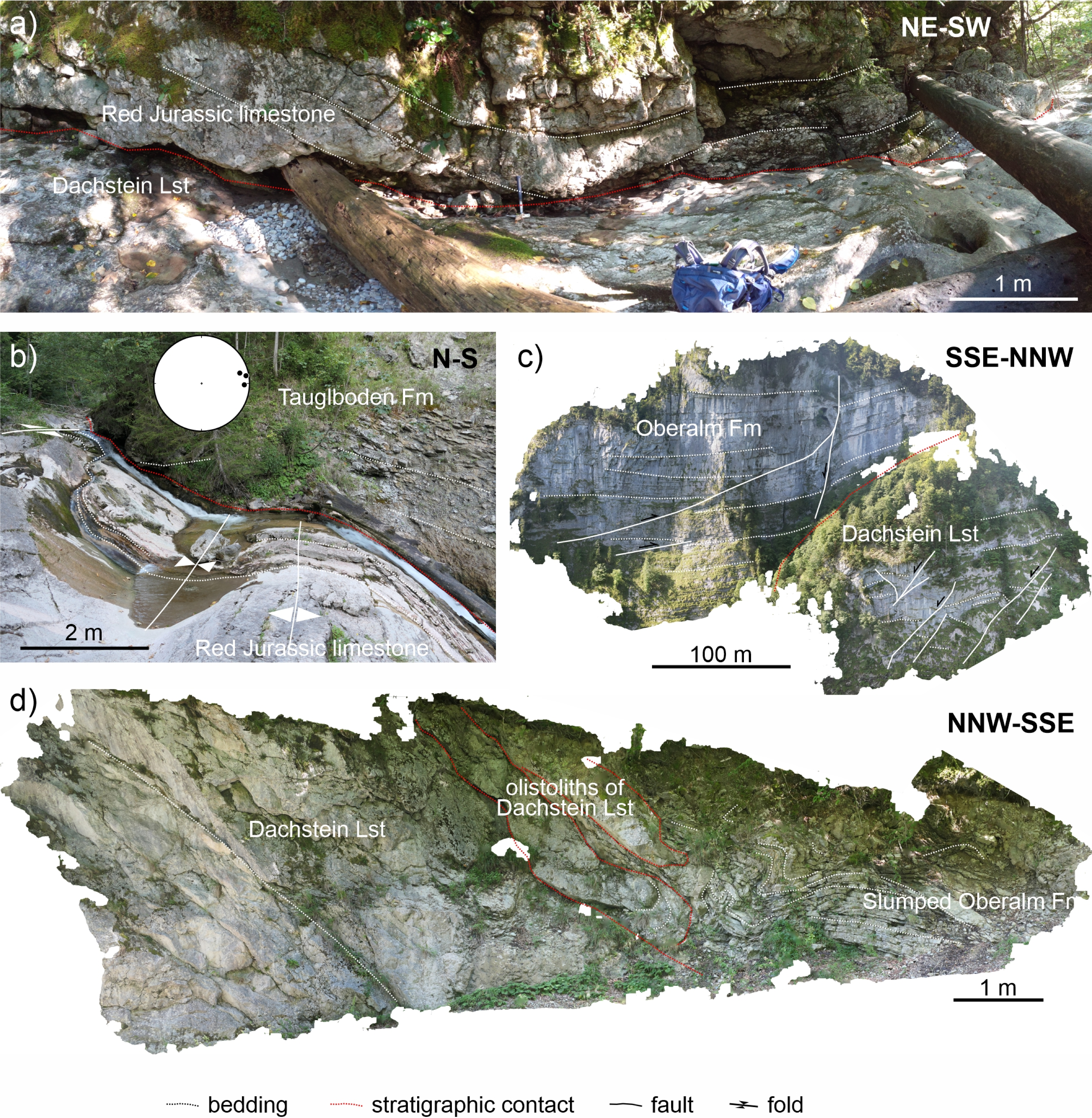
a)
NE-SW
Red Jurassic limestone
Dachstein Lst
1 m
b)
N-S
Tauglboden Fm
2 m
Red Jurassic limestone
c)
SSE-NNW
Oberalm Fm
Dachstein Lst
100 m
d)
NNW-SSE
olistoliths of Dachstein Lst
Dachstein Lst
Slumped Oberalm Fm
1 m
bedding
stratigraphic contact
fault
fold

Figure 5.

a)
NW-SE
Gamskogel
Oberalm Fm
Olistoliths of Dachstein Lst
Schönberg
200 m
Bärnkogel
Dachstein
Tauglboden
Fig. 5c
b)
NW-SE
Breccia of Dachstein Lst
Dachstein blocks
Bedded Oberalm Fm
1 m
c)
Bärnkogel
NW-SE
Dachstein Lst
erosional
truncation
surface
Red Jurassic limestone
Olistolith of Dachstein Lst
Tauglboden Fm
Fig. 5e
Fig. 5d
d)
NW-SE
Olistolith of Dachstein Lst
Tauglboden Fm
e)
NW-SE
Olistolith of Dachstein Lst
Tauglboden Fm
Red Jurassic limestone
1 m
bedding
foliation
stratigraphic contact
fault
fold

Figure 6.

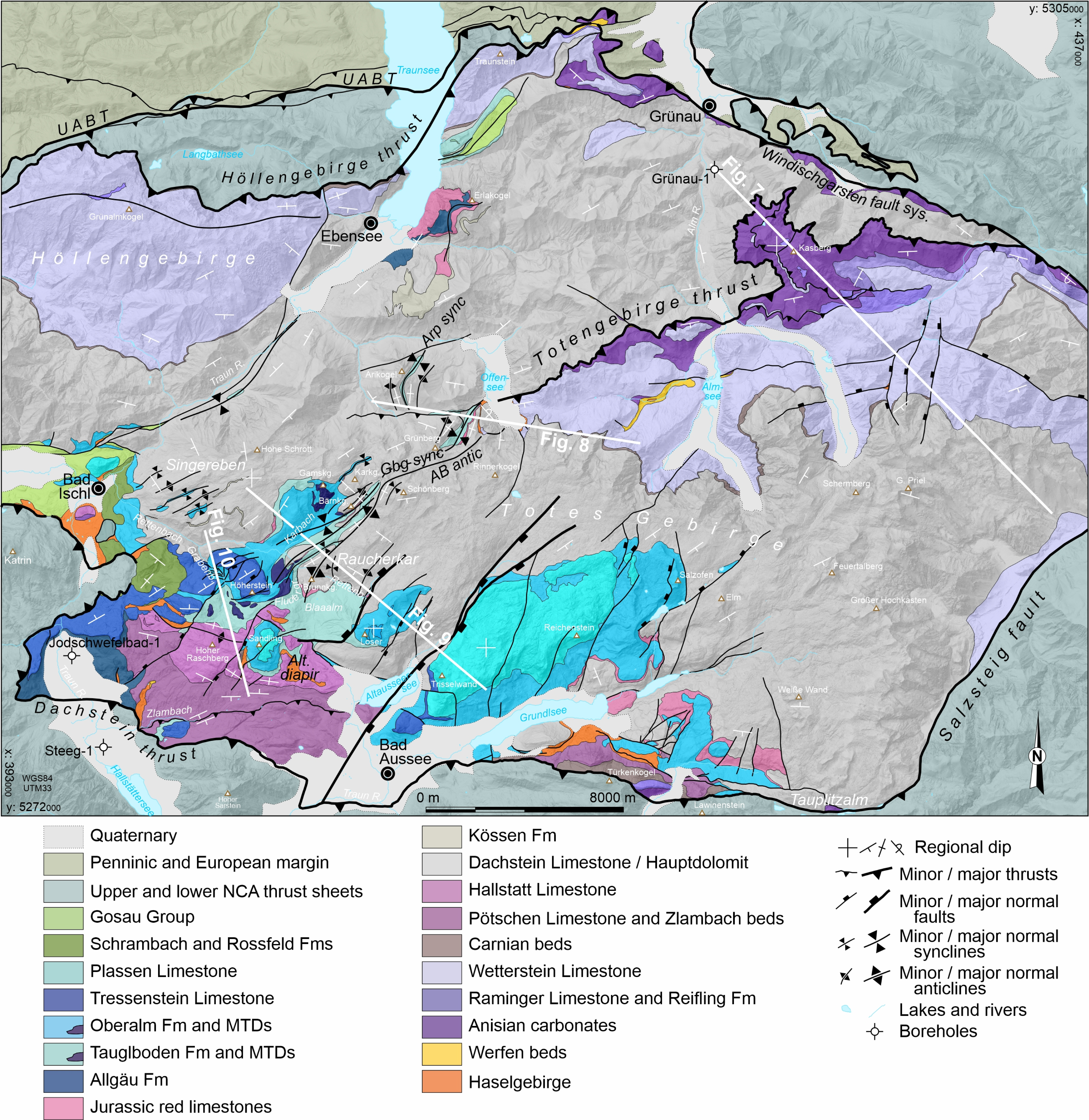
y: 5305000
x: 437000
Traunsee
UABT
UABT
Traunstein
Grünau
Grünau-1
Windischgarsten fault sys.
Langbathsee
Höllengebirge thrust
Grünalmkogel
Erlakogel
Ebensee
Höllengebirge
Alm R.
Kasberg
Fig. 7
Totengebirge thrust
Arp sync
Traun R.
Arikogel
Offensee
Almsee
Fig. 8
Grünberg
Hohe Schrott
Singereben
Bad Ischl
Gamskg.
Karkg.
Gbg sync
AB antic
Rinnerkogel
Schönberg
Bärnkg.
Schermberg
G. Priel
Totes Gebirge
Rettenbach
Fig. 10
Karbach
Raucherkar
Katrin
Grabenb.
Höherstein
Brunnkg.
Feuertalberg
Salzofen
Elm
Großer Hochkasten
Blaaalm
Fig. 9
Reichenstein
Salzsteig fault
Jodschwefelbad-1
Hoher Raschberg
Sandling
Loser
Alt. diapir
Traun R.
Altaussee
Trisselwand
Weiße Wand
Grundlsee
Zlambach
Dachstein thrust
Steeg-1
Bad Aussee
Türkenkogel
x: 393000
WGS84
UTM33
y: 5272000
Hallstättersee
Hoher Sarstein
Traun R.
0 m
8000 m
Lawinenstein
Tauplitzalm
N
Quaternary
Penninic and European margin
Upper and lower NCA thrust sheets
Gosau Group
Schrambach and Rossfeld Fms
Plassen Limestone
Tressenstein Limestone
Oberalm Fm and MTDs
Tauglboden Fm and MTDs
Allgäu Fm
Jurassic red limestones
Kössen Fm
Dachstein Limestone / Hauptdolomit
Hallstatt Limestone
Pötschen Limestone and Zlambach beds
Carnian beds
Wetterstein Limestone
Raminger Limestone and Reifling Fm
Anisian carbonates
Werfen beds
Haselgebirge
Regional dip
Minor / major thrusts
Minor / major normal faults
Minor / major normal synclines
Minor / major normal anticlines
Lakes and rivers
Boreholes

Figure 7.

a)
Grünau-1
Kasberg
Totengebirge
NNW-SSE
Totengebirge thrust
2000 m
0 m
-2000 m
Penninic and Helvetic units (sub-UABT)
Dachstein Lst (lagoonal carbonates)
Carnian beds (clastics, carbonates)
Wetterstein Lst (lagoonal carbonates)
Refiling Fm (pelagic marly limestones)
Anisian limestones (pelagic carbonates)
Werfen beds (clastics & carbonates)
Haselgebirge (evaporites & clastics)
b)
Rhaetian (Late Triassic)
0 m
-2000 m
-4000 m
Austroalpine basement
c)
Early Carnian (Late Triassic)
0 m
-2000 m
-4000 m
0 m
4000 m
Austroalpine basement

Figure 8.

a)
TT contractional system
WNW-ESE
Ariplan syn.
Grünbg. syn.
A.-B. ant.
Offensee rollover
Totengebirge
Offensee
2000 m
0 m
-2000 m
Penninic and Helvetic units (sub-UABT)
b)
Rhaetian (Late Triassic)
0 m
-2000 m
-4000 m
Austroalpine basement
0 m
4000 m
Tauglboden Fm (siliceous marls)
Red Jurassic limestone
Dachstein Lst (lagoonal carbonates)
Carnian beds (clastics, carbonates)
Wetterstein Lst (lagoonal carbonates)
Refiling Fm (pelagic marly limestones)
Anisian dolomites
Werfen beds (clastics & carbonates)
Haselgebirge (evaporites & clastics)

Figure 9.

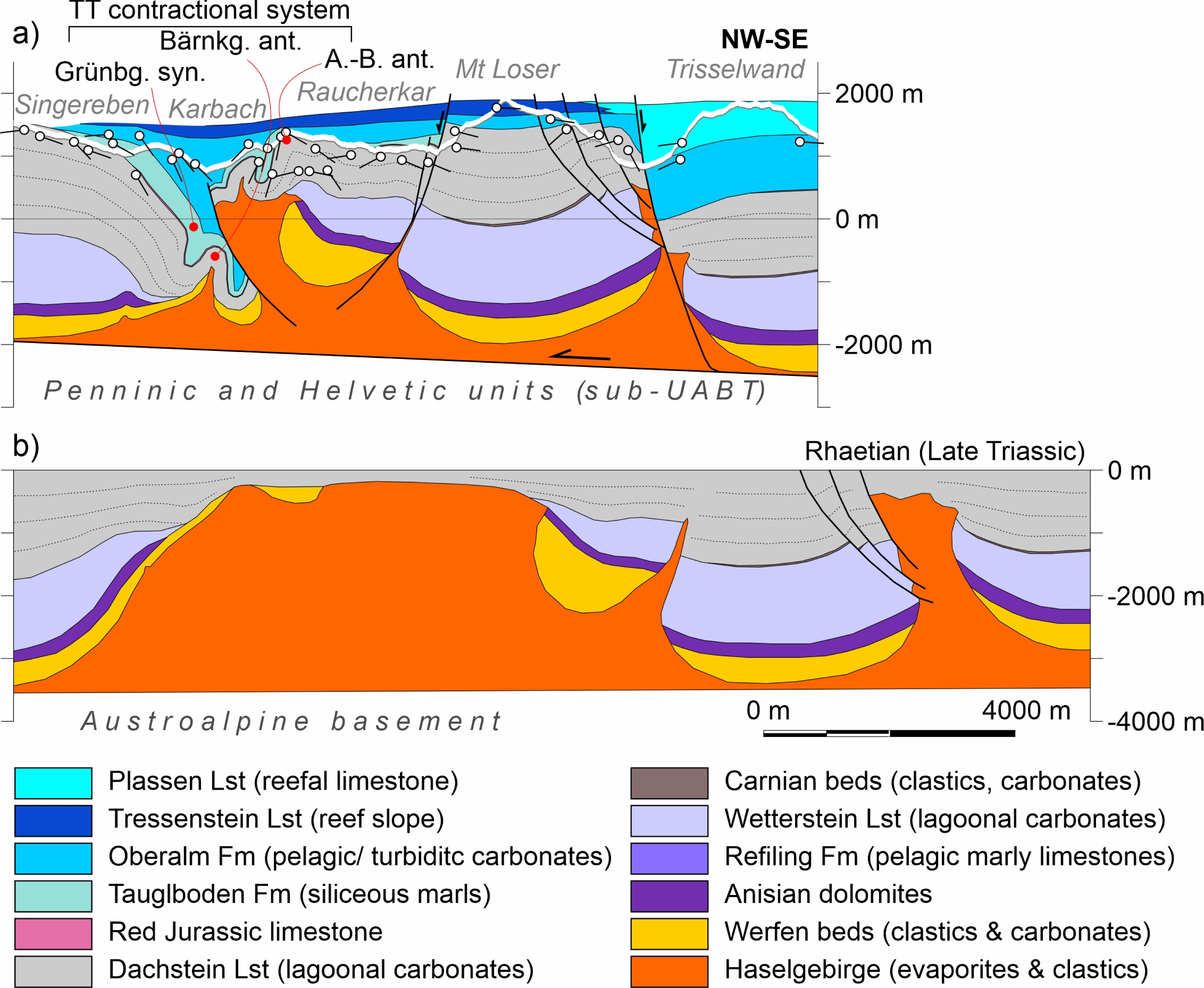

TT contractional system
a)
Bärnkg. ant.
NW-SE
A.-B. ant.
Grünbg. syn.
Mt Loser
Trisselwand
Raucherkar
Singereben
Karbach
2000 m
0 m
-2000 m
Penninic and Helvetic units (sub-UABT)
b)
Rhaetian (Late Triassic)
0 m
-2000 m
Austroalpine basement
0 m
4000 m
-4000 m
Plassen Lst (reefal limestone)
Tressenstein Lst (reef slope)
Oberalm Fm (pelagic/ turbiditc carbonates)
Tauglboden Fm (siliceous marls)
Red Jurassic limestone
Dachstein Lst (lagoonal carbonates)
Carnian beds (clastics, carbonates)
Wetterstein Lst (lagoonal carbonates)
Refiling Fm (pelagic marly limestones)
Anisian dolomites
Werfen beds (clastics & carbonates)
Haselgebirge (evaporites & clastics)

Figure 10.

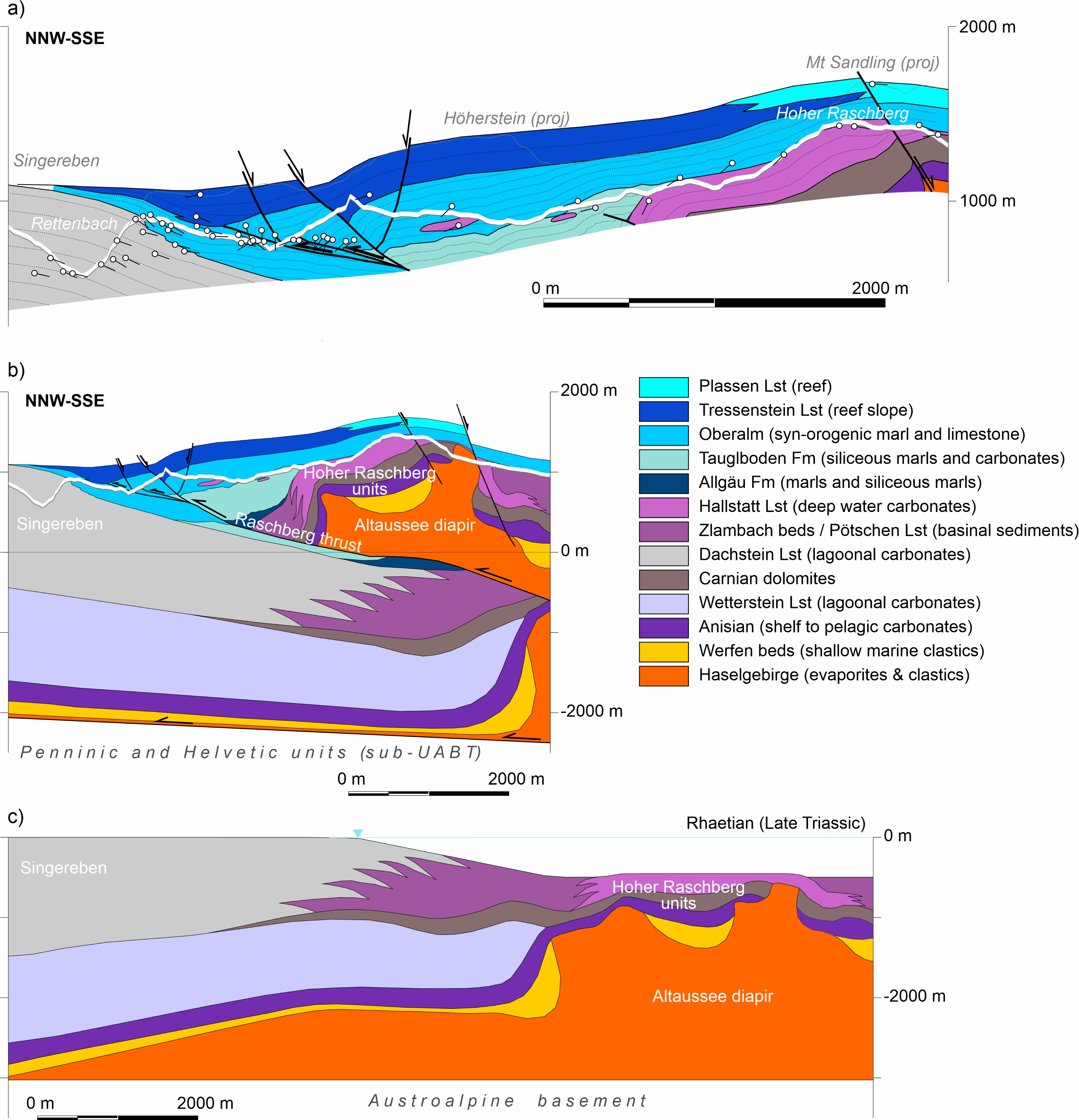

a)
NNW-SSE
2000 m
1000 m
Mt Sandling (proj)
Hoher Raschberg
Höherstein (proj)
Singereben
Rettenbach
0 m
2000 m
b)
NNW-SSE
2000 m
0 m
-2000 m
Hoher Raschberg units
Altaussee diapir
Singereben
Raschberg thrust
Penninic and Helvetic units (sub-UABT)
0 m
2000 m
Plassen Lst (reef)
Tressenstein Lst (reef slope)
Oberalm (syn-orogenic marl and limestone)
Tauglboden Fm (siliceous marls and carbonates)
Allgäu Fm (marls and siliceous marls)
Hallstatt Lst (deep water carbonates)
Zlambach beds / Pötschen Lst (basinal sediments)
Dachstein Lst (lagoonal carbonates)
Carnian dolomites
Wetterstein Lst (lagoonal carbonates)
Anisian (shelf to pelagic carbonates)
Werfen beds (shallow marine clastics)
Haselgebirge (evaporites & clastics)
c)
Rhaetian (Late Triassic)
0 m
-2000 m
Singereben
Hoher Raschberg units
Altaussee diapir
0 m
2000 m
Austroalpine basement

Figure 11.

Untersberg thrust sheet
Hallein diapir
Fig. 13
Berchtesgaden
Ahornalm thrust
Rossfeld sync.
Eckersattel
Kehlstein
Eckersattel thrust
Bluntautal thrust
Eckersattel thrust
Dürreckberg
Hoher Göll
Göll Massif
Jenner
Königs-see
Königssee fault
Bluntautal thrust
Schneibstein
Germany
Austria
Hagengebirge
Salzach R.
Golling
Tauglboden
Trattberg syncline
Trattberg
Hochwieskopf
Trattberg thrust
Einberg thrust
Postalm
Einberg
Rigaus - Postalm fault
Dachstein thrust sheet
Fig. 12
Schwarzer Berg
Schwarzerberg thrust
Lammer R.
Hochsattel anticline
Roadberg
Sattelberg
Sattelberg thrust
Gosau basin
Abtenau
Tennengebirge
Südlicher Wieselstein
0 m
4000 m
y: 5280000
x: 383000
x: 349000
y: 5265000
WGS84
UTM33
Quaternary
Gosau Group
Schrambach and Rossfeld Fms
Oberalm Fm and MTDs
Tauglboden Fm, Strubberg Fm and MTDs
Allgäu Fm
Jurassic red limestones
Rhaetian Lst
Kössen Fm
Dachstein Lst
Hallstatt Lst
Pötschen Lst and Zlambach beds
Carnian dolomite
Wetterstein Lst
Reifling Fm
Anisian carbonates
Werfen beds
Haselgebirge (evaporites and clastics)
Lakes and rivers
National boundary
Regional dip
Minor / major normal synclines
Minor / major normal anticlines
Minor / major thrusts
Minor / major normal faults
Buried trace of Trattberg - Eckersattel thrust
Buried trace of Untersberg - Dachstein thrust

Figure 12.

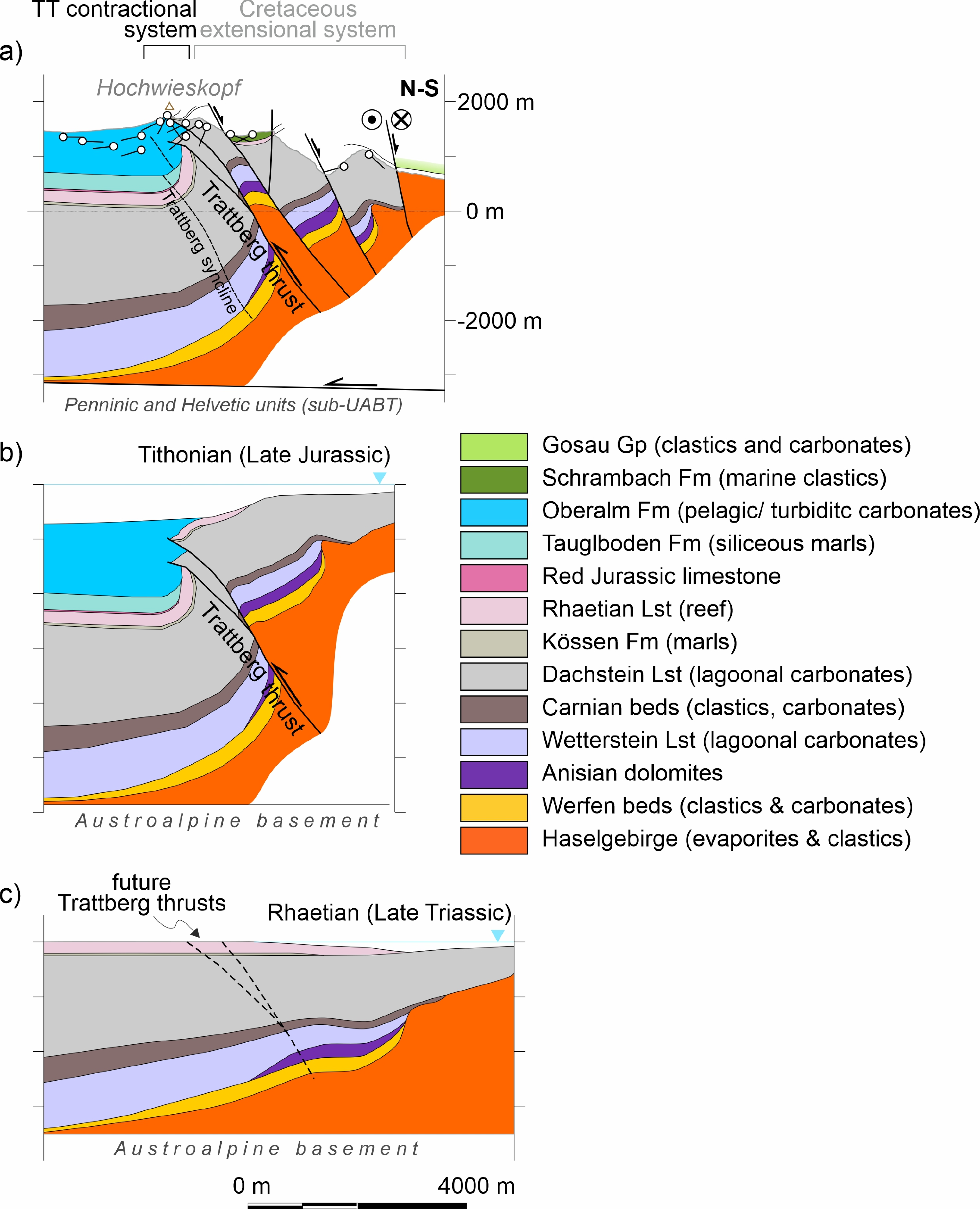

TT contractional system
Cretaceous extensional system
a)
Hochwieskopf
N-S
2000 m
0 m
-2000 m
Trattberg thrust
Trattberg syncline
Penninic and Helvetic units (sub-UABT)
b)
Tithonian (Late Jurassic)
Trattberg thrust
Austroalpine basement
Gosau Gp (clastics and carbonates)
Schrambach Fm (marine clastics)
Oberalm Fm (pelagic/ turbiditc carbonates)
Tauglboden Fm (siliceous marls)
Red Jurassic limestone
Rhaetian Lst (reef)
Kössen Fm (marls)
Dachstein Lst (lagoonal carbonates)
Carnian beds (clastics, carbonates)
Wetterstein Lst (lagoonal carbonates)
Anisian dolomites
Werfen beds (clastics & carbonates)
Haselgebirge (evaporites & clastics)
c)
future Trattberg thrusts
Rhaetian (Late Triassic)
Austroalpine basement
0 m
4000 m

Figure 13.

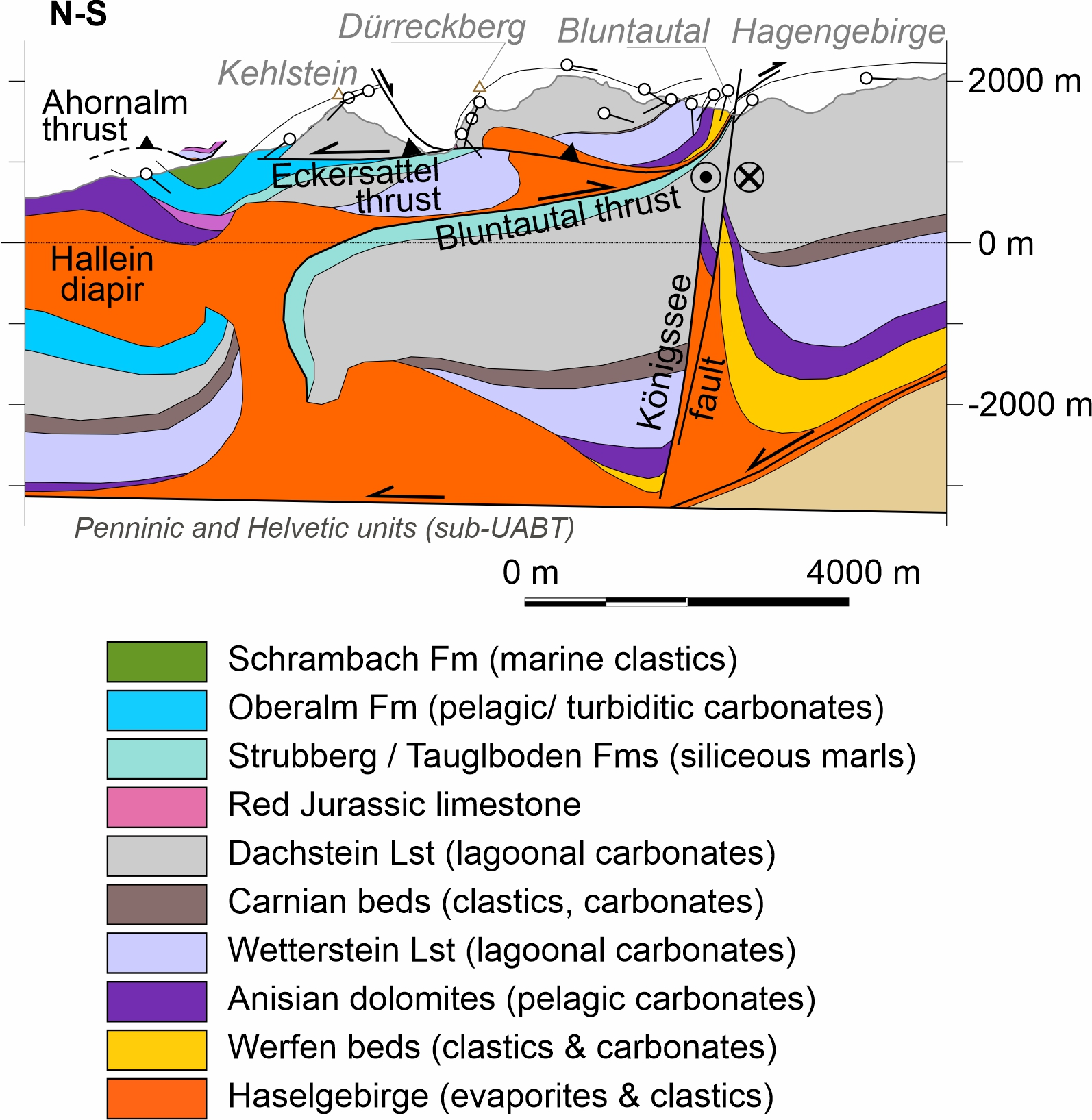
N-S
Dürreckberg
Bluntautal
Hagengebirge
Kehlstein
Ahornalm thrust
Eckersattel thrust
Bluntautal thrust
Hallein diapir
Königssee fault
2000 m
0 m
-2000 m
Penninic and Helvetic units (sub-UABT)
0 m
4000 m
Schrambach Fm (marine clastics)
Oberalm Fm (pelagic/ turbiditic carbonates)
Strubberg / Tauglboden Fms (siliceous marls)
Red Jurassic limestone
Dachstein Lst (lagoonal carbonates)
Carnian beds (clastics, carbonates)
Wetterstein Lst (lagoonal carbonates)
Anisian dolomites (pelagic carbonates)
Werfen beds (clastics & carbonates)
Haselgebirge (evaporites & clastics)

Figure 14.

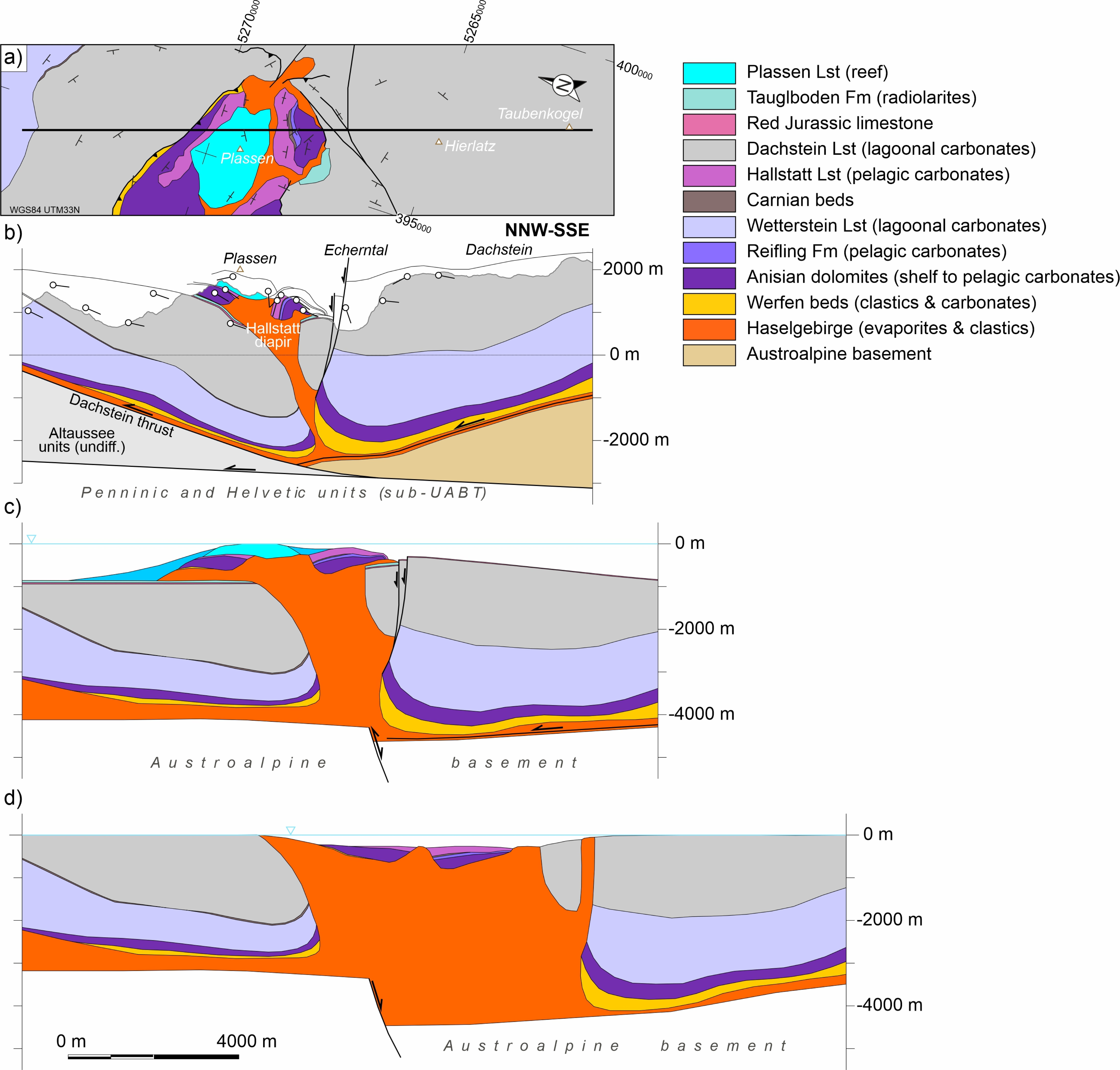
a)
5270000
5265000
400000
395000
Taubenkogel
Hierlatz
Plassen
WGS84 UTM33N
b)
NNW-SSE
Plassen
Echerntal
Dachstein
2000 m
0 m
-2000 m
Hallstatt diapir
Dachstein thrust
Altaussee units (undiff.)
Penninic and Helvetic units (sub-UABT)
c)
0 m
-2000 m
-4000 m
Austroalpine basement
d)
0 m
-2000 m
-4000 m
0 m
4000 m
Austroalpine basement
Plassen Lst (reef)
Taugiboden Fm (radiolarites)
Red Jurassic limestone
Dachstein Lst (lagoonal carbonates)
Hallstatt Lst (pelagic carbonates)
Carnian beds
Wetterstein Lst (lagoonal carbonates)
Reifling Fm (pelagic carbonates)
Anisian dolomites (shelf to pelagic carbonates)
Werfen beds (clastics & carbonates)
Haselgebirge (evaporites & clastics)
Austroalpine basement

Figure 15.

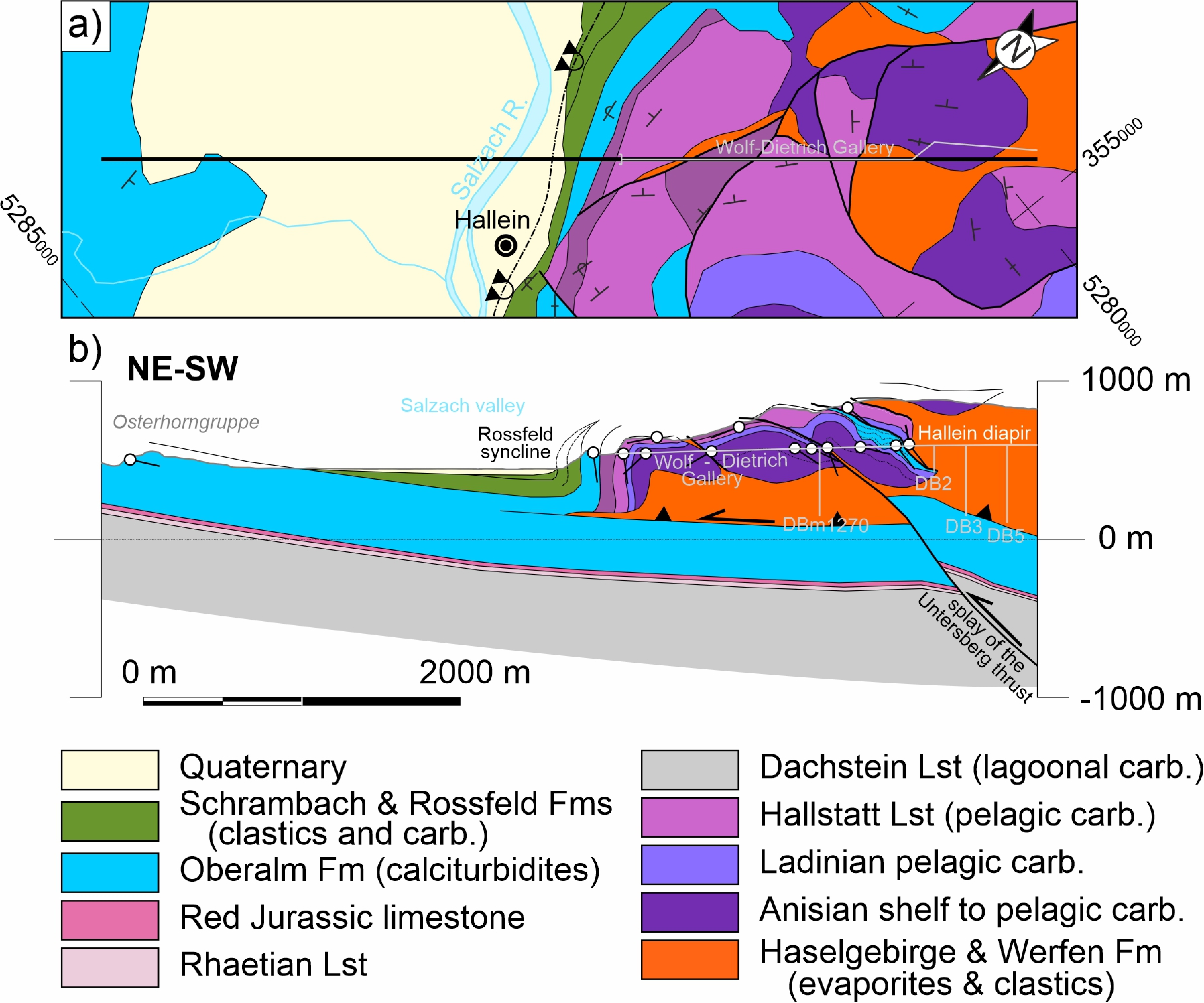
a)
Salzach R.
Hallein
Wolf-Dietrich Gallery
355000
5285000
5280000
b)
NE-SW
Osterhorngruppe
Salzach valley
Rossfeld
syncline
Hallein diapir
Wolf - Dietrich
Gallery
DB2
DBm1270
DB3
DB5
1000 m
0 m
-1000 m
splay of the
Untersberg thrust
0 m
2000 m
Quaternary
Schrambach & Rossfeld Fms
(clastics and carb.)
Oberalm Fm (calciturbidites)
Red Jurassic limestone
Rhaetian Lst
Dachstein Lst (lagoonal carb.)
Hallstatt Lst (pelagic carb.)
Ladinian pelagic carb.
Anisian shelf to pelagic carb.
Haselgebirge & Werfen Fm
(evaporites & clastics)

Figure 16.

a)
325000
5275000
330000
5270000
Grubhörndl
Kienberg
Grubhörndl thrust
Saalachtal Th-1
N
WGS84 UTM33N
b)
NW-SE
Grubhörndl
Gerhardstein-Lofer units
Kienberg
Saalachtal Th-1 (proj.)
Grubhörndl thrust
2000 m
0 m
-2000 m
Penninic and Helvetic units (sub-UABT)
c)
4000 m
0 m
Penninic and Helvetic units (sub-UABT)
0 m
4000 m
d)
NW-SE
Grubhörndl
Oberalm Fm
Rhaetian Lst
Kössen Fm
Rhaetian Lst
Dach-stein Lst
Plassen Lst
Schrambach Fm
Rhaetian Lst
Kössen Fm
Dachstein Lst
Dachstein Lst
Lower Cretaceous (marine clastics)
Plassen Lst (reef)
Oberalm Fm (pelagic/ turbiditc carbonates)
Upper Jurassic breccias
Red Jurassic limestone
Rhateian Lst (reef)
Kössen Fm (marls)
Dachstein Lst (lagoonal carbonates)
Hallstatt Lst (pelagic carbonates)
Wetterstein Lst (lagoonal carbonates)
Anisian dolomites
Werfen beds (clastics & carbonates)
Haselgebirge (evaporites & clastics)

Figure 17.


a)
sealevel
drowned platform
thin platform roof
drowned platform
pelagic roof
drowned platform
pelagic roof
drowned platform
minibasin
salt wall
minibasin
salt wall
minibasin
salt wall
minibasin
diapir
diapir
Austroalpine basement
??
inherited extensional offset?
b)
sealevel
isoclinal syncline
salt wall rim uplift
salt overthrust
inverted faults
squeezed salt wall
secondary weld
plug-fed thrust
erosion
syn-orogenic sediments
reef growth +/- erosion
salt-detached shortening
??
basement thrusting?
??
inherited extensional offset?

Figure 18.


a)
Pelagic Upper Triassic and evaporites (diapir/salt wall roof)
Thin Upper Triassic platform (diapir/salt wall roof)
Thick Upper Triassic platform (minibasin)
Direction of stratigraphic tapering of Middle / Upper Triassic platforms
Extensional rollover
Map area (km²)
1895
287
5220
Unken
Lofer
Hallein
Lammertal
Altaussee
Kasberg
Windischgarsten
Grundlsee
Bad Mitterndorf
Late Triassic
0 10 20 40 km
N
b)
Pelagic Upper Triassic and evaporites
Thin Upper Triassic platform
Thick Upper Triassic platform
Thrust
Fold system
Secondary weld
Reef trend
Age constraints
First breccias
Thrusting
Reef growth
Map area (km²)
1472
63
4904
Falkenstein
Lugberg
Jainzenberg
Ebensee
Totengebirge
Untersberg
Hallein
Grünberg
Raschberg
Trattberg
Grubhörndl
Eckersattel
Postalm
Sandling
Trisselwand
Salzsteig
Rote Wand
Wurzeralm
Lofer Gerhardstein
Klausbach
Königssee
Bluntautal
Sattelberg
Hallstatt
Plassen
Feuerkogel
Bad Mitterndorf
Late Triassic outline
Late Jurassic
0 10 20 40 km
N
c)
Pelagic Upper Triassic and evaporites
Thin Upper Triassic platform
Thick Upper Triassic platform
Thrust
Secondary weld
Leading edge eroded upper thrust(s)
Inherited structures
Leading edge basement wedge
Map area (km²)
732
37
4725
Untersberg
Unken
Lofer
Gerhardstein
Postalm
Dachstein
Salzsteig
Warscheneck
Obertraun
Worschach
Late Jurassic outline
Late Cretaceous
0 10 20 40 km
N
d)
Pelagic Upper Triassic and evaporites
Thin Upper Triassic platform
Thick Upper Triassic platform
Late Cretaceous - Neogene collapse
Thrust
Strike-slip faults
Inherited structures
Leading edge basement wedge
Map area (km²)
537
5
4662
Wolfgangsee
Traunsee
Windischgarsten
Nierental
Latten-gebirge
Lofer
Königssee
Lammertal
Postalm
Sandling
Wurzeralm
Pyhrn
SEMP
Gosau
Obertraun
Ramsau
Late Cretaceous outline
Present-day
0 10 20 40 km
N
e)
Key structures
Salzburg
Gmunden
Steyr
Bad Ischl
Liezen
Saalfelden
Bischofshofen
Schladming
Re
Ub
Ha
Oh
Hö
Sg
Tr
Ks
St
Gb
Lh
Ra
Ka
As
To
Ws
Lo
Wt
HG
Go
Sw
Tt
Sb
Pw
Zw
Ht
Gr
Mt
Gh
Lg
Hn
Tn
Dc
Rl
Mg

Figure 19.

a)
Erosion
Breccias (Tauglboden & Strubberg Fms)
Background radiolarite basin (Tauglboden & Strubberg Fms)
Reef (Plassen Fm)
Active structures
Squeezed salt walls or diapirs
Falkenstein
Osterhorngruppe
Raschberg
Grünberg
Totengebirge
Rettenbach - Sandlingalm
Loser
Wurzeralm
Grubhörndl
Bluntautal
Büchsenkopf
Sattelberg
Strubberg
Hallstatt
Rettenstein
Callovian-Oxfordian
0 10 20 40 km
N
b)
Erosion
Megabreccias (Barmstein)
Reef (Plassen Fm)
Reef slope (Tressenstein)
Pelagic basin carbonates (Oberalm Fm)
Active structures
Squeezed salt walls or diapirs
Falkenstein
Lugberg
Jainzenberg
Untersberg
Oberalm
Osterhorngruppe
Bad Ischl
Hallein
Trattberg
Moosegg
Eckersattel
Höherstein
Sandling
Trisselwand
Rote Wand
Raucherschober - Schafkogel
Lofereralm
Lofer
Gerhardstein
Hochkranz
Sarsteinalm
Feuerkogel
Krahstein
Plassen
Bosruck
Rettenstein
Ramsau
?
Kimmeridgian-Tithonian
0 10 20 40 km
N
c)
Onset of thrusting on the Lofer-Gerhardstein and Untersberg thrusts
Moosegg
Bad Ischl
Onset of thrusting on the Dachstein thrust
Approximate Oberalm Fm to Schrambach Fm boundary
~125
~129.4
~132.6
~139.8
~145.0
152.1
157.3
163.5
166.1
168.3
170.3
APTIAN
BARREMIAN
HAUTERIVIAN
VALANGINIAN
BERRIASIAN
TITHONIAN
KIMMERIDGIAN
OXFORDIAN
CALLOVIAN
BATHONIAN
BAJOCIAN
AALENIAN
CRETAC.
JURASSIC
Grubhörndl
Lofer-Gerhardstein
Hallein
Bluntautal
Eckersattel
Sattelberg
Trattberg
Rettenstein-Ramsau
Hallstatt
Plassen
Falkenstein
Raschberg
Sandling
Grünberg
Krahstein
Totengebirge
Wurzeralm
Rote Wand
Blue = Thrusts or folds
Orange = Squeezed diapir or salt allochthon
Pink = Reefs
Denotes unconstrained cessation
Thrusting / folding / uplift
Thrusting / folding (uncertain)
Erosion / breccia deposition
Reef growth